1996

INTERACTIONS AMONG THE STATIONARY PHASE, THE MOBILE PHASE, AND THE SOLUTE IN LIQUID CHROMATOGRAPHIC SYSTEMS

Zengbiao Li

College of Humanities and Sciences
Virginia Commonwealth University

This is to certify that the dissertation prepared by Zengbiao Li entitled INTERACTIONS AMONG THE STATIONARY PHASE, THE MOBILE PHASE, AND THE SOLUTE IN LIQUID CHROMATOGRAPHIC SYSTEMS has been approved by his committee as satisfactory completion of the dissertation requirement for the degree of Doctor of Philosophy in Chemistry.

[redacted]

Dr. Sarah C. Rutan, Director of Dissertation, Department of Chemistry

[redacted]

Dr. Fred M. Hawkridge, Committee Member, Department of Chemistry

[redacted]

Dr. Jennifer K. Stewart, Committee Member, Department of Biology

[redacted]

Dr. Charlene D. Crawley, Committee Member, Department of Chemistry

[redacted]

Dr. M. Samy El-Shall, Committee Member, Department of Chemistry

[redacted]

Dr. Robert G. Bass, Chairman, Department of Chemistry

[redacted]

Dr. Susan E. Kennedy, Interim Dean, College of Humanities and Sciences

[redacted]

Dr. Jack L. Haar, Dean, School of Graduate Studies

December 13, 1996

Date

INTERACTIONS AMONG THE STATIONARY PHASE, THE MOBILE PHASE, AND THE SOLUTE IN LIQUID CHROMATOGRAPHIC SYSTEMS

A dissertation
submitted in partial fulfillment of the requirements
for the degree of Doctor of Philosophy
at Virginia Commonwealth University

By

Zengbiao Li
M.Sc. Beijing Medical University 1987
B.Sc. Peking University 1984

Director:
Sarah C. Rutan, Ph.D.
Associate Professor
Department of Chemistry

Virginia Commonwealth University
Richmond, Virginia
December, 1996

Acknowledgments

I would like to thank Dr. Sarah Rutan, for her guidance and support throughout this work. I would also like to thank my committee, including Drs. Charlene Crawley, M. Samy El-Shall, Fred Hawkridge, Jennifer Stewart, Paul Ross (ex-committee member), and Vicki Wysocki (ex-committee member), for their advice. I am very grateful to our research group and the analytical group for their fellowship and for practice talks. I would like to thank the chemistry department for financial support. I would like to express my thanks to my family for their support throughout my educational experience. Finally, I would like to thank my wife, Yiling, for her love, understanding, and companionship.

Table of Contents

List of Tables

List of Figures

List of Abbreviations and Symbols

Abbreviations

ACN	Acetonitrile
DCMPVP	2,4-Dichloro-6-[2-(N-methyl-4-pyridinio)vinyl]phenolate (see page 38 for the structure of DCMPVP)
ET-30	2,6-Diphenyl-4-(2,4,6-triphenyl-1-pyridinio)-1-phenolate (see page 38 for the structure of ET-30)
ET-33	2,6-Dichloro-4-(2,4,6-triphenyl-N-pyridinio)phenolate (see page 38 for the structure of ET-33)
HPLC	High performance liquid chromatography
IND	Factor indicator function
IR	Infra-red spectroscopy
kK	Kilokayser (1000 cm^{-1})
MeOH	Methanol
NMR	Nuclear magnetic resonance spectroscopy
ODS	Octadecylsilylated silica
RPLC	Reversed-phase liquid chromatography
RSD	Residual standard deviation
SD	Standard deviation
SDS	Sodium dodecyl sulfate
THF	Tetrahydrofuran
vs.	versus

Symbols

% T	Percent transmittance in optical transmittance measurements
k'	Capacity factor
α	Hydrogen-bonding acidity parameter
β	Hydrogen-bonding basicity parameter
γ^{SV}	Surface tension of the solid-vapor interface
γ^{SL}	Surface tension of the solid-liquid interface
γ^{LV}	Surface tension of the liquid-vapor interface
ΔG	Free energy change
φ	Percent organic modifier (v/v) in organic modifier-water mixtures
λ_{max}	Wavelength at the absorption maximum in an electronic absorption spectrum
ν_{max}	Frequency at the absorption maximum in an electronic absorption spectrum
π^*	Dipolarity-polarizability parameter
θ	Contact angle formed at the three-phase (solid/liquid/vapor) boundary

Symbols in target factor analysis

D	Data matrix
$\mathbf{D}_{key}$	Key cobmination set used to reproduce data matrix **D** within experimental error
$\mathbf{D}_r$	Reproduced data matrix
E	Residual error matrix, representing the different between $\mathbf{D}_r$ and **D**
S	Diagonal matrix obtained from singular value decomposition of data matrix **D**, whose diagonal elements are the square roots of the respective eigenvalues for the eigenvectors in orthonormal matrices **U** and **V**
T	Transformation matrix used to reproduce data matrix **D** from the key combination set
U	Orthonormal matrix obtained from singular value decomposition of data matrix **D**, composed of eigenvectors of the row-factor space
V	Orthonormal matrix obtained from singular value decomposition of data matrix **D**, composed of eigenvectors of the column-factor space
c	Number of columns in data matrix **D**
n	Number of significant factors
r	Number of rows in data matrix **D**
λ_j	Eigenvalue for the jth eigenvector in orthonormal matrices **U** and **V**

Abstract

INTERACTIONS AMONG THE STATIONARY PHASE, THE MOBILE PHASE, AND THE SOLUTE IN LIQUID CHROMATOGRAPHIC SYSTEMS

By Zengbiao Li, Ph.D.

A dissertation submitted in partial fulfillment of the requirements for the degree of Doctor of Philosophy at Virginia Commonwealth University.

Virginia Commonwealth University, 1996.

Director: Sarah C. Rutan, Ph.D., Associate Professor, Department of Chemistry

Interactions among the stationary phase, the mobile phase, and the solute in liquid chromatography have been studied. A strong dependence of the stationary phase properties on the mobile phase composition may arise from their interactions.

The solvatochromic comparison method, which can give estimates for the dipolarity-polarizability, the hydrogen-bonding acidity, and the hydrogen-bonding basicity of a solvent, represented by the solvatochromic parameters π^*, α, and β, respectively, was used to study the surface properties of silica in the presence of *n*-hexane-chloroform or *n*-hexane-ethyl ether mixtures. A high dipolarity-polarizability, a high hydrogen-bonding acidity, and a low hydrogen-bonding basicity were obtained for silica in *n*-hexane. The π^* and α

values for silica were not affected by the addition of chloroform into *n*-hexane. The hydrogen-bonding basicity of silica, however, decreased with increasing amounts of chloroform. The π^* value for silica decreased with increasing contents of ethyl ether. The decrease in π^* and β values for silica may have resulted from the competition between the polar solvent and the solvatochromic dyes for the strong adsorption sites on silica.

Electronic absorption spectra of a solvatochromic dye, N,N-dimethyl-4-nitroaniline, in *n*-hexane-ethyl ether mixtures were used to elucidate solute-solvent interactions. Target factor analysis indicated that solute-solvent interactions in a binary solvent can only be reproduced using three or four significant factors, instead of a linear combination of solute-solvent interactions in the two pure components, which is probably caused by the existence of various microenvironments in mixtures of *n*-hexane and ethyl ether.

Optical transmittance measurements were established to study the wetting of alkyl bonded silicas in organic solvent-water mixtures. When the percent organic solvent content in the eluent, φ, was high, alkyl bonded silica was wetted and well solvated. With decreasing φ, alkyl bonded silica became less solvated. When φ was lower than the nonwetting limit (less than 10% of organic solvent), alkyl bonded silica became nonwetted. With increasing φ, a nonwetted alkyl bonded silica

remains nonwetted until φ reaches the rewetting limit (around 60%), which is much higher than the nonwetting limit. Wetting hysteresis can be observed clearly in optical transmittance measurements. Slow kinetics may be a prerequisite for the appearance of wetting hysteresis. Different alkyl bonded phases have different wetting behaviors. Much longer column equilibration time is required if the stationary phase is nonwetted or not well solvated. Both the surface dipolarity and solute retention are affected by the wetting of the stationary phase.

Chapter 1

Introduction

Liquid chromatography is one of the most important modern separation techniques. According to the relative polarity of the stationary phase and the mobile phase, there are two separation modes in liquid chromatography: the normal-phase mode, in which the stationary phase is more polar than the mobile phase, and the reversed-phase mode, in which the stationary phase is less polar than the mobile phase. Silica is the most frequently used stationary phase in normal-phase liquid chromatography. In reversed-phase liquid chromatography (RPLC), chemically modified silica with alkyl substituents is the most frequently used stationary phase. To make stationary phases for RPLC, some surface silanols are removed by alkylsilylation,

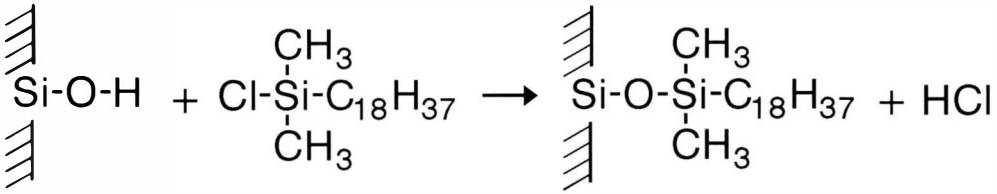

A chromatographic process is determined by the interactions among the stationary phase, the mobile phase, and the solute. A strong dependence of the stationary phase properties on the mobile phase composition may arise from their interactions. In most cases in liquid chromatography, the mobile phase is not a pure solvent, but a mixture of two

or more solvents. The interactions between the solute and the mobile phase is often complicated by preferential solvation of the solute by one component of the mixture and molecular interactions between different components in the mobile phase.

The surface of silica is composed of silanol and siloxane groups. Surface silanols are mainly responsible for the retention of solutes on silica. In RPLC, surface silanol groups are also instrumental in the wetting of alkylsilylated silica and the retention of some solutes. There are several types of surface silanols. Different types of silanols may have different acidities. Most of the studies on silica surfaces are under conditions without the presence of a solvent. One question posed in this research is how a solvent modifies the properties of surface silanols or the interactions between surface silanols and solutes. This effect must be understood to elucidate the retention mechanism and predict retention in liquid chromatography.

The solvatochromic comparison method, which can give estimates for the dipolarity-polarizability, represented by the solvatochromic parameter π^*, the hydrogen-bonding acidity, represented by the solvatochromic parameter α, and the hydrogen-bonding basicity, represented by the solvatochromic parameter β, of the surface of silica, was used in this research. The solvatochromic parameters was used to elucidate the surface chemistry of silica. The ultimate goal is the

prediction of retention based on the solvatochromic parameters of solutes, the stationary phase, and the mobile phase according to the following equation:

$$\ln k' = c + s \cdot \pi_2^* \cdot \Delta\pi^* + a \cdot \beta_2 \cdot \Delta\alpha + b \cdot \alpha_2 \cdot \Delta\beta \qquad (1\text{-}1)$$

where k' is the capacity factor, π_2^*, α_2, and β_2 are the solvatochromic parameters for the solutes, $\Delta\pi^*$, $\Delta\alpha$, and $\Delta\beta$ are the differences of the solvatochromic parameters between the stationary phase and the mobile phase, and s, a, and b are regression coefficients.

The mobile phase in normal-phase liquid chromatography is often a mixture of a nonpolar solvent and a polar solvent, e.g., *n*-hexane and ethyl ether. The interactions between a polar organic solute and the mobile phase are complicated by the potential preferential solvation of the polar solute by ethyl ether and dipolar interactions between ethyl ether molecules. Factor analysis was conducted on the electronic spectra of a solvatochromic dye, N,N-dimethyl-2-nitroaniline, in mixtures with different ethyl ether contents. Information about the molecular interactions between the dye and the mobile phase can be obtained from the results of the factor analysis study.

The surface of alkylsilylated silica is composed of bonded alkyl chains and residual silanols. The stationary phase materials for RPLC are relatively hydrophobic because of the alkylsilylation of some of the surface silanol groups.

The mobile phase used in RPLC, however, is usually a mixture of water and organic solvents. Therefore, in RPLC, problems with wetting the alkylsilylated silicas are expected, especially in water-rich eluents. The wetting of a bonded alkyl phase, more specifically, the interfacial tension between the stationary phase and the mobile phase, may strongly affect various chromatographic behaviors of the bonded phase. Unlike a flat surface, however, there are not many experimental techniques available to characterize the wetting and interfacial behaviors of porous particles. In this research, the measurements of the optical transmittance of the stationary phase/mobile phase system was proposed as a means to study the interfacial behavior of the stationary phase particles in the mobile phase. The solvatochromic method, chromatographic measurements, and direct wetting tests were also applied to study the wetting, or the interfacial behavior, and its effects on chromatographic performance.

Although liquid chromatography has been practiced for a long time, the interactions among the stationary phase, the mobile phase, and the solute are still far from well understood. In this research, solvent effects on the properties of silica and alkylsilylated silica were studied by the solvatochromic comparison method, optical transmittance measurements, direct wetting tests, and chromatographic measurements. Factor analysis was applied to study the

interactions between a solute and binary solvent mixtures. The results from this research may solve some problems in chromatographic applications and improve our understanding of the mechanism of a liquid chromatographic process.

Chapter 2

Background

2-1 Surface Chemistry of Silica

Basic knowledge about silica can be found in two frequently cited books in this field.[1,2] Several recent articles have reviewed advances in elucidating the chemical nature of the surface of silica for chromatographic applications.[3-6] The chemical nature of the surface of silica has been characterized by various techniques, including infrared spectroscopy (IR),[7-10] nuclear magnetic resonance spectroscopy (NMR),[7,9,11-13] adsorption methods,[14,15] and chromatographic methods.[8,16] The information provided by these techniques is summarized here. The surface of silica is composed of silanol and siloxane groups. There are three types of silanols——free silanols, hydrogen-bonded silanols, and geminal silanols,[17] as shown in Figure 2-1. ^{29}Si NMR can be used to distinguish the silicon atoms in siloxane groups, [(≡Si-O-)$_4$**Si**], the silicon atoms with one hydroxyl group, [(≡Si-O-)$_3$**Si**OH], and the silicon atoms with two hydroxyl groups, [(≡Si-O-)$_2$**Si**(OH)$_2$].[11] But this method can not distinguish free and hydrogen-bonded silanol groups. IR is capable of distinguishing free and hydrogen-bonded silanol groups.[7,18] Isotherm adsorption[14,15] and chromatographic methods[8,16] give information about the activities of different adsorption sites on the surface of silica.

The surface silanol concentration, the ratio of the three

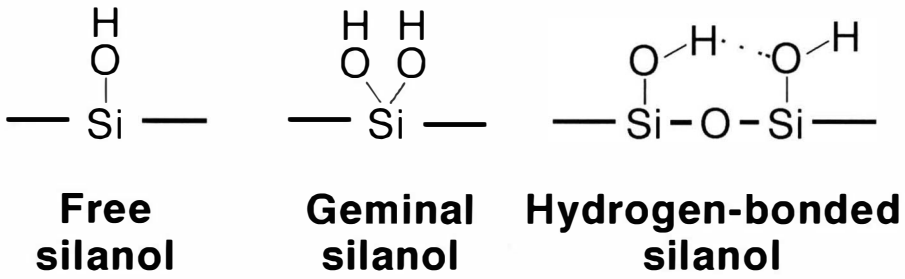

Figure 2-1. Different types of silanol groups.

types of silanol groups and the content of metal impurities are among the most important parameters for silica in chromatographic applications.[9,14,17] The surface silanol concentration can be changed by the degree of hydration. For fully hydrated porous silica in chromatographic applications, it is generally agreed that the surface silanol concentration is around 8 μmol/m^2 (4.8 silanol groups/nm^2).[4,19,20] The ratio of the three types of silanol groups is related to the degree of hydration of silica. For fully hydrated silica, geminal silanol groups account for about 30% of the total silanol groups.[7,12] Different types of silanols have different acidities. It is generally believed that free silanols are more acidic than hydrogen-bonded silanols.[7,9] But there are arguments about whether hydrogen-bonded silanols are the most acidic.[15] Strong evidence was provided by Pfleiderer and Bayer that geminal silanols were responsible for the abnormal chromatographic behavior of basic solutes on silica.[21] Metal impurities in silica may have a large effect on the acidity of silica[14,22] and the retention of hydrogen-bonding acceptor solutes[23] or solutes capable of chelating metals.[24,25]

Dehydration of silica is usually performed by thermal treatment under vacuum. The first stage is the removal of physically adsorbed water at relatively low dehydration temperatures. Then hydrogen-bonded silanols are eliminated. Finally free silanols can be removed at very high

temperatures. Sindorf and Maciel have studied dehydration and rehydration of silica by ^{29}Si NMR and thermogravimetric methods.[12] Most of the physically adsorbed and bulk molecular water was removed at temperatures lower than 100°C. Most of the silanol groups were removed at temperatures lower than 500°C. At temperatures below 500°C, geminal silanols were removed to a larger degree than single silanols. Geminal silanols removed below 500°C can be completely restored by exposure to water. But only about half of the single silanol groups removed below 500°C can be recovered. At temperatures between 500°C and 700°C, the surface concentration of geminal silanols remained constant. But the restoration of geminal silanols decreased rapidly in this temperature range. At temperatures higher than 700°C, both geminal and single silanol groups were further eliminated. Little restoration of surface silanols was observed for silica dehydrated at temperatures higher than 700°C. Kinney et al. demonstrated by ^{1}H NMR that hydrogen-bonded silanols seldom existed on the surface of silica dehydrated at 500°C.[13]

IR studies conducted by Mauss and Engelhardt showed little evidence of hydrogen-bonded silanols for silica dehydrated above 600°C.[8] It was observed that capacity factor values for benzyl alcohol and phenol, solutes with hydroxyl groups, decreased with the dehydration temperature of silica. The largest decrease in retention on silica for benzyl alcohol

and phenol occurred within the dehydration temperature range between 400°C and 600°C. It was concluded that benzyl alcohol and phenol were mainly retained by hydrogen-bonded silanols on the surface of silica. In contrast, the retention of ketones and esters was seldom affected by dehydration in the temperature range between 100°C and 600°C. It is believed that these solutes were adsorbed preferentially on the free silanols. Some earlier research showed that solutes with hydroxyl groups adsorbed preferentially on hydrogen-bonded silanols whereas solutes with only hydrogen-bonding accepting ability preferred to interact with free silanols.[18]

From the enthalpy of adsorption of various molecules as a function of coverage, Fubini et al. showed that the surface of silica was highly heterogeneous.[15] The decrease of the enthalpy of adsorption of water on silica after thermal treatment at 800°C was attributed to the removal of hydrogen-bonded silanols, which may have stronger interactions with water than free silanols. From the decrease of the enthalpy of adsorption of ammonia on silica after thermal treatment, it was concluded that hydrogen-bonded silanols were more acidic than free silanols.

Pfleiderer and Bayer believe that geminal silanols are responsible for the abnormal chromatographic behavior of basic solutes on silica or chemically modified silica.[21] They found that the modification of silica by Fe^{3+} can reduce the

retention of basic solutes and improve the column efficiency for basic solutes. Solid state NMR showed that the Fe^{3+} on the silica was localized on the geminal silanols by chelation. Only about 40% of the geminal silanol groups were strong adsorption sites for basic solutes. An ion-exchange mechanism was proposed for the interactions between basic solutes and acidic geminal silanol groups. Heidrich et al.[26] demonstrated by ab initio calculations that the geminal silanols were more acidic than single silanols in the gas phase.

Nawrocki and Szczepaniak studied strong adsorption sites on silica surfaces by gas chromatography.[22] The population of strong adsorption sites was correlated to the trace amount of calcium in silica. It is believed that silanol groups close to metal impurities, not the metal impurities themselves, are the strong adsorption sites.[22,23] Ab initio calculations showed that the acidity of a silanol group can be significantly increased by its interactions with a Lewis center.[26] Köhler et al.[7] correlated the pH value of 9.2 of LiChrospher Si-200 silica with the high sodium content of the silica. But basic solutes were still strongly adsorbed on to the silica with a high pH value. It is believed that acid treatment can only remove surface metals, but not the metal impurities embedded within the silica structure.[24]

A quantitative estimation of the surface polarity of silica is very important for chromatographic applications.

Boudreau and Cooper[27,28] evaluated the surface polarity of silica by a heterogeneous gas-solid chromatographic method. In this method, the monolayer adsorption energies of indicator solutes are used to build polarity scales. The indicator solutes for the acidity, basicity, and dipolarity of a surface are pyridine, chloroform, and dichloromethane, respectively. In this method, the contribution of dipolar interactions to the adsorption energies of chloroform and pyridine is not excluded in measuring the acidity and basicity of a surface. Therefore, the parameters for the acidity and basicity include some contribution from the dipolarity of the surface. In addition, this approach cannot be applied to study the effect of the overlying solvent on the surface properties.

2-2 Solvent-Solvent and Solvent-Solute Interactions in Binary Solvent Mixtures

In liquid chromatography, the mobile phase is usually a binary solvent mixture. To a rough approximation, a property of the binary solvent mixture can be considered as a linear combination of the corresponding properties of the two pure components, i.e., a linear function of the solvent composition. This linear relationship holds only, however, for binary solvent mixtures consisting of two components with their molecular interactions similar both in type and in

magnitude. In most cases, a non-linear relationship is observed because solvent mutual-interactions, i.e., interactions between a solvent molecule of one component and a solvent molecule of another component, are significantly different from solvent self-interactions, i.e., interactions among solvent molecules of the same component. When a solute used to probe the properties of the solvent mixture is added into the binary solvent mixture, the situation becomes more complicated because of the solute-solvent interactions. In a word, interpretation of interactions between a solute and a binary solvent mixture are complicated by solvent self-interactions and solvent mutual-interactions.

Non-linear dependence on the solvent composition in binary solvents has been observed for various properties, e.g., volume, density, viscosity, dielectric constant, and refractive index. Based on the changes of these physical properties of binary solvent mixtures, solvent-solvent interactions in the solvent mixture can be investigated.[29,30] Spectroscopic measurements, however, may provide more detailed information about solute-solvent interactions and interactions between the solvent components. NMR has been used to study the structure of water-acetonitrile mixtures.[31,32] Most of the research work concerning the structure of binary solvent mixtures and interactions between the solute and binary solvent mixtures was conducted based on electronic absorption

and emission spectroscopic measurements with probe molecules which are sensitive to solvent environments.[33-35] Some of the probe molecules have been used as solvatochromic indicators to measure solvent polarity. Their electronic excitation energies have been well correlated with solvent polarity. Preferential solvation, defined as the difference between the solvent composition in the immediate surroundings of the solute, and the bulk solvent composition, is often observed for probe molecules. The solvent composition in the immediate surrounding of the solute can be calculated from the experimental excitation energy of the solute, assuming a linear dependence of excitation energy on solvent composition in the local region. Preferential solvation as defined herein is a composite effect of solvent self-association, solvent mutual interactions, and solvent-solute interactions. The three types of interactions are interrelated. Solvent self-association may result in microheterogeneity in solvent mixtures, i.e., microphases of one component coexist with microphases of another component. Solvent-solute interactions may play a much more significant role in preferential solvation than solvent-solvent interactions and it is not easy to separate the contributions of different types of interactions to preferential solvation. Therefore, to elucidate the structure of binary solvent mixtures relying solely on preferential solvation data is unwise.

Aqueous binary solvent mixtures. Aqueous binary mixtures are subjects of intensive research because of their widespread applications and their complexity in structure. Some polar organic solvents may complex with water. The presence of complexes, which may have significantly different chemical and physical properties from the individual components, may strongly affect the properties of the mixtures. For binary mixtures of water with methanol (MeOH), acetonitrile (ACN), and tetrahydrofuran (THF), Katz et al.[29] calculated the association constants and the molar volumes of the organic solvent-water complexes using an iterative procedure to minimize the difference between the volume change on mixing obtained from tentative association constants and molar volumes and the experimental volume change. A water molecule complexes strongly with a MeOH molecule. Binary mixtures of water and MeOH should be considered as 'ternary' mixtures of self-associated water, self-associated MeOH, and water-MeOH complexes. With the volume fraction of MeOH in the range from 45% to 80%, the major component in the mixtures is the water-MeOH complex. For ACN-water mixtures, complex formation is almost negligible. Complex formation in THF-water mixtures is considerable, but much less significant than in MeOH-water mixtures. For MeOH-water mixtures, the density change and refractive index change data have also been used to calculate the association constant and similar results were obtained.[30]

ACN-water mixtures are the most studied binary solvent system.[31,32,36,37] A generally believed picture for ACN-water mixtures from various studies has been presented.[31,32,37] With the mole fraction of ACN in the mixtures in the range from 0 to about 0.2, ACN molecules gradually occupy cavities in the water structure. The presence of ACN molecules leaves the water structure intact or even enhances the water structure. Further addition of ACN disrupts the water structure. Self-association leads to a microheterogeneous structure, i.e., microphases of structured water coexist with microphases of ACN. Separation into microphases persists until the mole fraction of ACN reaches about 0.7. With the mole fraction of ACN in the range from 0.7 to 0.95, the ACN-water mixtures can be described as discrete water-ACN complexes surrounded by ACN. With more than 0.95 mole fraction of ACN in the mixtures, an ACN structure as in the neat solvent, almost unmodified by the presence of water, is formed.

Solvatochromic indicators have often been used to study aqueous binary mixtures. The solvatochromic behavior of 2,6-diphenyl-4-(2,4,6-triphenyl-1-pyridinio)-1-phenolate (ET-30) has been studied in mixtures of water with MeOH, ethanol, 1-propanol, THF, and acetone.[38] ET-30 is preferentially solvated by alcohol in all three water-alcohol systems. Using the organic solvents with no hydrogen-bonding acidity, i.e., THF and acetone, as the cosolvent, however, preferential solvation

by the organic component occurs only in the water-rich region. In the organic-rich region, ET-30 is preferentially solvated by water. Similar behavior was observed for 4-[2-(1-methyl-4-pyridinio)ethenyl]phenolate in the mixtures of water with MeOH, ethanol, 1-propanol, and acetone.[39] The phenomenon of preferential solvation of ET-30 by different solvent components in different composition ranges was also observed in ACN-water mixtures[36] and 1,4-dioxane-water mixtures.[40] For N-ethyl-4-cyanopyridinium iodide and N-ethylpyrazinium iodide in the mixtures of 1,4-dioxane-water and THF-water, this behavior was also observed.[41] The common feature of these solvatochromic indicators is that they are highly polarized with a high degree of ionic character in their ground states.

For many aqueous binary systems, the dipolarity-polarizability, represented by the solvatochromic parameter π^*, was determined with solvatochromic indicators. For most of the aqueous binary systems, e.g., MeOH-water,[42] ACN-water,[37,42] 2-propanol-water,[42] and THF-water,[42,43] the curve of π^* against the solvent composition reflects the preferential solvation of the indicator molecules by the organic cosolvent. For mixtures of water with dimethyl sulphoxide, formamide, and formic acid, however, a maximum π^* value higher than either of the two pure components was observed.[43] It is believed that a complex between water and the organic cosolvent is formed, which has a larger dipole moment than either component.[43]

Non-aqueous binary solvent mixtures. Most of the studies for the non-aqueous binary solvent mixtures were conducted to characterize preferential solvation. In a few cases, no preferential solvation was observed. Such systems are usually thermodynamically ideal, but not of much practical value, e.g., mixtures of tributyl phosphate and trimethyl phosphate[40] and mixtures of 1,2-dibromomethane and 1,2-dibromopropane.[40,44] Whether an indicator dye is preferentially solvated by the more polar component or the less polar component depends on the nature of the dye and the two solvent components.

In alcoholic binary mixtures, dyes with some ionic character in their ground states, e.g., ET-30, 4-[2-(1-methyl-4-pyridinio)ethenyl]phenolate, N-ethyl-4-cyanopyridinium iodide, 1-ethyl-4-methoxycarbonylpyridinium iodide, and N-ethylpyrazinium iodide, are usually preferentially solvated by the alcohol cosolvent.[33,38-41,44-46] In mixtures of a non-polar solvent and a polar solvent, solvatochromic indicators are preferentially solvated by the polar solvent because the indicator molecules are polar.[47] Various factors, including dielectric enrichment, hydrogen-bonding interactions, hydrophobic interactions, have been cited to explain preferential solvation phenomena.[47-49]

In some non-aqueous binary solvent mixtures, synergistic effects, i.e., the mixture is more polar than either of its two pure components, were observed.[44,45] A maximum in

electronic excitation energy was observed for ET-30 in the chloroform-tributyl phosphate binary system.[45] A solvent mutual attraction weaker than self-association is believed to be the reason for the appearance of the maximum.[45] Similar behavior was observed for ET-30 and 1-ethyl-4-methoxycarbonylpyridinium iodide in mixtures of acetone-chloroform and acetone-dichloromethane, which is, however, attributed to the complexation between acetone and its cosolvent,[44] as proposed for some aqueous mixtures.

2-3 Wetting

Wetting refers to the macroscopic manifestations of the molecular interactions between a liquid and a solid in direct contact. Such manifestations can be quantitative, e.g., measurements of contact angle and capillary rise, or qualitative, e.g., the immersion of fine particles in a liquid and the spreading of a liquid over a solid surface. The quantitative manifestations can be used as wetting parameters to characterize the wetting phenomena. The wetting between a liquid and a solid is opposed by the cohesive forces among the molecules of the liquid and facilitated by the adhesive forces between the molecules of the liquid and the molecules on the surface of the solid.

The contact angle, θ, can be related to surface tensions

by Young's equation,[50]

$$\gamma^{SV} = \gamma^{SL} + \gamma^{LV} \cdot \cos\theta \qquad (2\text{-}1)$$

where γ^{SV}, γ^{SL}, and γ^{LV} are the surface tensions of the solid-vapor interface, the solid-liquid interface, and the liquid-vapor interface, respectively.

As a thermodynamic quantity, the contact angle is expected to have a unique value for any particular system. Different contact angles are obtained, however, depending on whether a liquid drop in contact with a solid tends to advance or recede; this phenomenon is usually referred to as wetting hysteresis. The maximum and minimum stable contact angles are called the advancing and receding contact angles, respectively. It is not clear which, if either, of the two contact angles represents the true equilibrium value.[50] According to Berg, the most useful contact angle to describe wetting behavior is the static advancing contact angle.[51] Contact angles reported in the literature, if not specified, represent static advancing contact angles.

The origins of wetting hysteresis are still controversial.[50] According to Johnson and Dettre,[52] hysteresis is always present. They attribute contact angle hysteresis to the existence of many thermodynamic metastable states at the three-phase (solid/liquid/vapor) boundary. The energy barriers between these metastable states are larger than kT. While the thermodynamic arguments for hysteresis effects are

very convincing, the molecular mechanism for contact angle hysteresis has yet to be clarified. The most prevalent explanations for contact angle hysteresis are surface roughness and heterogeneity.[52,53] The advancing and receding contact angles are believed to be associated with regions of low wettability and regions of high wettability, respectively.[52]

Wetting processes can be classified into three categories, adhesional wetting, immersional wetting, and spreading wetting, as shown in Figure 2-2.[53] In adhesional wetting, a liquid-vapor interface and a solid-vapor interface are replaced by a solid-liquid interface, involving the following free energy change

$$\Delta G = (\gamma^{SL} - \gamma^{SV} - \gamma^{LV}) \cdot A \qquad (2\text{-}2)$$

if every interface involved has an area of A. In immersional wetting, a solid-vapor interface is replaced by a solid-liquid interface, involving the free energy change

$$\Delta G = (\gamma^{SL} - \gamma^{SV}) \cdot A \qquad (2\text{-}3)$$

In spreading wetting, a solid-vapor interface is replaced by a liquid-vapor interface and a solid-liquid interface, involving the free energy change

$$\Delta G = (\gamma^{SL} + \gamma^{LV} - \gamma^{SV}) \cdot A \qquad (2\text{-}4)$$

Substituting Young's equation into equations 2-2, 2-3, and 2-4 results in equations 2-5, 2-6, and 2-7

$$\Delta G = - A \cdot \gamma^{LV} \cdot (\cos\theta + 1) \qquad (2\text{-}5)$$

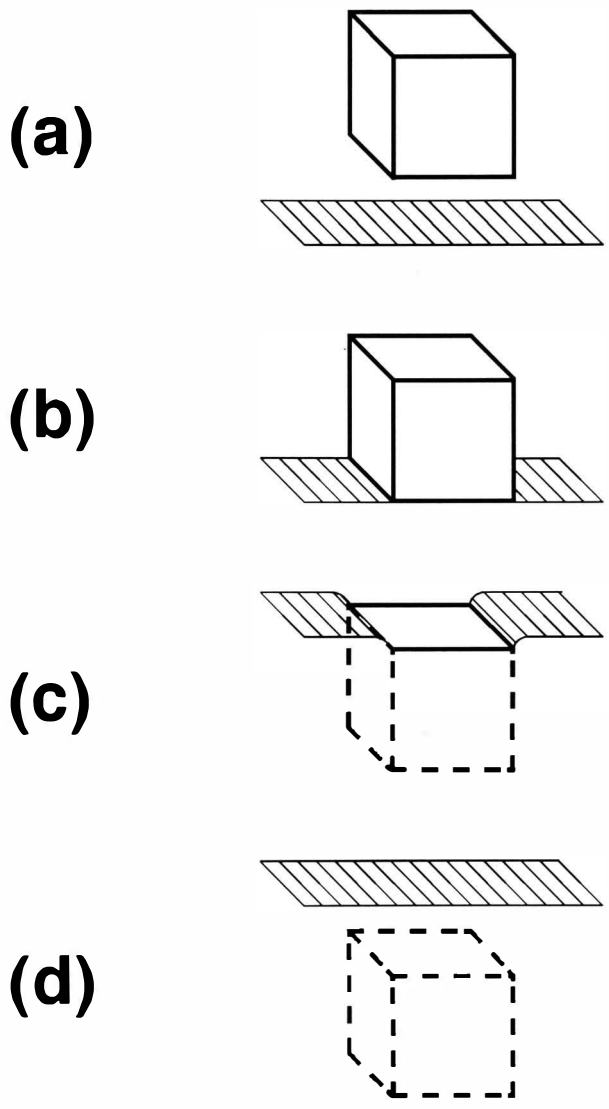

Figure 2-2. Adhesional (a → b), immersional (b → c), and spreading (c → d) wetting.

$$\Delta G = - A \cdot \gamma^{LV} \cdot \cos\theta \qquad (2\text{-}6)$$

$$\Delta G = - A \cdot \gamma^{LV} \cdot (\cos\theta - 1) \qquad (2\text{-}7)$$

ΔG must be negative for a wetting process to occur spontaneously. This requires the contact angle to be less than 180°, less than 90°, and 0° for spontaneous adhesional wetting, spontaneous immersional wetting, and spontaneous spreading wetting, respectively.

A wetting process can also be described by capillary rise. The penetration of a liquid into a capillary is determined by the pressure difference across the curved surface of a meniscus, ΔP, which can be estimated from the surface tension of the liquid, γ^{LV}, the contact angle, θ, and the radius of the capillary, r,

$$\Delta P = 2\gamma^{LV} \cdot \cos\theta / r \qquad (2\text{-}8)$$

The contact angle is required to be less than 90° for spontaneous penetration of the liquid into the capillary.

The state of wetting can be classified into three stages according to the magnitude of the contact angle. Usually, complete wetting means a contact angle of zero between the liquid and the solid, with spontaneous spreading of the liquid over the solid surface.[54] Nonwetting is used when the contact angle is larger than 90°.[55] The situation in between can be described by the term partial wetting.[51]

2-4 Wetting and Related Behavior of Alkylsilylated Silica

The surface of alkylsilylated silica is composed of bonded alkyl chains and residual silanol groups. Wetting of octadecylsilylated silica is influenced by chain-chain interactions, chain-eluent interactions, and residual silanol-eluent interactions.[56,57] The macroscopic wetting phenomenon, i.e., the contact angle, however, has not been well correlated with interactions on a molecular level or the nanoscopic structure at the mobile phase/stationary phase boundary.[58]

Behavior of alkylsilylated silica in water-rich eluents. In water-rich eluents, abnormal chromatographic behavior is often observed.[59-66] A very long time is required to bring a column to equilibrium if water alone is used as the eluent.[59,60,64] With water as the eluent, a plot of column equilibration time versus C_{18} bonding density shows a maximum at bonding density of about 2.9 $\mu mol/m^2$.[64] The addition of 3% 1-propanol in water significantly reduces column equilibration time.[64] The sorption capacity of a C_{18} column with water as the eluent decreases with time, but can be restored by washing with MeOH.[65] Conventional retention models can not predict retention in water-rich eluents.[61,62] In mobile phases with less than 10% MeOH or ACN, the increase in the retention of non-polar compounds with decreasing organic modifier content is much less than expected.[66] Retention may even decrease with

decreasing organic modifier content in water-rich eluents.[59,62,63] If changes in the stationary phase with changing eluent are considered in the retention model, the prediction is much better.[62,67] In addition, column efficiency decreases in water-rich eluents.[68] All of these phenomena are presumed to reflect the state of wetting of the stationary phase.

When the organic modifier content in the eluent is lower than a certain value, preequilibration of the column with organic modifier leads to a longer retention time than preequilibration with water.[69] This indicates that the stationary phase may exist in different states even when in contact with the same eluent. Gilpin et al. observed that with pure water as the eluent, a bonded phase may exist in a different state after heating.[56,70,71] Even the rate of cooling after heating may affect the properties of bonded phases.[72]

Wetting studies for alkyl bonded phases. The wettability of a bonded phase can be tested by titrating its suspension in an organic solvent[73] or in water[57,60] using water or an organic solvent as the titrant, respectively. About 50% of water was needed to bring a persistent film of alkyl bonded phase particles to the surface of a bonded phase suspension in MeOH.[73] About 60% (v/v) MeOH was required to wet bonded phases used extensively in RPLC.[57,60] Less organic modifier was required to wet a bonded phase with a lower surface coverage

of alkyl groups.[57,73]

Contact angles on bonded phases can be calculated from the capillary rise in alkyl bonded glass capillaries.[74,75] Contact angles in the range from 15° to 70° were obtained using ACN, MeOH, ethanol, and their aqueous mixtures with less than 50% of water as the wetting agent. Contact angles can also be calculated from solvent migration rates on reversed-phase thin layer chromatographic plates.[75]

Park and Kim conducted a thorough study on the wetting of monomeric C_1, C_4, C_8, and C_{18} phases on borosilicate glass surfaces in MeOH-water mixtures by measuring advancing contact angles.[76] The contact angle increases with increasing bonding density and increasing percentage of water. With increasing chain length, the contact angle first decreases, then increases. The minimum contact angle value was observed for the C_8 or C_4 phase, depending on the bonding density. The rigidity and hydrophobicity of the methyl groups on the surface of the C_1 phase are considered the reasons for the high contact angle for the C_1 phase. With intermediate chain lengths, the alkyl chains are more mobile and disordered, exposing many methylene groups to the surface. It is well known that surfaces composed of methylene groups have a higher critical surface tension, i.e., are less hydrophobic, than surfaces formed by methyl groups.[52] For surfaces bonded with C_{18} chains, due to the higher degree of van der Waals

interactions among the chains, the chains are well packed and only the methyl groups are exposed to the overlaying liquid, leading to higher contact angles. Contact angles for all the C_4 and C_8 surfaces, in the whole composition range, are less than 90°. In water, contact angles are more than 90° for the C_1 and C_{18} surfaces with the highest bonding density.

For polymeric phases, the situation is obviously different. Wasserman et al.[77] observed that for C_1, C_2, and C_3 phases, the water contact angle is less than 90°. For phases from C_6 to C_{18}, the water contact angle is around 110° and is not affected by chain length.

Schwartz et al.[78] synthesized bonded C_{18} layers by reacting octadecyltrichlorosilane with steam treated mica surfaces. The water contact angle obviously increases with the surface coverage. The surface with a complete coverage has a water contact angle of 112°.

Montgomery et al. observed that octadecyl derivatized silica plates are not wetted by pure water, and show a contact angle of 93°.[79] Aqueous eluents with 20% of MeOH or 5% 1-propanol have contact angles of 65° and 69°, respectively.

Correlation between wetting and the other properties of alkyl bonded phases. Wetting can be ultimately traced to interactions on the molecular level. Therefore, it is important to correlate wetting with the microscopic manifestations of molecular interactions, e.g., mobility,

orientation, and conformation of bonded alkyl chains and orderness of bonded alkyl layer. For alkyl bonded surfaces, a more closely packed and more ordered layer usually indicates a surface of lower surface tension and larger contact angle.[80,81] Using a fluorescence probe, Montgomery el al.[79,82-84] were able to determine the orientational distributions of C_{18} chains bonded on a silica plate. In water, on average, the chains tilt away from the surface normal at an angle of about 80°.[82] With the addition of 20% MeOH or 5% 1-propanol, the chains tilt about 70° from the surface normal. With the introduction of a submonolayer amount of heptanol, octanol, or decanol into the C_{18} layer, the average tilt angle is a little more than 50°. In addition, the orientational distribution is narrower with the introduction of the long-chain alcohols. The tilt angle decreases with the chain length of alcohol. It was proposed that the addition of a small amount of short-chain alcohol may make the C_{18} phase partially wetted, but not solvated.[79] The long-chain alcohols are believed to interpenetrate into the C_{18} layer.[82] The addition of sodium dodecyl sulfate (SDS) in the mobile phase at the level of millimoles per liter also decreases the tilt angle to a little more than 50° and makes the orientational distribution narrower.[83,84] The tilt angle reaches a minimum at a SDS concentration just below the critical micelle concentration of 8.3 mM. It is believed that the chains from bonded C_{18} layer

and those from the adsorbed SDS layer interpenetrate one another.[83] Burbage and Wirth[85] studied the reorientation of a fluorophor, acridine orange, on a C_{18} layer bonded to a silica plate. Acridine orange is believed to sit at the C_{18}/solvent interface. The addition of a small amount of MeOH or propanol into water causes a broader out-of-plane orientational distribution, i.e., makes the interface rougher. Based on changes in NMR line shape, Gilpin and Gangoda[63] studied the mobility of alkyl chains bonded on silica by ^{13}C-labeling of the terminal methyl group. For a polymeric C_7 phase with a low bonding density (4.75% C), upon the addition of at least 1% dioxane in D_2O, the line from the terminal methyl group suddenly becomes sharp. For the phase with a medium coverage (6.47% C), the content of dioxane required to bring the change is 8%. The content of dioxane required is 2% and 25% for polymeric C_8 phases with a bonding density of 6.18% and 9.50% C, respectively. Obviously, upon the addition of a small amount of dioxane, the alkyl chains become more mobile. For monomeric C_8 and C_{10} phases, however, no sudden line-sharpening occurs upon the addition of dioxane.

A general knowledge about the structure, composition, and properties of solvated alkyl bonded silicas may be useful in studying the wetting process. Residual silanols usually account for over half of the total silanols before alkylsilylation[86] and prefer to interact with water over

organic modifier.[86,87] Organic modifier is enriched on alkyl bonded silica throughout the whole composition range, except at very low contents of water.[88] The amount of sorbed organic modifier at first rises rapidly with increasing organic modifier content, then increases much slower as the organic modifier content is higher than about 50% (v/v).[89,90] Molecular motion increases along the bonded alkyl chain moving outward from the surface and the methyl group at the unbound end is much more mobile than the other part of the chain.[91] The mobility of bonded alkyl chains decreases with increasing water content.[92] A predominantly ordered structure of a bonded C_{18} layer slightly lowers its degree of order after exposure to organic modifier.[93] The diffusion coefficient of a solute in a bonded C_{18} layer increases with increasing MeOH content.[94] The polarity of C_{18} phases decreases with increasing MeOH content approximately in the range from 0% to 50%.[95,96] A fusion-like transition of bonded C_{18} layers is often observed around room temperature.[97,98] All of these are ultimately determined by molecular interactions among the stationary phase, the mobile phase, and the solute.

Chapter 3

Solvatochromic Studies of the Surface Polarity of Silica under Normal Phase Conditions

3-1 Introduction

It is obvious from the background chapter that although the surface chemistry of silica has been extensively investigated for a long period, there are still many controversies and ambiguities about the origin of the acidity, the molecular interactions between solutes and the silica surfaces, and the surface polarity of silica. In this chapter, the dipolarity and hydrogen-bonding ability of the surface of silica and solvent effects on them are studied. The results are explained based on molecular interactions between silanol groups, solvent molecules, and the solute.

Generally speaking, there are two strategies to study the surface chemistry of silica. One of them is direct characterization by NMR, IR, elemental analysis, thermogravimetric analysis, and pH measurements. The other strategy is indirect and based on the interactions between probe molecules and the surface. It includes adsorption methods, chromatographic methods, and IR, NMR, fluorescence, and UV-visible spectroscopy of probe molecules. Using the latter strategy, the information on molecular interactions allows for the prediction of the chromatographic retention of solutes, since the probes serve as models for chromatographic solutes.

The polarity of a medium can be probed using electronic

spectroscopy.[99-101] Among them, the solvatochromic comparison method developed by Kamlet and Taft[102-106] distinguishes itself from other techniques by quantitatively decomposing the molecular interactions of a medium with a solute into dipolarity-polarizability (π^*), hydrogen-bonding basicity (β), and hydrogen-bonding acidity (α). This method has been successfully applied to elucidate interactions between homogeneous media and solutes. It will be the main approach used to investigate the surface chemistry of silica in this research.

The electronic excitation energy of a molecule depends on the properties of the medium because the ground and excited states of the molecule have different electronic distributions. In other words, the properties of a medium can be deduced from the energy of electronic excitation of probe molecules. With right choices of probe molecules, the ability of the medium to participate by different types of interactions, i.e., dipolarity-polarizability, hydrogen-bonding acidity, and hydrogen-bonding basicity, can be measured. This is the basic idea of the solvatochromic comparison method.

The electronic excitation energies of certain dyes are strongly affected by dipolarity-polarizability of solvents, but seldom affected by hydrogen-bonding or any other specific interactions with solvents. The solvent dipolarity-

polarizability scale was established with these dyes.[102,103,106] 4-Nitroanisole, 2-nitroanisole, N,N-diethyl-3-nitroaniline, 4-methoxy-β-nitrostyrene, 1-ethyl-4-nitrobenzene, and N-methyl-2-nitroaniline are among the dyes used to establish the solvent dipolarity-polarizability scale.[106] The solvent dipolarity-polarizability scale is called the π^* scale because the electronic transition of the dyes is of the π to π^* type. The π^* value representing the dipolarity-polarizability of a solvent is calculated from the frequency at the absorption maximum of the π^* indicator dye in the solvent, ν_{max}, in kK (kilokayser, 1000 cm^{-1}), by equation 3-1,[106]

$$\pi^* = (\nu_{max} - \nu_0)/s \qquad (3\text{-}1)$$

where ν_0 is the frequency at the absorption maximum of the π^* dye in cyclohexane, which is assigned a π^* value of zero, and s is a normalization factor, obtained by setting the π^* value of dimethyl sulfoxide to one.

The establishment of the α-scale of solvent hydrogen-bonding acidities requires an α dye, the electronic transition energy of which is sensitive to the hydrogen-bonding acidity of a solvent, and a π^* dye, to cancel the contribution of dipolarity-polarizability of the solvent to the energy shift of the electronic transition of the α dye.[102,105,107] The structures of some α dyes, ET-30, 2,6-dichloro-4-(2,4,6-triphenyl-N-pyridinio)phenolate (ET-33),[108] and 2,4-dichloro-6-[2-(N-methyl-4-pyridinio)vinyl]phenolate (DCMPVP),[109] are shown

in Figure 3-1. The construction of the α-scale of solvent hydrogen-bonding acidities[102,105,107] can be explained diagrammatically, as shown in Figure 3-2. In solvents with no hydrogen-bonding acidity, a linear correlation between the ν_{max} for an α dye (DCMPVP) and the ν_{max} for a reference π^* dye (N,N-dimethyl-4-nitroaniline) is expected,

$$\nu_{max}(\alpha \text{ dye}) = a \cdot \nu_{max}(\pi^* \text{ dye}) + b \qquad (3\text{-}2)$$

where a is the slope, and b is the intercept. In a solvent with hydrogen-bonding acidity, the $\nu_{max}(\alpha$ dye) value will deviate from the straight line described by equation 3-2. The deviation, which is the difference between the observed $\nu_{max}(\alpha$ dye) value and the $\nu_{max}(\alpha$ dye) value calculated from equation 3-2, is used to calculate the α value of solvent hydrogen-bonding acidity,

$$\alpha = [\nu_{max}(\alpha \text{ dye})(\text{obsd}) - \nu_{max}(\alpha \text{ dye})(\text{calcd})]/c \qquad (3\text{-}3)$$

where c is a normalization factor obtained by setting the α value of MeOH to one.

The β-scale of solvent hydrogen-bonding basicities was constructed in a way similar to the α-scale.[102,104,110] Typical dye pairs for the measurement of the β value of solvent hydrogen-bonding basicity are 4-nitroaniline/N,N-diethyl-4-nitroaniline, 2-nitroaniline/N,N-dimethyl-2-nitroaniline, 2-nitro-p-toluidine/N,N-dimethyl-2-nitro-p-toluidine, 2-nitro-p-anisidine/N,N-dimethyl-2-nitro-p-anisidine, as shown in Figure 3-3. Hydrogen-bonding interactions between solvents and α or

ET-30

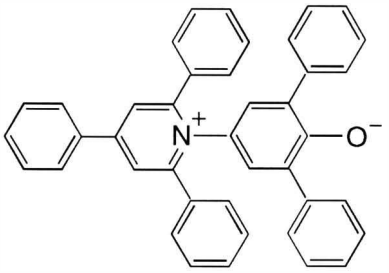

ET-33

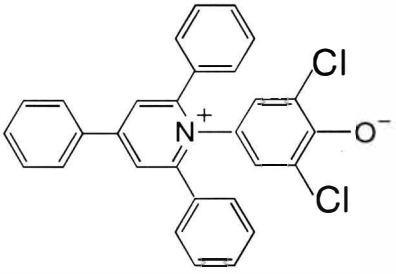

DCMPVP

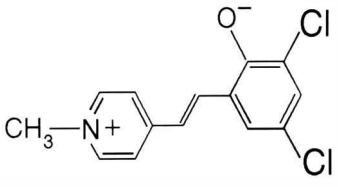

Figure 3-1. Structures of ET-30, ET-33, and DCMPVP.

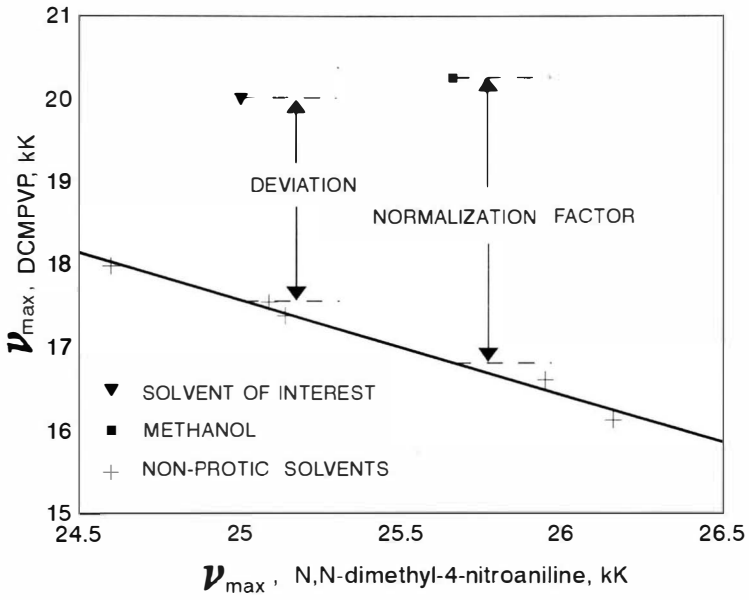

Figure 3-2. α-Scale of solvent hydrogen-bonding acidities.

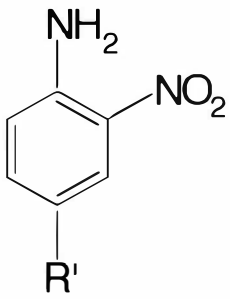

R'	Dye
H	2-Nitroaniline
Me	2-Nitro-p-toluidine
MeO	2-Nitro-p-anisidine

Figure 3-3. Structures of β dyes.

β dyes are illustrated in Figure 3-4. Equations 3-4 and 3-5 are used to obtain the β value of solvent hydrogen-bonding basicity,

$$\nu_{max}(\beta \text{ dye}) = a \cdot \nu_{max}(\pi^* \text{ dye}) + b \qquad (3\text{-}4)$$

$$\beta = [\nu_{max}(\beta \text{ dye})(\text{calcd}) - \nu_{max}(\beta \text{ dye})(\text{obsd})]/c \qquad (3\text{-}5)$$

where c is a normalization factor obtained by setting the β value of hexamethylphosphoramide to one.

The solvatochromic comparison method has been applied successfully to the characterization of various solvents. This method has also been applied to the characterization of dry solid surfaces, including silica,[111] silicalite and zeolites,[112,113] and alumina.[114] Recently, the solvatochromic parameters of silica in the presence of 1,2-dichloroethane or cyclohexane were also measured.[115] Solvatochromic parameters for a heterogeneous surface measured by different dyes were much less reproducible than for a homogeneous medium.[111] This was attributed to the more specific interactions between silica and dyes.[111] The solvatochromic parameters for a heterogeneous interface may be less reliable than the ones for a homogeneous medium in principle because specific interactions are more likely to exist between the heterogeneous interface and the probe. Technical difficulties, e.g., dye overloading[111,114] and large interferences from background absorption, may also affect the quality of the data.

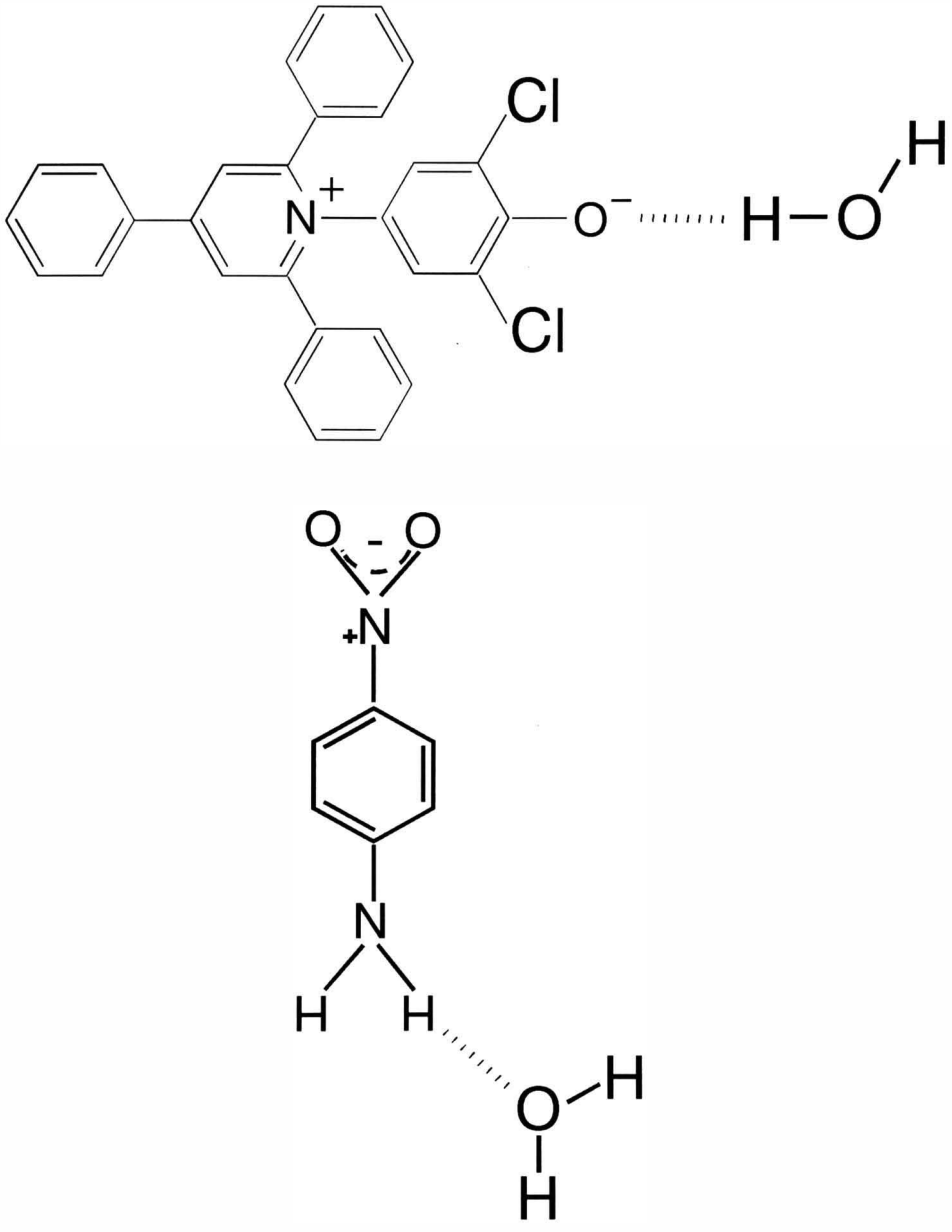

Figure 3-4. Hydrogen-bonding interactions between solvents (i.e., water) and α or β dyes.

The solvatochromic comparison method has been applied to the characterization of solvated bonded phases.[99,116] The π^* values of octadecylsilylated silica exposed to reversed-phase mobile phases are generally lower than the corresponding mobile phase values, but much higher than alkane values.[99,116] This is consistent with the generally held view that the stationary phases are solvated by mobile phases. The α values of solvated octadecylsilylated silica are higher than the corresponding mobile phase values.[116] This was explained by specific interactions between the α dye and residual surface silanol groups.[116]

In this research, the solvatochromic comparison method is used to characterize the surface of silica in mixtures of *n*-hexane and a polar solvent. The α, β, and π^* values of the surface of silica are calculated from electronic spectral data of dyes on the surface. These values can be used to predict chromatographic retention of various solutes. The effects of solvent composition and the nature of the polar solvent on the surface properties of silica are studied. This method, developed for silica in mixtures of *n*-hexane and a polar solvent, may also be useful for characterization of other solid-liquid interfaces.

3-2 Experimental

3-2-1 Materials and Chemicals

LiChrosorb SI 100 (30 μm, 100 Å pores) was purchased from E. Merck (Darmstadt, Germany). Molecular sieves 3Å, obtained from Aldrich (Milwaukee, WI, USA), were pretreated at 220 ± 5 °C for more than 48 hours before use, except when specified otherwise.

2-Nitroaniline, 4-nitroaniline, and 4-nitroanisole were supplied by Aldrich (Milwaukee, WI, USA). N,N-Dimethyl-4-nitroaniline, N,N-diethyl-4-nitroaniline, N-methyl-2-nitroaniline, and ET-33 were obtained from Kodak (Rochester, NY, USA), Frinton Laboratories (Vineland, NJ, USA), Lancaster Synthesis Ltd (White Lund, Morecambe, England), and Lambda (Graz, Austria), respectively. DCMPVP was synthesized and purified in our laboratory.[109]

All solvents were HPLC or spectrophotometric grade.

3-2-2 Acquisition of Electronic Spectral Data

All electronic absorption spectra were obtained on a Shimadzu UV-265 spectrophotometer equipped with an integrating sphere attachment. A diagram of the quartz flow cell used for these measurements is shown in Figure 3-5. There is

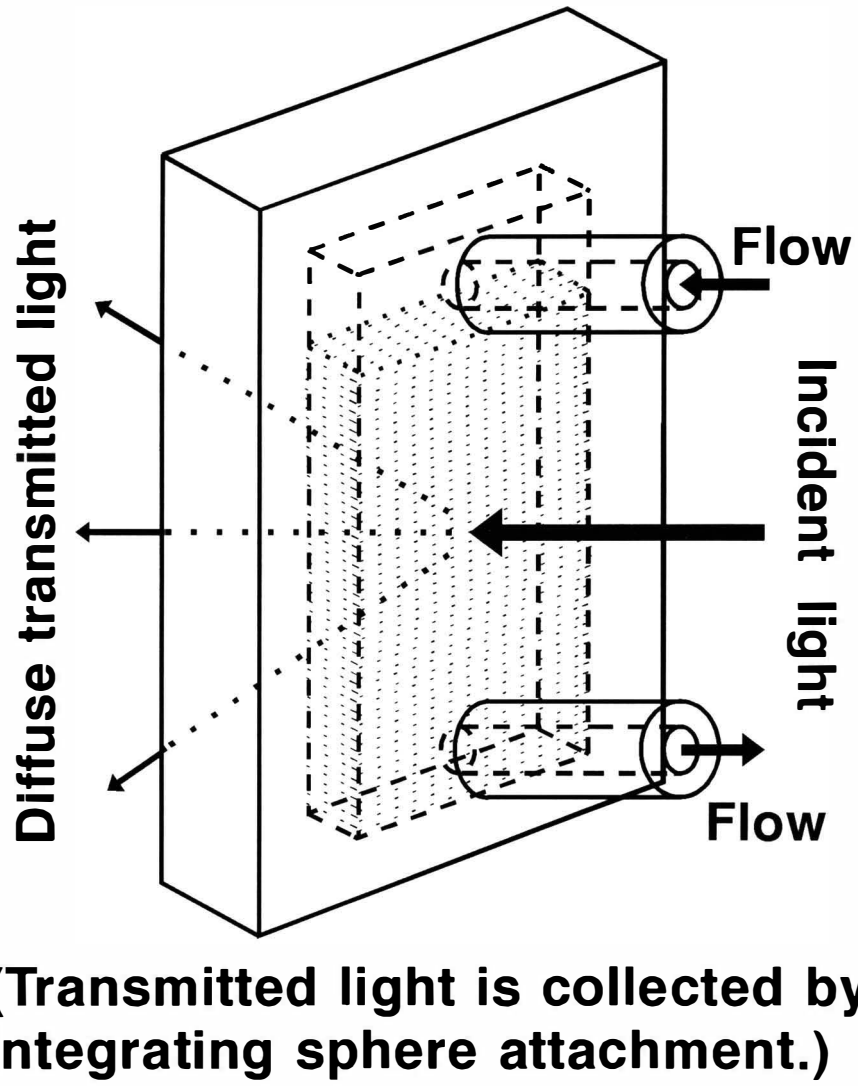

Figure 3-5. Diagram of flow cell used for solvatochromic measurements.

considerable transmittance of light through silica and chemically modified silica wetted by solvents. The transmitted light is highly diffuse, so the integrating sphere attachment used in the transmittance mode was adopted for the measurement of spectra of dyes on the surface of silica in the presence of a mobile phase. The slit width was set to give a bandpass of 5 nm. A flow cell with a 1 mm path length was packed with the stationary phase of interest. For conditions where the retention of the dye was not very large, a solution of the dye in the selected mobile phase with an appropriate concentration was passed through the flow cell until the spectrum did not change with time. If the retention of the dye on a stationary phase in the selected mobile phase was very large, a solution of the dye in a mobile phase with an appropriate elution strength was passed through the flow cell until the dye was uniformly distributed on the stationary phase throughout the flow cell. Then the flow cell was equilibrated with the mobile phase of interest, and the spectrum was measured. The spectra of the background contributions were measured with the silica-filled flow cell equilibrated with the appropriate mobile phases and were subtracted from the spectra with dyes in the flow cell to obtain the spectra of the dyes. Solvents were dried over molecular sieves for more than 24 hours, except for the measurements of π^* values for mixtures of *n*-hexane and

chloroform. A drying tube filled with silica was installed on the top of the solvent or solution reservoir during the process of equilibrating the silica in the flow cell with the dye solution or mobile phase. This reduced the amount of moisture absorbed by the solvents.

Solution spectra of the dyes were obtained in the transmittance mode without the integrating sphere attachment. In this case, 10 mm path length cuvettes were used, and the slit width was set to give a bandpass of 2 nm.

The dye spectra were smoothed by a quadratic polynomial smoothing program.[117] The wavelength of maximum absorbance, λ_{max}, was obtained from the first derivative of each spectrum with the assistance of linear regression analysis to determine the point at which the derivative was zero.

All measurements for the solvatochromic parameters of silica were repeated several times. But only the highest value, not the average, for each solvatochromic parameter is reported because trace amounts of water in the mobile phases always lowered the measured π^*, α, and β values. The care taken above can not guarantee the complete elimination of the systematic error caused by trace amounts of water, but the results described here give an estimate for the lower bound for the solvatochromic parameters of the silica surface.

3-2-3 Interference from the Dye in the Mobile Phase

In a flow cell packed with silica particles, the light path in Beer's law is decreased by the occupation of some of the space by silica. However, the light path is increased by reflection and refraction of light by silica. When there is no retention on the silica surface, the pathlength correction factor, K, is the ratio of the absorbance of a dye solution in the flow cell in the presence of silica over the absorbance in the absence of silica. A K value of 0.91 was determined, so the net pathlength through the solution is decreased by 9% in the presence of silica particles.

The mobile phase interference is estimated as shown in Figure 3-6. Spectrum 1, $A_1(\lambda)$, is from a dye solution with the mobile phase of interest as the solvent in the absence of silica (molar concentration C_1; pathlength b_1). A dye solution with a molar concentration of C_2 was kept flowing through a flow cell (pathlength b_2) packed with silica until an equilibrium was reached. Spectrum 2, $A_2(\lambda)$, including contributions both from the dye in the mobile phase (spectrum 3, $A_3(\lambda)$) and from the dye retained on the surface of silica (spectrum 4, $A_4(\lambda)$), was obtained. At equilibrium the dye concentration in the mobile phase is C_2. Therefore,

$$A_3(\lambda) = K \cdot A_1(\lambda) \cdot (b_2 \cdot C_2) / (b_1 \cdot C_1) \qquad (3\text{-}6)$$

The spectrum of the dye retained on the surface of

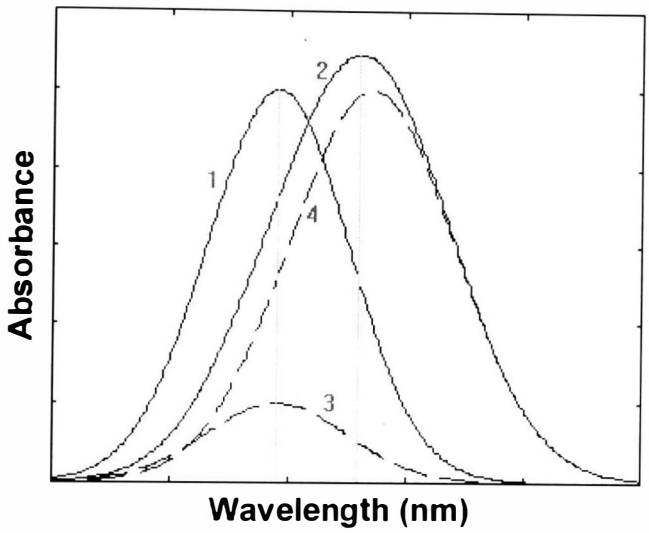

Figure 3-6. Spectra from a dye solution with the mobile phase as the solvent (1) and from the dye in the flow cell (in the mobile phase and adsorbed on silica) (2), which is composed of spectra 3 (in the mobile phase) and 4 (adsorbed on silica).

silica, $A_4(\lambda)$, is the difference between $A_2(\lambda)$ and $A_3(\lambda)$,

$$A_4(\lambda) = A_2(\lambda) - K \cdot A_1(\lambda) \cdot (b_2 \cdot C_2)/(b_1 \cdot C_1) \quad (3\text{-}7)$$

The absorbance maxima of spectra 1 to 4 is at the wavelengths of λ_{max1}, λ_{max2}, λ_{max3}, and λ_{max4}, respectively. The absorbance contribution from the dye in the mobile phase at λ_{max2} can be obtained by substituting $A_1(\lambda_{max2})$ into equation 3-6. The ratio of the amount of the dye adsorbed on the silica surface to the amount of the dye present in the mobile phase, i.e., the capacity factor k', approximately equals to the ratio of $A_4(\lambda_{max4})$ to $A_3(\lambda_{max3})$. When the contribution from the mobile phase is small, $A_4(\lambda_{max4})$ approximately equals to the difference between $A_2(\lambda_{max2})$ and $A_3(\lambda_{max2})$. Therefore,

$$k' = [A_2(\lambda_{max2}) - A_3(\lambda_{max2})]/A_3(\lambda_{max3}) \quad (3\text{-}8)$$

where $A_3(\lambda_{max2})$ and $A_3(\lambda_{max3})$ can be obtained from equation 3-6.

3-2-4 Chromatographic Measurements

Measurements of the retention of dyes on LiChrosorb SI 100 were performed on a Hewlett-Packard 1050 series liquid chromatograph, fitted with a quaternary pump, an autosampler, and a variable wavelength detector. A 100 x 4.6 mm column was filled with LiChrosorb SI 100 by dry-packing. Solvents were dried over molecular sieves for more than 24 hours. Drying tubes filled with silica were installed on the top of the solvent reservoirs.

3-3 Results

3-3-1 π^* Values for Mixtures of *n*-Hexane and Chloroform

The dyes used for measuring π^* values for mixtures of *n*-hexane and chloroform are 4-nitroaniline (**1**), 2-nitroaniline (**2**) and N,N-dimethyl-4-nitroaniline (**3**). 4-Nitroaniline and 2-nitroaniline can be used to measure π^* values of solvents that have negligible hydrogen-bonding basicity. The electronic spectra of these probes in mixtures of *n*-hexane and chloroform were obtained. These solutions were not subjected to any special precautions to minimize the water content. The ν_0 and s values for the calculation of π^* values are from reference 106. The ν_{max} values for the three dyes, and the π^* values from each of the three dyes are listed in Table 3-1.

The π^* values of these solvents were not affected by drying. The π^* values of dried *n*-hexane probed by 4-nitroaniline, 2-nitroaniline and N,N-dimethyl-4-nitroaniline were -0.085, -0.094, and -0.092, respectively. The π^* values of dried chloroform probed by 4-nitroaniline, 2-nitroaniline and N,N-dimethyl-4-nitroaniline were 0.706, 0.744, and 0.710, respectively.

Table 3-1. ν_{max} values (in kK) of 4-nitroaniline (**1**) (ν_0 31.10 kK; s -3.138), 2-nitroaniline (**2**) (ν_0 26.55 kK; s -1.536) and N,N-dimethyl-4-nitroaniline (**3**) (ν_0 28.10 kK; s -3.436) in mixtures of *n*-hexane and chloroform and the calculated π^* values

% $CHCl_3$ (v/v)	0	2	5	10	20	30	50	70	100
ν (**1**)$_{max}$	31.41	31.29	31.09	30.83	30.38	30.05	29.60	29.25	28.87
$\pi^*_{(1)}$	-0.098	-0.060	0.002	0.087	0.231	0.335	0.477	0.590	0.711
ν (**2**)$_{max}$	26.71	26.65	26.53	26.40	26.18	26.00	25.75	25.59	25.41
$\pi^*_{(2)}$	-0.104	-0.067	0.012	0.098	0.242	0.357	0.523	0.626	0.740
ν (**3**)$_{max}$	28.39	28.18	27.93	27.60	27.14	26.77	26.31	25.91	25.56
$\pi^*_{(3)}$	-0.085	-0.022	0.049	0.145	0.278	0.386	0.521	0.638	0.739
$\pi^*_{(Aver.)}$	-0.10	-0.05	0.02	0.11	0.25	0.36	0.51	0.62	0.73

3-3-2 π^* Values for Silica in *n*-Hexane-Chloroform Mixtures

4-Nitroanisole (**4**), N-methyl-2-nitroaniline (**5**), N,N-dimethyl-4-nitroaniline (**3**) and N,N-diethyl-4-nitroaniline (**6**) were used to probe the dipolarity-polarizability of the silica surface. It was originally assumed that N-methyl-2-nitroaniline could be used as a π^* dye because of its intramolecular hydrogen-bonding interactions.[106] The ν_0 and s values are from reference 106. The ν_{max} values for these dyes and the π^* values from these dyes are listed in Table 3-2. From the data in Table 3-2 it can be concluded that the surface of silica has a very high dipolarity-polarizability.

Significantly lower and less reproducible π^* values for silica were obtained when the solvents were not dried.

The π^* values for silica in contact with mixtures of *n*-hexane and chloroform and the π^* values for the mixtures vs. the composition are plotted in Figure 3-7. It is obvious from Figure 3-7 that the dipolarity-polarizability of silica in contact with mixtures of *n*-hexane and chloroform is not affected by the composition of the mobile phase, but that the values obtained are somewhat dependent on the nature of the dye used as the probe molecule.

In chloroform, i.e., the case with the least retention on silica, the absorbance contribution from N,N-dimethyl-4-nitroaniline in the mobile phase, obtained as described in the

Table 3-2. ν_{max} values (in kK) of N,N-dimethyl-4-nitroaniline (**3**) (ν_0 28.10 kK; s -3.436), 4-nitroanisole (**4**) (ν_0 34.12 kK; s -2.343), N-methyl-2-nitroaniline (**5**) (ν_0 24.59 kK; s -1.593) and N,N-diethyl-4-nitroaniline (**6**) (ν_0 27.52 kK; s -3.182) on silica in mixtures of *n*-hexane and chloroform and the calculated π^* values

% $CHCl_3$ (v/v)	$\nu(4)_{max}$	$\pi^*_{(4)}$	$\nu(5)_{max}$	$\pi^*_{(5)}$	$\nu(3)_{max}$	$\pi^*_{(3)}$	$\nu(6)_{max}$	$\pi^*_{(6)}$
0	31.42	1.152	22.15	1.533	23.66	1.291	22.94	1.439
2	31.37	1.174	22.16	1.523	23.71	1.277	23.00	1.420
5	31.38	1.169	22.16	1.523	23.64	1.299	23.01	1.417
10	31.31	1.199	22.09	1.567			23.00	1.420
20	31.22	1.238			23.71	1.277	22.97	1.430
30	31.24	1.229			23.67	1.290	22.95	1.436
50	31.37	1.174			23.66	1.291	22.88	1.458
70	31.49	1.122			23.70	1.282	22.81	1.480
100					23.66	1.291	22.73	1.505
Average	31.35	1.182 ±0.039	22.14	1.537 ±0.021	23.68	1.287 ±0.008	22.92	1.445 ±0.030

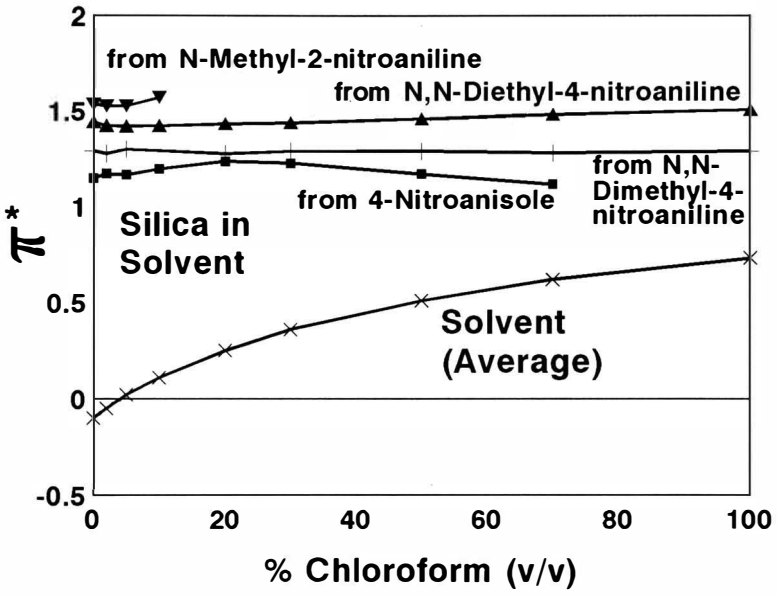

Figure 3-7. π^* values for silica in n-C_6H_{14}-$CHCl_3$ and π^* values for n-C_6H_{14}-$CHCl_3$.

experimental section, is 9.5%. However, from Figure 3-7 there is no evidence that the ν_{max} value is affected to any significant extent by dye present in the mobile phase, otherwise the line for N,N-dimethyl-4-nitroaniline would approach the curve for the solvent. The absorbance contributions from N,N-dimethyl-4-nitroaniline in the mobile phase with 70%, 50%, 30%, 20%, 10%, 5%, and 0% (v/v) of chloroform are 3.5%, 0.73%, 0.10%, 0.015%, 0.0086%, 0.00051%, and 0.00020%, respectively. In this section and the sections below, only the ν_{max} values which are not affected by the dye present in the mobile phase are listed and used to calculate the solvatochromic parameters for the surface of silica, except when specified otherwise. Chromatographic tests described later will give more information about the magnitude of the interference from the dyes present in the mobile phase.

3-3-3 Equations for α Measurements with ET-33 and DCMPVP as Probes

ET-33 (**7**) and DCMPVP (**8**), paired with N,N-dimethyl-4-nitroaniline (**3**) or 4-nitroanisole (**4**), were used to probe the hydrogen-bonding acidity of silica. The ν_{max} values of these dyes in various solvents with no hydrogen-bonding acidity and in MeOH are listed in Table 3-3.

In solvents with no hydrogen-bonding acidity, the ν_{max}

Table 3-3. ν_{max} values (in kK) of N,N-dimethyl-4-nitroaniline (**3**), 4-nitroanisole (**4**) (from reference 105), ET-33 (**7**), and DCMPVP (**8**) in various solvents with no hydrogen-bonding acidity and in MeOH

Solvent	$\nu(3)_{max}$	$\nu(4)_{max}$	$\nu(7)_{max}$	$\nu(8)_{max}$
Ethyl ether	27.10	33.45	14.10	
Ethyl acetate	26.16	32.79	15.92	16.13
THF	25.95	32.79	16.32	16.61
Dimethylacetamide	25.14	32.05	18.06	17.38
Dimethylformamide	25.09	32.05	18.37	17.54
Dimethyl sulfoxide	24.60	31.70	19.24	17.97
MeOH	25.66	32.79	22.59	20.26

values for the α dyes (ET-33 and DCMPVP) are expected to correlate linearly with the ν_{max} values for the π^* dyes. Correlations for dye pairs (**7**)/(**3**), (**7**)/(**4**), (**8**)/(**3**), and (**8**)/(**4**) are expressed by equations 3-9, 3-10, 3-11, and 3-12, respectively.

$$\nu(\mathbf{7})_{max} = (70.6 \pm 1.4) - (2.089 \pm 0.053)\nu(\mathbf{3})_{max}$$
$$(n = 6;\ r = -0.9987;\ SD = 0.11) \qquad (3\text{-}9)$$

$$\nu(\mathbf{7})_{max} = (111.6 \pm 4.1) - (2.91 \pm 0.13)\nu(\mathbf{4})_{max}$$
$$(n = 6;\ r = -0.9962;\ SD = 0.18) \qquad (3\text{-}10)$$

$$\nu(\mathbf{8})_{max} = (45.9 \pm 2.2) - (1.135 \pm 0.087)\nu(\mathbf{3})_{max}$$
$$(n = 5;\ r = -0.9913;\ SD = 0.11) \qquad (3\text{-}11)$$

$$\nu(\mathbf{8})_{max} = (64.6 \pm 6.8) - (1.47 \pm 0.21)\nu(\mathbf{4})_{max}$$
$$(n = 6;\ r = -0.9987;\ SD = 0.21) \qquad (3\text{-}12)$$

Equations 3-13, 3-14, 3-15, and 3-16, obtained using the method described in the introduction section, are used for dye pairs (**7**)/(**3**), (**7**)/(**4**), (**8**)/(**3**), and (**8**)/(**4**), respectively, to calculate α values.

$$\alpha_{(7)/(3)} = [\nu(\mathbf{7})_{max}(obsd) - \nu(\mathbf{7})_{max}(calcd)]/5.56 \qquad (3\text{-}13)$$

$$\alpha_{(7)/(4)} = [\nu(\mathbf{7})_{max}(obsd) - \nu(\mathbf{7})_{max}(calcd)]/6.52 \qquad (3\text{-}14)$$

$$\alpha_{(8)/(3)} = [\nu(\mathbf{8})_{max}(obsd) - \nu(\mathbf{8})_{max}(calcd)]/3.44 \qquad (3\text{-}15)$$

$$\alpha_{(8)/(4)} = [\nu(\mathbf{8})_{max}(obsd) - \nu(\mathbf{8})_{max}(calcd)]/3.90 \qquad (3\text{-}16)$$

3-3-4 α Values for Silica in *n*-Hexane-Chloroform Mixtures

The ν_{max} values for ET-33 and DCMPVP on silica in mixtures

of *n*-hexane and chloroform and the corresponding α values are listed in Table 3-4. In calculating the α values, $\nu(\mathbf{3})_{max}$ in equations 3-9 and 3-11 and $\nu(\mathbf{4})_{max}$ in equations 3-10 and 3-12 are taken as 23.68 and 31.35, respectively, which are the average ν_{max} values for N,N-dimethyl-4-nitroaniline and 4-nitroanisole on silica in mixtures of *n*-hexane and chloroform (Table 3-2). From the data in Table 3-4 it can be concluded that the surface of silica has a moderate to high hydrogen-bonding acidity, which does not depend on the composition of the overlying solvent.

3-3-5 Equations for β Measurements with 4-Nitroaniline and 2-Nitroaniline as Probes

4-Nitroaniline (**1**), paired with N,N-diethyl-4-nitroaniline (**6**) or N,N-dimethyl-4-nitroaniline (**3**), and 2-nitroaniline (**2**), paired with N-methyl-2-nitroaniline (**5**), are used to probe the hydrogen-bonding basicity of silica. The ν_{max} values of these dyes in solvents with no hydrogen-bonding basicity and hexamethylphosphoramide are listed in Table 3-5.

In media with no hydrogen-bonding basicity, the ν_{max} values for a β dye are expected to correlate linearly with the ν_{max} values of the corresponding π^* dye. Correlations for dye pairs (**1**)/(**6**), (**1**)/(**3**) and (**2**)/(**5**) are expressed by equations 3-17, 3-18, and 3-19, respectively.

Table 3-4. ν_{max} values of ET-33 (**7**) and DCMPVP (8) on silica in mixtures of *n*-hexane and chloroform and the calculated α values with N,N-dimethyl-4-nitroaniline (**3**) or 4-nitroanisole (**4**) as the reference π^* dyes

% $CHCl_3$ (v/v)		0	10	100	Average
ET-33	ν_{max} (kK)	22.87	22.67	22.71	22.75
	$\alpha_{(7)/(3)}$	0.306	0.270	0.277	0.284±0.019
	$\alpha_{(7)/(4)}$	0.399	0.368	0.374	0.380±0.016
DCMPVP	ν_{max} (kK)	22.28	22.36	22.34	22.33
	$\alpha_{(8)/(3)}$	0.934	0.958	0.951	0.948±0.012
	$\alpha_{(8)/(4)}$	0.975	0.996	0.991	0.987±0.011

Table 3-5. ν_{max} values (in kK) of 4-nitroaniline (**1**), N,N-diethyl-4-nitroaniline (**6**), N,N-dimethyl-4-nitroaniline (**3**), 2-nitroaniline (**2**) and N-methyl-2-nitroaniline (**5**) in various solvents with no hydrogen-bonding basicity and in hexamethylphosphoramide

Solvent	$\nu(\mathbf{1})_{max}$	$\nu(\mathbf{6})_{max}$	$\nu(\mathbf{3})_{max}$	$\nu(\mathbf{2})_{max}$	$\nu(\mathbf{5})_{max}$
n-Hexane	31.37	27.96	28.42	26.70	24.70
Cyclohexane	31.11	27.65	28.18	26.53	24.57
Carbon tetrachloride	30.49	26.92	27.38	26.18	24.20
Trichloroethylene	29.52	25.90	26.26	25.75	23.79
Chloroform	28.89	25.22	25.66	25.41	23.31
Methylene chloride	28.55	25.11	25.52	25.34	23.30
1,2-Dichloroethane	28.47	25.14	25.54	25.29	23.35
Hexamethylphosphoramide	25.53	24.93	25.18	24.09	23.20

$$\nu(\mathbf{1})_{max} = (0.986 \pm 0.044)\nu(\mathbf{6})_{max} + (3.9 \pm 1.2)$$
$$(n = 7;\ r = 0.9950;\ SD = 0.13) \qquad (3\text{-}17)$$

$$\nu(\mathbf{1})_{max} = (0.956 \pm 0.045)\nu(\mathbf{3})_{max} + (4.3 \pm 1.2)$$
$$(n = 7;\ r = 0.9944;\ SD = 0.14) \qquad (3\text{-}18)$$

$$\nu(\mathbf{2})_{max} = (0.964 \pm 0.038)\nu(\mathbf{5})_{max} + (2.85 \pm 0.91)$$
$$(n = 7;\ r = 0.9961;\ SD = 0.06) \qquad (3\text{-}19)$$

Equations 3-20, 3-21, and 3-22, obtained using the method described in the introduction section, are used for dye pairs (**1**)/(**6**), (**1**)/(**3**) and (**2**)/(**5**), respectively, to calculate β values.

$$\beta_{(1)/(6)} = [\nu(\mathbf{1})_{max}(calcd) - \nu(\mathbf{1})_{max}(obsd)]/2.92 \qquad (3\text{-}20)$$

$$\beta_{(1)/(3)} = [\nu(\mathbf{1})_{max}(calcd) - \nu(\mathbf{1})_{max}(obsd)]/2.78 \qquad (3\text{-}21)$$

$$\beta_{(2)/(5)} = [\nu(\mathbf{2})_{max}(calcd) - \nu(\mathbf{2})_{max}(obsd)]/1.13 \qquad (3\text{-}22)$$

The equations for dye pair (**1**)/(**6**) are slightly different from the ones reported by Kamlet and Taft[104] and Krygowski et al.[118] As pointed out by Krygowski et al.,[118] two solvents with slight hydrogen-bonding basicity, toluene and benzene, were included to build the correlation between $\nu(\mathbf{1})_{max}$ and $\nu(\mathbf{6})_{max}$ in the equations reported by Kamlet and Taft.[104] The correlation reported by Krygowski et al.[118] has a higher precision, and no solvents with hydrogen-bonding basicity were used to build the correlation. But the $\nu(\mathbf{1})_{max}$ and $\nu(\mathbf{6})_{max}$ values reported by Krygowski et al.[118] are always lower than our values. The reason for this is not clear. For consistency, equations 3-17 and 3-20 are used to calculate β values here.

3-3-6 β Values for Silica in *n*-Hexane-Chloroform Mixtures

The ν_{max} values for 4-nitroaniline and 2-nitroaniline on silica in mixtures of *n*-hexane and chloroform and the corresponding β values are listed in Table 3-6. In calculating β values, $\nu(\mathbf{6})_{max}$, $\nu(\mathbf{3})_{max}$ and $\nu(\mathbf{5})_{max}$ in equations 3-17, 3-18, and 3-19 are taken as 22.92, 23.68 and 22.14, respectively, which are the average ν_{max} values for N,N-diethyl-4-nitroaniline, N,N-dimethyl-4-nitroaniline and N-methyl-2-nitroaniline on silica in mixtures of *n*-hexane and chloroform (Table 3-2). From the data in Table 3-6 it can be concluded that the surface of silica has a low to moderate hydrogen-bonding basicity. The β value for silica vs. the composition of the mobile phase is plotted in Figure 3-8.

3-3-7 Dye Retention on Silica in *n*-Hexane-Chloroform Mixtures

Chromatographic tests were carried out to estimate the extent of the interference from the dyes present in the mobile phase on the measurements of the surface solvatochromic parameters. The solvent peak was used as the dead volume marker. The capacity factors for all the π^* and β dyes used in this research are listed in Table 3-7. The retention values for the α dyes used in this research were not measured because they have very strong retention even in ACN, which is

Table 3-6. ν_{max} values (in kK) of 4-nitroaniline (**1**) and 2-nitroaniline (**2**) on silica in mixtures of *n*-hexane and chloroform and the calculated β values with N,N-dimethyl-4-nitroaniline (**3**), N-methyl-2-nitroaniline (**5**), or N,N-diethyl-4-nitroaniline (**6**) as the reference π^* dyes

% $CHCl_3$ (v/v)	0	2	5	10	20	30	50	70	100
ν (**1**)$_{max}$	25.45	25.47		25.61	26.12	26.12	26.22	26.30	26.68
$\beta_{(1)/(6)}$	0.349	0.342		0.295	0.120	0.120	0.086	0.058	-0.072
$\beta_{(1)/(3)}$	0.514	0.507		0.457	0.273	0.273	0.237	0.209	0.072
ν (**2**)$_{max}$	24.06	24.06	24.07	24.09	24.14	24.15	24.28		
$\beta_{(2)/(5)}$	0.124	0.124	0.115	0.097	0.053	0.044	-0.071		

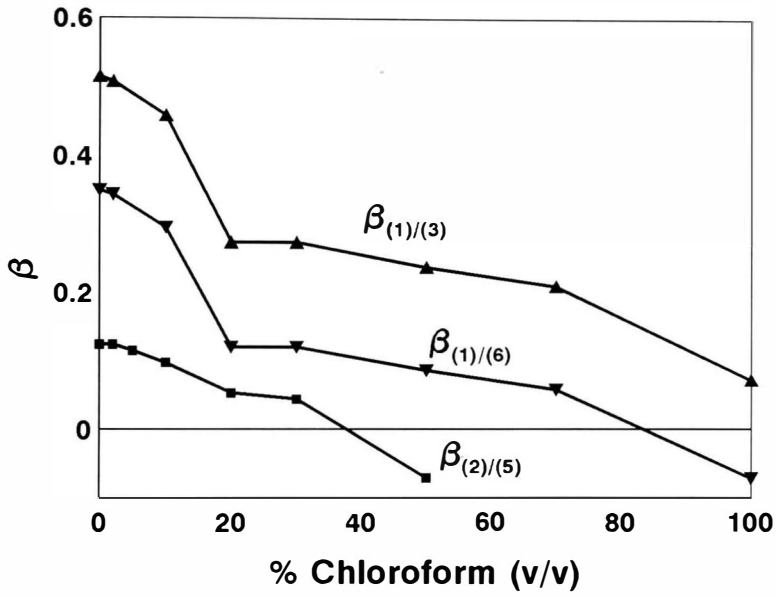

Figure 3-8. β values for silica in n-C_6H_{14}-$CHCl_3$ mixtures.

Table 3-7. Capacity factors for various π^* and β dyes on silica in *n*-hexane-chloroform mixtures

% $CHCl_3$ (v/v)	100	70	50	30	20	10
N-Methyl-2-nitroaniline	2.0	3.7	6.9	15.3	23.9	46.6
4-Nitroanisole	1.5	3.1	6.4	15.4	26.7	56.3
N,N-Dimethyl-4-nitroaniline	5.6	11.1	23.0	56.2	107	
N,N-Diethyl-4-nitroaniline	6.4	14.3	26.8	69.7	121	
2-Nitroaniline	3.5	7.6	14.6	34.5	56.6	106
4-Nitroaniline	9.6	22.8	62.6	183		

a much stronger normal phase eluent than chloroform. From Table 3-7 it can be seen that N,N-dimethyl-4-nitroaniline, N,N-diethyl-4-nitroaniline, and 4-nitroaniline have relatively high retention over the entire composition range. For 2-nitroaniline with chloroform as the mobile phase, the absorbance contribution from the dye present in the mobile phase cannot be neglected. For N-methyl-2-nitroaniline and 4-nitroanisole in a mobile phase with more than 70% (v/v) of chloroform, the absorbance contribution from the dyes present in the mobile phase may be significant. The phase ratios and the degree of drying of the mobile phases in the flow cell tests and in the chromatographic tests may not be the same. Despite these differences, the chromatographic tests can give an estimate of the extent of interference from the dyes present in the mobile phase.

3-3-8 Dye Retention on Silica in *n*-Hexane-Ethyl Ether Mixtures

From preliminary spectrophotometric measurements it was observed that π^* dyes in mixtures of *n*-hexane and ethyl ether had a much lower retention on silica than in mixtures of *n*-hexane and chloroform. Dyes present in the mobile phase may strongly interfere the measurements of solvatochromic parameters for silica in the presence of *n*-hexane-ethyl ether mixtures. It is necessary to estimate the significance of

such interference before calculating solvatochromic parameters. The ratio of the amount of a dye adsorbed on the silica surface over the amount of the dye present in the mobile phase, i.e., the capacity factor, can be estimated from spectroscopic measurements, as described in the experimental section. The capacity factors for N,N-dimethyl-4-nitroaniline and N,N-diethyl-4-nitroaniline on silica in mixtures of *n*-hexane and ethyl ether are listed in Table 3-8. From Table 3-8 it can be seen that the amount of dyes present in the mobile phase starts to surpass that adsorbed on silica when the ethyl ether content in the mobile phase is larger than 10% (v/v).

3-3-9 π^* Values for Mixtures of *n*-Hexane and Ethyl Ether and for Silica in Mixtures of *n*-Hexane and Ethyl Ether

N,N-Dimethyl-4-nitroaniline (**3**) and N,N-diethyl-4-nitroaniline (**6**) were used to measure the π^* values for mixtures of *n*-hexane and ethyl ether and for silica in mixtures of *n*-hexane and ethyl ether. The ν_{max} values for the two π^* dyes in mixtures of n-hexane and ethyl ether and the corresponding π^* values for the mixtures are listed in Table 3-9. For the measurements of the π^* values for silica in mixtures of *n*-hexane and ethyl ether, the absorbance contribution from the dyes in the mobile phase was subtracted from the total spectra as described in the experimental

Table 3-8. Capacity factors for N,N-dimethyl-4-nitroaniline (**3**) and N,N-diethyl-4-nitroaniline (**6**) on silica in *n*-hexane-ethyl ether mixtures

% Ethyl ether (v/v)	$k'_{(3)}$	$k'_{(6)}$
100	0.213	0.068
80	0.346	0.069
60	0.413	0.124
40	0.862	0.219
20	1.78	0.588
10	3.23	1.20
8	3.25	1.42
6	4.09	1.77
4	5.10	3.08
3	6.26	3.87
2	9.51	5.21
1	23.0	15.0
0.5	58.2	43.0

Table 3-9. ν_{max} values (in kK) for N,N-dimethyl-4-nitroaniline (**3**) and N,N-diethyl-4-nitroaniline (**6**) in mixtures of *n*-hexane and ethyl ether and the corresponding π^* values for the mixtures

% Ethyl ether (v/v)	$\nu(\mathbf{3})_{max}$	$\pi^*_{(3)}$	$\nu(\mathbf{6})_{max}$	$\pi^*_{(6)}$	$\pi^*_{(Aver.)}$
0	28.43	-0.096	27.82	-0.094	-0.095
0.5	28.39	-0.084	27.79	-0.085	-0.085
1	28.35	-0.073	27.77	-0.079	-0.076
2	28.34	-0.070	27.75	-0.072	-0.071
3	28.33	-0.067	27.72	-0.063	-0.065
4	28.30	-0.058	27.63	-0.035	-0.047
6	28.28	-0.052	27.58	-0.019	-0.036
8	28.22	-0.035	27.59	-0.022	-0.029
10	28.21	-0.029	27.55	-0.009	-0.019
20	28.03	0.020	27.42	0.031	0.026
40	27.75	0.102	27.20	0.101	0.102
60	27.52	0.169	27.04	0.151	0.160
80	27.34	0.221	26.83	0.217	0.219
100	27.17	0.271	26.69	0.261	0.266

section. The subtracted spectrum represents only the dye adsorbed on the silica surface. The π^* values obtained from the subtracted spectra represent the dipolarity-polarizability of the silica surface. The ν_{max} values for these dyes from the total spectra and the subtracted spectra and the corresponding π^* values from these dyes are listed in Table 3-10. The ν_0 and s values are from reference 106. Spectral subtraction and the calculation of π^* values for the silica surface are only performed for systems containing up to 10% ethyl ether in the mobile phase. With more than 10% ethyl ether in the mobile phase, the capacity factors for the dyes are too low to allow accurate estimation of the π^* values for the silica surface.

The π^* values for silica in contact with mixtures of *n*-hexane and ethyl ether (after correction) and the π^* values for the mixtures vs. the ethyl ether content in the range of 0-10% (v/v) are plotted in Figure 3-9. It is obvious from Figure 3-9 that the dipolarity-polarizability of silica in contact with mixtures of *n*-hexane and ethyl ether decreases with the ethyl ether content in the mobile phase. It is also instructive to plot the π^* values before correction and those for the mixtures vs. the ethyl ether content in the whole composition range, as shown in Figure 3-10. The lines for silica before correction approach the solution line at high ethyl ether contents because of the low retention of dyes on silica.

Table 3-10. ν_{max} values (in kK) for N,N-dimethyl-4-nitroaniline (**3**) and N,N-diethyl-4-nitroaniline (**6**) on silica in mixtures of *n*-hexane and ethyl ether before and after correction for the mobile phase contribution and the corresponding π^* values

% Ethyl ether (v/v)	Before correction				After correction			
	$\nu(3)_{max}$	$\pi^*_{(3)}$	$\nu(6)_{max}$	$\pi^*_{(6)}$	$\nu(3)_{max}$	$\pi^*_{(3)}$	$\nu(6)_{max}$	$\pi^*_{(6)}$
0	23.50	1.339	23.18	1.367	23.50	1.339	23.18	1.367
0.5	23.82	1.246	23.57	1.241	23.82	1.246	23.57	1.241
1	24.11	1.161	23.90	1.138	24.11	1.161	23.90	1.138
2	24.86	0.943	24.56	0.930	24.86	0.943	24.56	0.930
3	25.40	0.786	25.00	0.792	25.33	0.806	24.91	0.820
4	25.69	0.701	25.69	0.575	25.63	0.719	25.18	0.735
6	26.10	0.582	26.50	0.321	25.87	0.649	25.42	0.660
8	26.57	0.445	26.62	0.283	25.95	0.626	25.54	0.622
10	27.01	0.320	26.74	0.245	26.16	0.565	25.55	0.619
20	27.15	0.276	26.92	0.189				
40	27.25	0.247	26.95	0.179				
60	27.17	0.271	26.87	0.204				
80	27.12	0.285	26.77	0.236				
100	27.04	0.308	26.60	0.289				

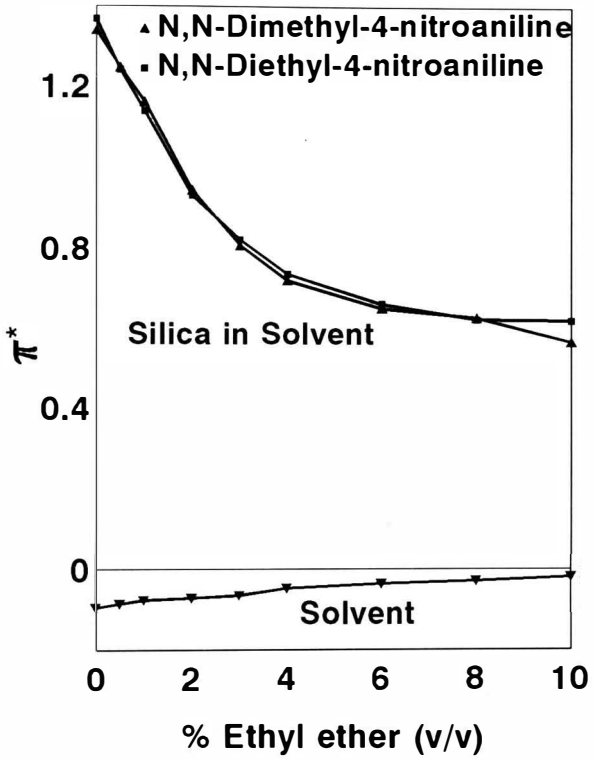

Figure 3-9. π^* values for silica in mixtures of *n*-hexane and ethyl ether (after correction) and π^* values for the mixtures.

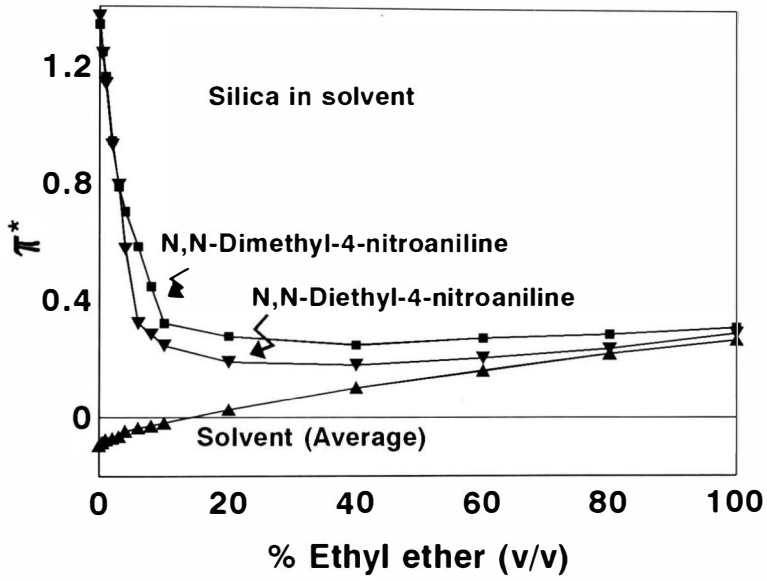

Figure 3-10. π^* values for silica before correction and the π^* values for the mixtures of *n*-hexane and ethyl ether.

3-3-10 Transition Energies of ET-33 on Silica in Mixtures of *n*-Hexane and Ethyl Ether

ET-33 is well retained on silica in mixtures of *n*-hexane and ethyl ether. The amount of ET-33 present in the mobile phase is negligible throughout the whole composition range. The ν_{max} values for ET-33 on silica in mixtures of *n*-hexane and ethyl ether and the corresponding α values are listed in Table 3-11. In calculating the α values, $\nu(\mathbf{3})_{max}$ values after correction in Table 3-10 are used in equation 3-9. The data in Table 3-11 show that the α value for silica increases with the ethyl ether content, which is obviously contrary to chemical intuition. The possible reason for this behavior will be discussed in the next section. Instead of the α values, the transition energy of ET-33 on silica is calculated and plotted vs. the ethyl ether content, as shown in Figure 3-11. From Figure 3-11 it can be seen that the overall polarity of the silica surface decreases with the ethyl ether content.

Table 3-11. ν_{max} values for ET-33 on silica in mixtures of *n*-hexane and ethyl ether and the corresponding α values

% Ethyl ether (v/v)	ν_{max} (kK)	ν_{max} (kcal/mol)	α
0	22.76	65.07	0.225
0.5	22.43	64.13	0.286
1	22.30	63.76	0.372
2	22.13	63.28	0.623
3	22.00	62.89	0.775
4	21.93	62.70	0.876
6	21.83	62.42	0.949
8	21.67	61.96	0.950
10	21.64	61.86	1.022
20	21.34	61.02	
25	21.25	60.75	
30	21.20	60.62	
40	20.99	60.01	
50	20.90	59.76	
60	20.75	59.35	
80	20.59	58.88	
100	20.47	58.51	

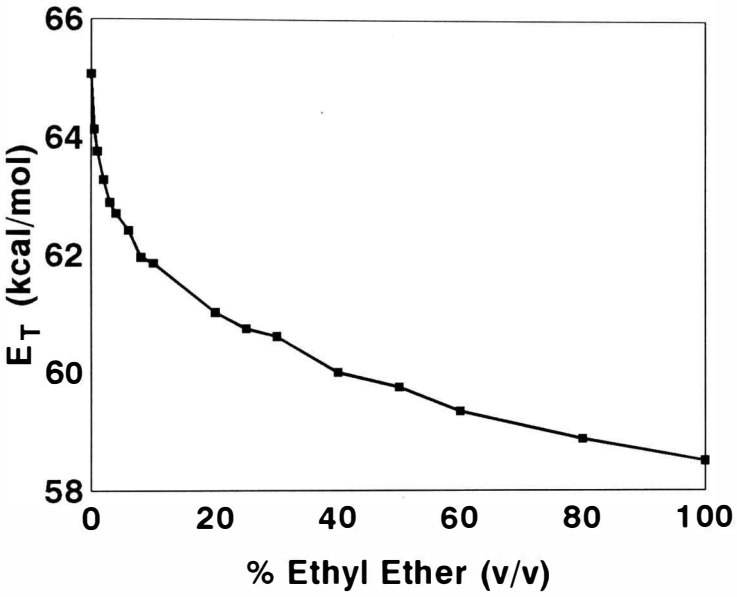

Figure 3-11. Transition energy of ET-33 on silica in mixtures of *n*-hexane and ethyl ether.

3-4 Discussion

3-4-1 Experimental Setup and Solvent Drying

The use of a flow cell allows the sample optical spectrum and the background spectrum to be obtained using exactly the same cell position and the same batch of silica. This makes the background subtraction much more reliable. This is very important as we know from experience that the background interferences may be severe in some cases.

The π^* values obtained for the solvents were not affected by drying. But it was observed that the electronic absorption data for DCMPVP were sensitive to trace amounts of water in the solvents.[109] This can be attributed to the preferential solvation of the α dyes[40] by water due to the zwitterionic nature of these dyes, whereas the π^* dyes used in this research are not significantly preferentially solvated by water. The much larger effect of trace amounts of water in the mobile phase on the π^* values of silica than on the π^* values of the mobile phases can be attributed to the enrichment of water on the surface of silica[119] and the blocking of adsorption sites with high dipolarities by water. The amount of water in the mobile phase can significantly affect the retention of solutes on silica, especially with the water content in the mobile phase lower than 100 ppm.[119] In

solvents dried over molecular sieves, as in our case, there is approximately 10 ppm of water remaining.[119]

3-4-2 π^* Values for Silica in *n*-Hexane-Chloroform or *n*-Hexane-Ethyl Ether Mixtures

N-Methyl-2-nitroaniline was originally proposed for the π^* measurements of protic solvents.[106] However, in solvents with a high hydrogen-bonding acidity, the π^* values from N-methyl-2-nitroaniline are usually higher than the values from the other π^* dyes,[42,99] as was observed in this research. Casassas et al. found by factor analysis that the spectral shift of N-methyl-2-nitroaniline is significantly affected by hydrogen-bonding interactions.[120] They suggested the rejection of N-methyl-2-nitroaniline as a π^* dye.

The π^* measurements for solvents with strong hydrogen-bonding acidity may not be very reliable because the effect of hydrogen-bonding interactions on the electronic spectral data of π^* dyes can not always be neglected in such solvents.[102,115] The π^* dyes used in this research are more polar in their excited state than in their ground state,[102] as shown in Figure 3-12. Hydrogen-bonding interactions between the nitro group in the dyes and protic solvents are expected to be slightly stronger when the dyes are in their excited states than when the dyes are in their ground states. This may make the

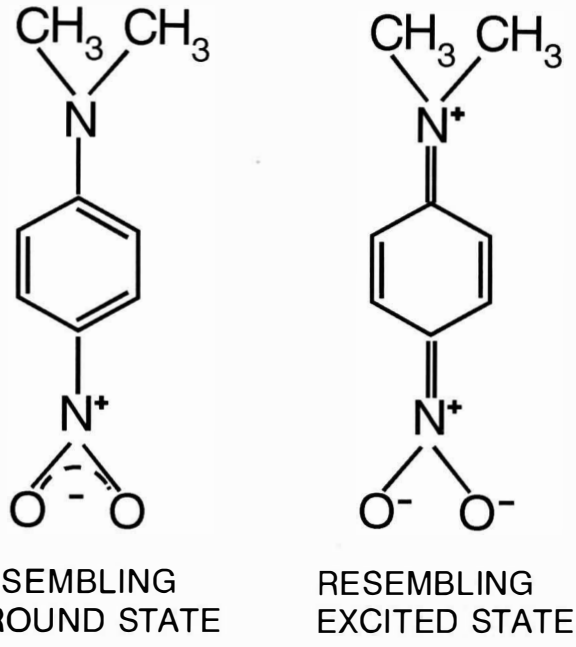

Figure 3-12. Approximate structures of N,N-dimethyl-4-nitroaniline in the ground and excited states.

measured π^* values higher than the actual ones.[102] The π^* values for silica in this research should therefore be considered the upper limit of the dipolarity-polarizability of silica. For silica in contact with mixtures of *n*-hexane and chloroform, the lowest π^* value, $\pi^*_{(4)}$ obtained from 4-nitroanisole, may be the one most closely reflecting the actual dipolarity-polarizability of the silica surface. There is still a considerable dispersion among the π^* values obtained from different π^* dyes, ranging from 1.182 to 1.537, though the dispersion is much smaller than that observed for the π^* values for dry silica, which range from 0.81 to 4.00.[111]

In mixtures of *n*-hexane and chloroform, it is obvious from Figure 3-7 that the dipolarity-polarizability of silica is not affected by the solvent composition. The average value of $\pi^*_{(4)}$ **at different compositions** (not the average value from different dyes), 1.182 (See Table 3-2), should be used to represent the surface dipolarity-polarizability of silica in contact with mixtures of *n*-hexane and chloroform. It can be concluded that though the π^* values of the surface of silica vary from dye to dye, the relative trends in the π^* values obtained from one π^* dye can certainly be trusted.

An adsorbed π^* dye molecule interacts not only with surface silanol groups, but also with solvent molecules (both adsorbed and in the mobile phase).[121] Most aromatic molecules are believed to adsorb in a flat configuration on the

adsorbent surface.[121] Such a configuration will expose one face of the adsorbed π^* dye molecule to the mobile phase. If interactions between the adsorbed π^* dye molecule and solvent molecules are significant, the ν_{max} value for the adsorbed π^* dye is expected to change with the solvent composition. Such a dependence is not observed for π^* dyes adsorbed on silica in contact with mixtures of *n*-hexane and chloroform. This indicates that interactions between an adsorbed solute molecule and solvent molecules are negligible compared with interactions between the solute molecule and the adsorbent surface.

In contrast to the case with chloroform as the cosolvent, the dipolarity-polarizability of silica decreases with the content of ethyl ether in *n*-hexane-ethyl ether mixtures. The silica surface has adsorption sites with different energies. Ethyl ether molecules may compete for high energy adsorption sites with dye molecules and force some dye molecules to adsorb onto weaker sites, resulting in the decreasing dipolarity-polarizability of silica in *n*-hexane-ethyl ether mixtures.

The π^* values before correction in Figure 3-10 include contributions both from the silica surface and the mobile phase. With the ethyl ether content lower than 40%, the π^* value decreases with the ethyl ether content, indicating the contribution from the silica surface is dominant. In the

range of 40-100% ethyl ether, the π^* value increases with the ethyl ether content, indicating the contribution from the mobile phase is dominant. These results are consistent with the retention data in Table 3-8.

3-4-3 Hydrogen-Bonding Acidity of Silica in *n*-Hexane-Chloroform or *n*-Hexane-Ethyl Ether Mixtures

It can be seen from Table 3-4 that the α values obtained from DCMPVP are much larger than the α values obtained from ET-33. Hydrogen-bonding is a specific interaction which requires steric compatibility. It is well known in the literature that hydrogen-bonding interactions of an adsorbate with a solid surface are strongly affected by steric factors.[9,14,15,122,123] From Raman spectra, hydrogen-bonding interactions between pyridine and the silica gel surface were observed.[122] But no hydrogen-bonding interactions were present between 2-chloropyridine and the silica gel.[122] This was attributed to steric hindrance.[122] The two *ortho* chlorine atoms in ET-33 may bring significant steric hindrance to hydrogen-bonding interactions between the phenolate in ET-33 and surface silanol groups. In addition, hydrogen-bonding interactions between the reference π^* dye and the surface silanol groups may cause the measured α value to be lower than the α value representing the actual hydrogen-bonding acidity

of the silica surface. From the above analysis, it is proposed that the highest α value in Table 3-4, $\alpha_{(8)/(4)}$, obtained by using DCMPVP paired with 4-nitroanisole, is the one that most closely represents the actual hydrogen-bonding acidity of the silica surface. This value should be considered the lower limit of the hydrogen-bonding acidity of the silica surface. It is obvious from the data in Table 3-4 that the hydrogen-bonding acidity of the silica is not affected by the composition of *n*-hexane-chloroform mixtures. The average value of $\alpha_{(8)/(4)}$ for all compositions, 0.987 (see Table 3-4), should be used to represent the lower limit for the surface hydrogen-bonding acidity of silica.

The π^* dyes may not be as effective as ET-33 in competing for strong adsorption sites on silica with solvent molecules. In the same mobile phase, ET-33 may occupy stronger adsorption sites than the reference π^* dyes. With the presence of ethyl ether in the mobile phase, use of a reference π^* dye can only cancel part of the dipolar contribution to the interactions between ET-33 and the silica surface, leading to an overestimated α value for the silica surface. The degree of overestimation increases with the ethyl ether content, resulting in changes in the α value of the silica surface contrary to chemical intuition. The decrease in the transition energy of ET-33 on silica with the ethyl ether content is likely caused by occupation of some of the strong

adsorption sites by ethyl ether molecules.

3-4-4 β Values for Silica in *n*-Hexane-Chloroform Mixtures

As described above, N-methyl-2-nitroaniline may not be an appropriate reference π^* dye. The β values probed by 2-nitroaniline/N-methyl-2-nitroaniline, $\beta_{(2)/(5)}$, should therefore be rejected. The $\beta_{(2)/(5)}$ values are always lower than the β values from the other dye pairs in the same mobile phase composition, presumably because of the hydrogen-bonding interactions between N-methyl-2-nitroaniline and the surface silanol groups.

There is a significant difference between the β values from 4-nitroaniline with different π^* reference dyes, as shown in Table 3-6. In measuring β values, it is assumed that the effects of solvent dipolarity-polarizability and hydrogen-bonding acidity on the electronic spectral data of β dyes can be canceled by referencing to the appropriate π^* dye. But it is believed that in the excited state, the nitro groups of β dyes are stronger hydrogen-bonding acceptors than the nitro groups of their alkylated derivatives, the reference π^* dyes.[102] This may make the measured β values higher than the actual ones for media with high hydrogen-bonding acidities. The β values probed by 4-nitroaniline/N,N-diethyl-4-nitroaniline, $\beta_{(1)/(6)}$, are believed to most closely reflect the

actual hydrogen-bonding basicity of the silica surface. Again, the relative trends of the β values from one β dye should be emphasized. It is obvious from Figure 3-8 that all three sets of β values change in a similar way with the concentration of chloroform in the *n*-hexane-chloroform mixture, i.e., the β value of the silica surface decreases as the concentration of chloroform in the binary mixture is increased. Hydrogen-bonding interactions between chloroform and the surface silanol groups may reduce the effective hydrogen-bonding basicity of the silica surface. For solutes with hydrogen-bonding acidity, the decrease of the effective hydrogen-bonding basicity of the silica surface with the concentration of chloroform must be considered in order to predict changes in retention with the mobile phase composition.

3-4-5 Comparisons to the Literature Results

From the experimental results and the above arguments, it can be concluded that the surface of silica has a high dipolarity-polarizability, a high hydrogen-bonding acidity and a low hydrogen-bonding basicity. According to the above arguments, the π^* and α value for the surface of silica in *n*-hexane-chloroform mixtures are 1.182 and 0.987, respectively. In *n*-hexane-ethyl ether mixtures, the π^* value for the surface

of silica decreases with the ethyl ether content. The β value for the surface of silica in *n*-hexane is not higher than 0.35 (See $\beta_{(1)/(6)}$ in Table 3-6), and the value decreases with increasing concentration of chloroform in the mobile phase.

These results are in good qualitative agreement with the values reported for dry silicas.[111] The π^*, α, and β values are 1.98, 1.22, and 0.43, and 2.08, 0.93, and 0.48 for two different dry silicas, respectively. These π^* values are much higher than ours, but the α and β values are more consistent with ours. It should be noted that the presence of solvent is not the only difference between the two reports. The types of silicas, the solvatochromic dyes used, and the amounts of dyes applied to silica are not the same either. The amounts of dyes applied to the surface of silica in our case are about one tenth of the lowest amount applied in reference 111, which is 0.24% (w/w). So direct comparisons should be made with caution. The surface properties of silica have also been deduced from the coefficients of the multiple linear correlation between normal phase solvent eluotropic strength ε^0 and the solvatochromic parameters of solvents.[124] The coefficients for the parameters π^*, α, and β in the reported multiple linear correlation are 0.45, 0.03, and 0.41, respectively, which reflect the magnitudes of dipolarity-polarizability, hydrogen-bonding basicity, and hydrogen-bonding acidity of the silica surface, respectively.[124] Though

these values can not be compared quantitatively with our solvatochromic parameters for the surface of silica, they are qualitatively in very good agreement with our results.

The two cosolvents, ethyl ether (π^* 0.27; α 0.00; β 0.47) and chloroform (π^* 0.58; α 0.44; β 0.00), have significantly different effects on the properties of the silica surface. Though chloroform has a higher dipolarity-polarizability, ethyl ether has a higher elution strength. Ethyl ether may have a stronger interactions with the silica surface because of the high hydrogen-bonding acidity and low hydrogen-bonding basicity of the silica surface. This is consistent with the observation that on silica, Snyder's eluent strength parameter ε^0 for ethyl ether is higher than the one for chloroform.[121] Spange et al. also found that solvents with hydrogen-bonding basicity can modify the surface properties of silica.[125]

As measured by Spange et al., π^*, α, and β values for silica in 1,2-dichloroethane are 0.5, 1.41, and 0.06, respectively.[115] Using a different dye from the measurements in 1,2-dichloroethane, a π^* value of 1.5 was obtained for silica in cyclohexane.[115] Spange et al. attributed the higher π^* value for silica in cyclohexane and all the higher π^* values measured for silica in the literature to hydrogen-bonding interactions between the π^* dyes and surface silanols. As observed in this work, however, solvents may significantly modify the dipolarity-polarizability of silica. It is very

likely that in 1,2-dichloroethane (π^* 0.81; α 0.00; β 0.00), the surface dipolarity-polarizability of silica is significantly reduced.

3-5 Conclusion

Using the solvatochromic comparison method, a high dipolarity-polarizability (π^* 1.182) , a high hydrogen-bonding acidity (α 0.987), and a low hydrogen-bonding basicity (β < 0.35) were obtained for silica in *n*-hexane. The π^* and α values for silica are not affected by the addition of chloroform into *n*-hexane. The hydrogen-bonding basicity of silica, however, decreases with increasing amount of chloroform in *n*-hexane-chloroform mixtures. In *n*-hexane-ethyl ether mixtures, the π^* value for silica decreases with increasing content of ethyl ether. The decrease in π^* and β values for silica with increasing amount of the polar solvent component may result from the competition between the polar solvent and the solvatochromic dyes for the strong adsorption sites on silica. Such changes in the solvatochromic parameters for the surface of silica should be considered in predicting solute retention.

Chapter 4

Solvent-Solute Interactions in Binary Solvents Studied by Target Factor Analysis of Electronic Absorption Spectra of Solvatochromic Dyes

4-1 Introduction

Interactions between a solute and a binary solvent mixture are complicated by solute-solvent interactions, solvent self-interactions, and solvent mutual-interactions. Electronic absorption spectra of the solute can be used to elucidate solvent-solute interactions. It is very difficult, however, to characterize the different interactions individually.

Factor analysis has been widely used to solve various complex problems in almost every branch of chemistry. Using factor analysis, the number of significant factors and the abstract significant factors can be obtained. The abstract significant factors can then be target-transformed to identify potentially significant factors. The effects of pure solvents on various physicochemical properties have been studied by factor analysis.[126-128] Casassas et al. have studied solvent effects on the wavelength shift of different solvatochromic dyes and on pK_a values of several acidic compounds in dioxane-water mixtures by factor analysis.[120,129] Macroscopic parameters, such as mole fraction and dielectric constant, and microscopic parameters, such as $E_T(30)$ values of solvent polarity and solvatochromic parameters α, β, and π^*, representing hydrogen-bonding acidity, hydrogen-bonding basicity, and dipolarity of solvents, respectively, were

target tested to evaluate their significance as physical factors. The result is not trivial because the authors were able to determine that the shift of the absorption maximum wavelengths of one of the π^* dyes, N-methyl-2-nitroaniline, is significantly affected by the α and β values of the solvent mixtures. The finding is consistent with results in an earlier report[42] and with our results in Chapter 3. Though factor analysis has been used to analyze the shift of the absorption maximum wavelength, it has not been applied to study the complete spectra.

In this research, target factor analysis will be used to study solvent effects on the electronic absorption spectra of N,N-dimethyl-4-nitroaniline in mixtures of *n*-hexane and ethyl ether. Both solvent-solute interactions and solvent-solvent interactions are cited to explain the dependence of solute spectra on the solvent composition.

4-2 Experimental

N,N-Dimethyl-4-nitroaniline was purchased from Kodak (Rochester, NY). Ethyl ether and *n*-hexane are spectrophotometric grade. All electronic absorption spectra were obtained on a Shimadzu UV-265 spectrophotometer.

Solutions of N,N-dimethyl-4-nitroaniline at $1x10^{-4}$ M in each of the *n*-hexane-ethyl ether mixtures with 100, 80, 60,

40, 20, 10, 8, 6, 4, 3, 2, 1, 0.5, and 0% (v/v) of ethyl ether, called mixtures 1, 2, ..., and 14, respectively, were prepared, which will be referred to as solutions 1, 2, ..., and 14, respectively. Electronic absorption spectra for the 14 solutions were obtained in the wavelength range of 250 nm to 500 nm at an interval of 0.1 nm.

4-3 Target Factor Analysis

4-3-1 Data Matrix

As a first approximation, an electronic absorption spectrum of a dye in a binary solvent mixture can be considered as a linear combination of the spectra of the dye in each of the two pure solvent components. Specifically, the absorbance value of a dye in a binary solvent mixture can be considered a linear combination of the absorbance values of the dye in each of two pure solvent components, i.e.,

$$A_m(\lambda) = c_1 \cdot A_1(\lambda) + c_2 \cdot A_2(\lambda) \qquad (4\text{-}1)$$

where A_m, A_1, and A_2 represent the absorbance of the dye solution in the mixture, pure solvent 1, and pure solvent 2, respectively, λ represents the wavelength, and c_1 and c_2 are coefficients, depending on the composition of the mixture.

The data matrix for this research is built up by taking the absorbance values of each of the 14 spectra as a column,

$$\mathbf{D} = [A_{m1}\ A_{m2}\ \ldots\ldots\ldots\ A_{m13}\ A_{m14}] \qquad (4-2)$$

where A_{m1}, A_{m2}, ..., and A_{m14} are the absorbance values of the spectrum of N,N-dimethyl-4-nitroaniline in mixtures 1, 2, ..., and 14, respectively. The dimensions of the data matrix are 2500x14. The wavelengths at the maximum absorbance for the 14 solutions are listed in Table 4-1. The spectra of solutions 1 (in ethyl ether), 7 (in 10% ethyl ether), and 14 (in *n*-hexane) are shown in Figures 1, 2, and 3, respectively.

4-3-2 Singular Value Decomposition

Singular value decomposition can decompose a data matrix into eigenvectors,

$$\mathbf{D} = \mathbf{USV}' \qquad (4-3)$$

where **U** and **V** are orthonormal matrices, composed of eigenvectors of the row-factor space and eigenvectors of the column-factor space, respectively. **S** is a diagonal matrix whose diagonal elements are the square roots of the respective eigenvalues. Singular value decomposition was performed for the data matrix in MATLAB, using the command

```
[u,s,v] = svd(D,0)
```

The first column in **U**, representing the most significant eigenvector (i.e., abstract factor) of the row-factor space, is shown as the solid curve in Figure 4-4. It can be considered the average of the 14 spectra. The second most

Table 4-1. Wavelength at the maximum absorbance, λ_{max}, for N,N-dimethyl-4-nitroaniline in mixtures of *n*-hexane and ethyl ether

% Ethyl ether (v/v)	λ_{max} (nm)
0	351.7
0.5	352.2
1	352.7
2	352.9
3	353.0
4	353.4
6	353.6
8	354.3
10	354.5
20	356.8
40	360.3
60	363.4
80	365.7
100	368.1

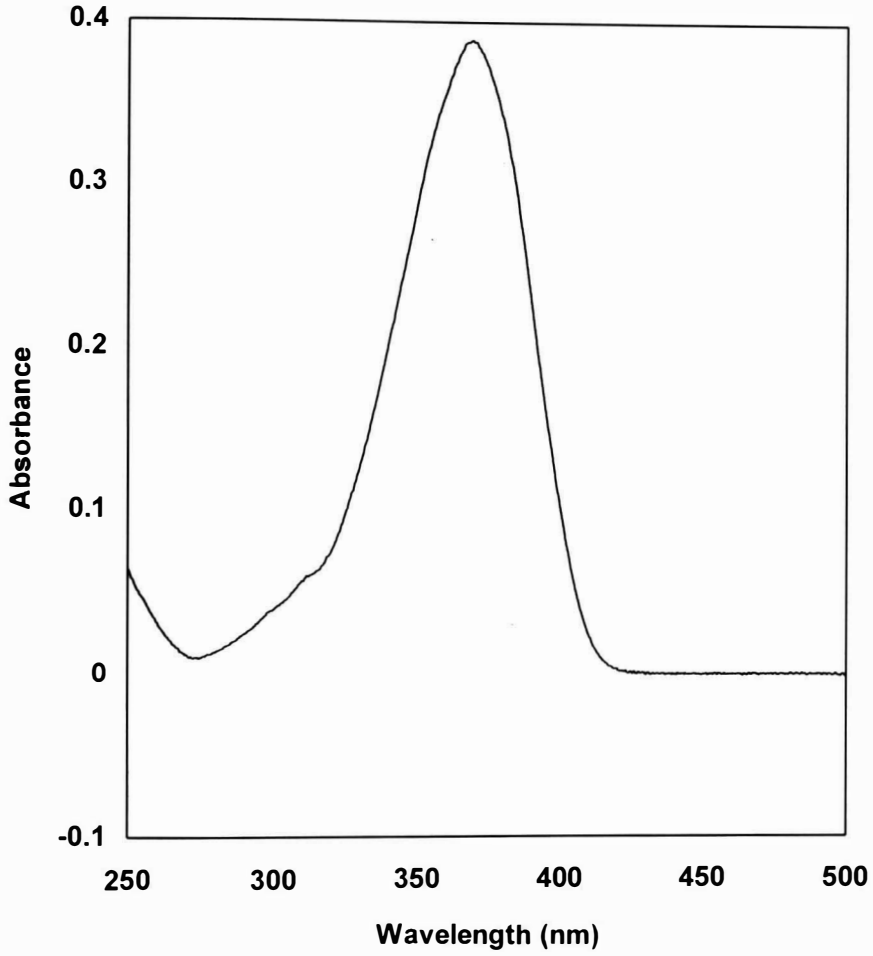

Figure 4-1. Electronic absorption spectrum of N,N-dimethyl-4-nitroaniline in ethyl ether.

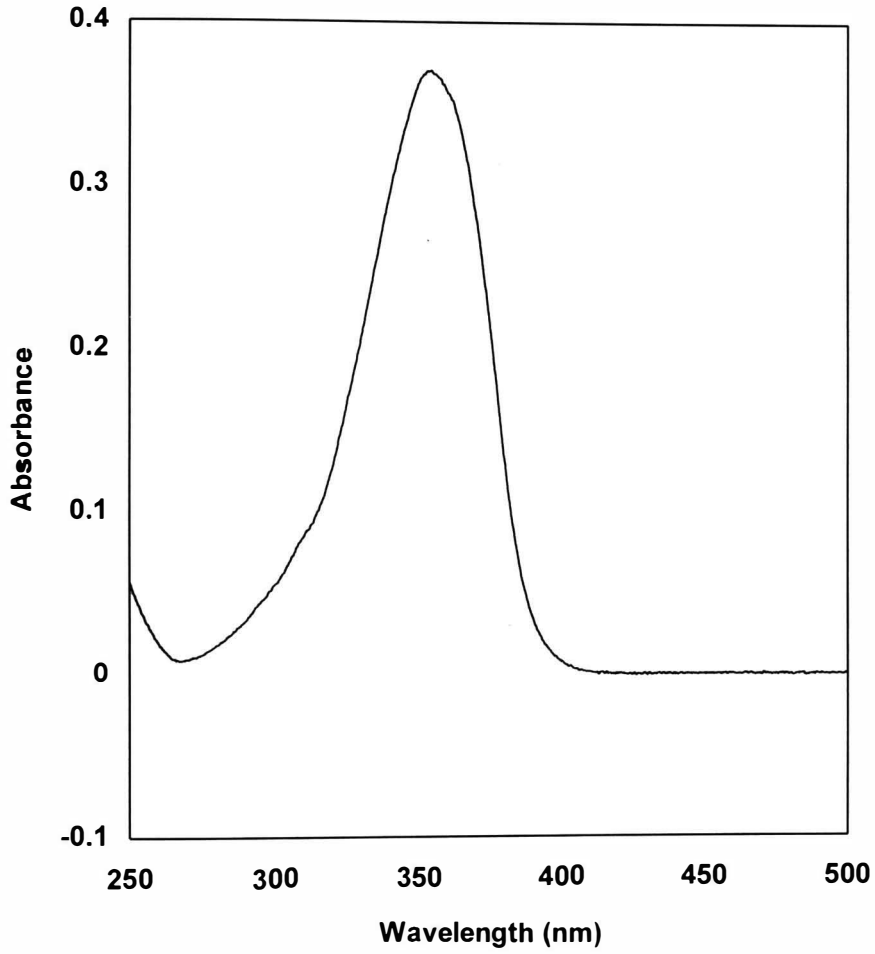

Figure 4-2. Electronic absorption spectrum of N,N-dimethyl-4-nitroaniline in an *n*-hexane-ethyl ether mixture containing 10% (v/v) ethyl ether.

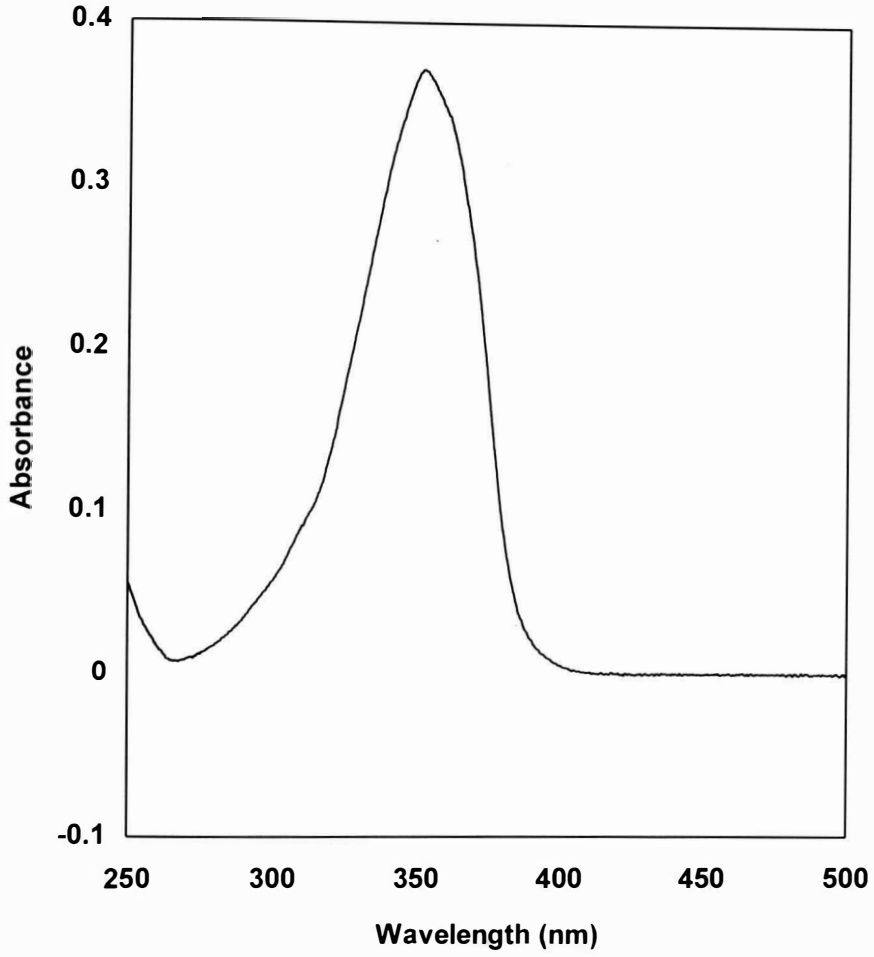

Figure 4-3. Electronic absorption spectrum of N,N-dimethyl-4-nitroaniline in *n*-hexane.

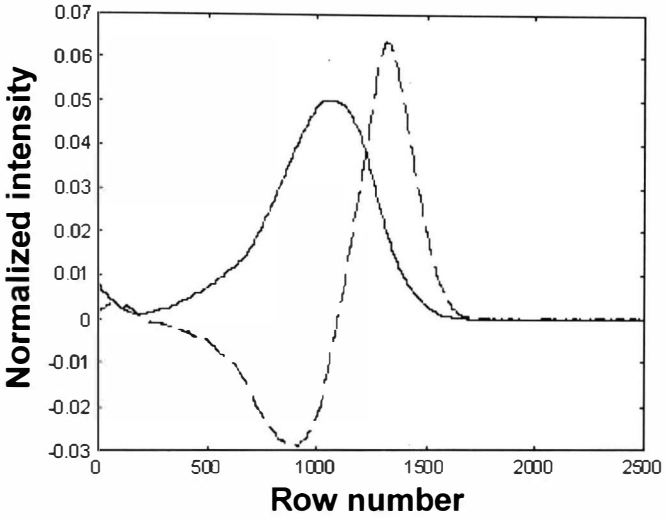

Figure 4-4. The first (solid curve) and the second (dashed curve) most significant abstract factors of the row-factor space.

significant abstract factor, shown as the dashed curve in Figure 4-4, was obtained from the residue after extracting the most significant factor. The third, forth, and fifth most significant abstract factors are shown in Figure 4-5, 4-6, and 4-7, respectively. There are totally 14 abstract factors. Only the first *n* largest abstract factors are required to account for the data within experimental error. The other abstract factors only account for experimental error.

4-3-3 Number of Significant Factors

The number of significant factors can be determined by a method based on comparison between the estimated experimental error and the residual standard deviation (RSD) and an empirical method using the factor indicator function developed by Malinowski.[126] RSD must be obtained first in both methods. RSD can be calculated by

$$RSD = \sqrt{\frac{\sum_{j=n+1}^{c} \lambda_j}{r(c-n)}} \qquad (4-4)$$

where r, c, and n are the number of rows in the matrix **D**, the number of columns in the matrix **D**, and the number of significant factors, respectively. λ_j is an eigenvalue,

$$\lambda_j = s(j,j) \cdot s(j,j) \qquad (4-5)$$

where $s(j,j)$ is the jth diagonal element in matrix **S** in

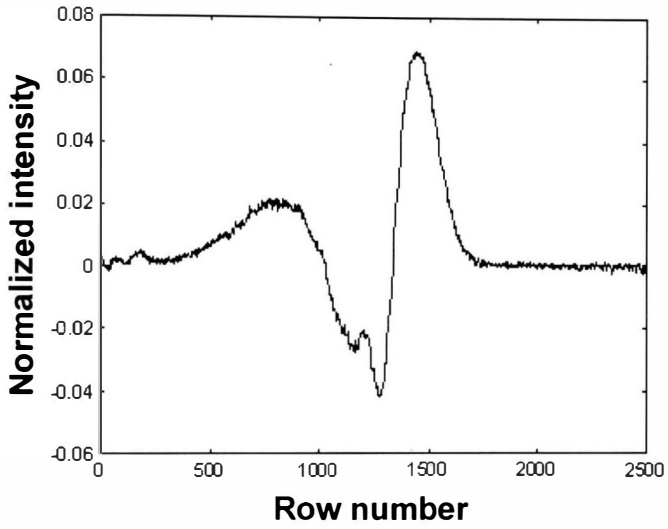

Figure 4-5. The third most significant abstract factor of the row-factor space.

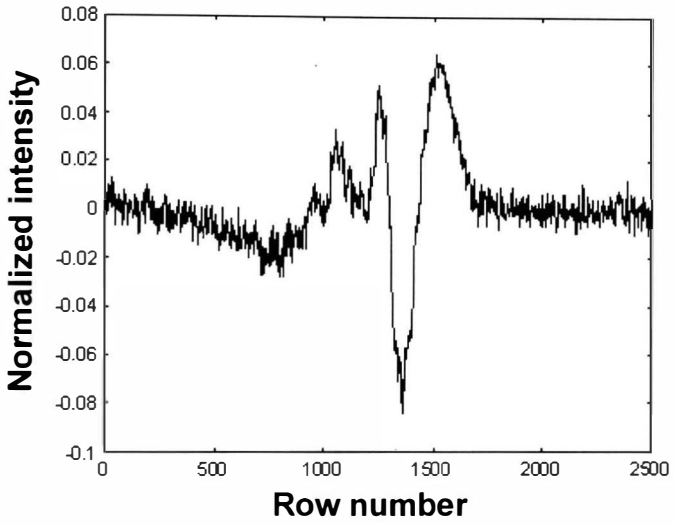

Figure 4-6. The forth most significant abstract factor of the row-factor space.

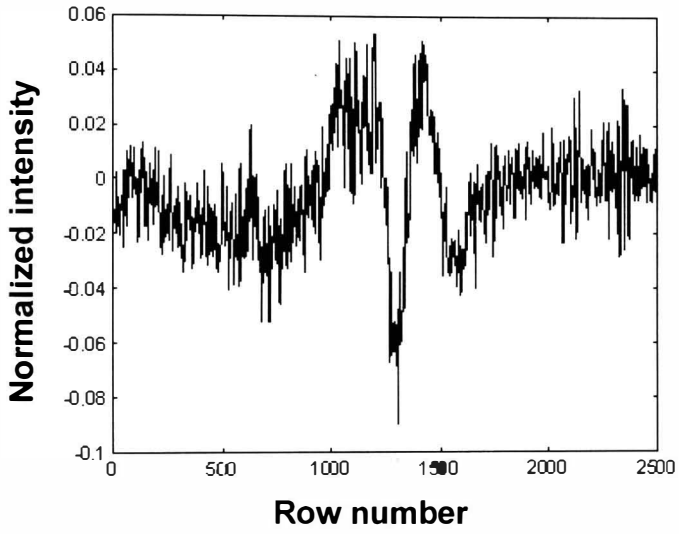

Figure 4-7. The fifth most significant abstract factor of the row-factor space.

equation 4-3.

The empirical method using the factor indicator function (IND) was explored first. IND is defined as

$$IND = RSD/(c - n)^2 \qquad (4\text{-}6)$$

In a plot of IND vs. the number of factors considered n, the n value at the minimum IND is considered the number of significant factors. With a MATLAB program (see Appendix A), which is adapted from a program described by Malinowski,[126] the plot is obtained, as shown in Figure 4-8. From the plot it can be see that the number of significant factors is 4.

For the method based on comparison between the estimated experimental error and RSD, the experimental error must be estimated first. Four flat parts of spectra are used to estimate the experimental error. Among them two are from the short wavelength region and the other two are from the long wavelength region. The experimental error is estimated to be in the range of 0.0005 to 0.0015 absorbance unit, which is same as estimated by Bulmer and Shurvell.[130] A plot of RSD vs. the number of factors considered n was obtained with the MATLAB program, as shown in Figure 4-9. When the number of significant factors is chosen as 4, RSD (0.0005) is at the lower bound of the estimated experimental error.

Based on the results from the two methods, the number of significant factors is chosen as 4.

The variance, which measures the importance of an

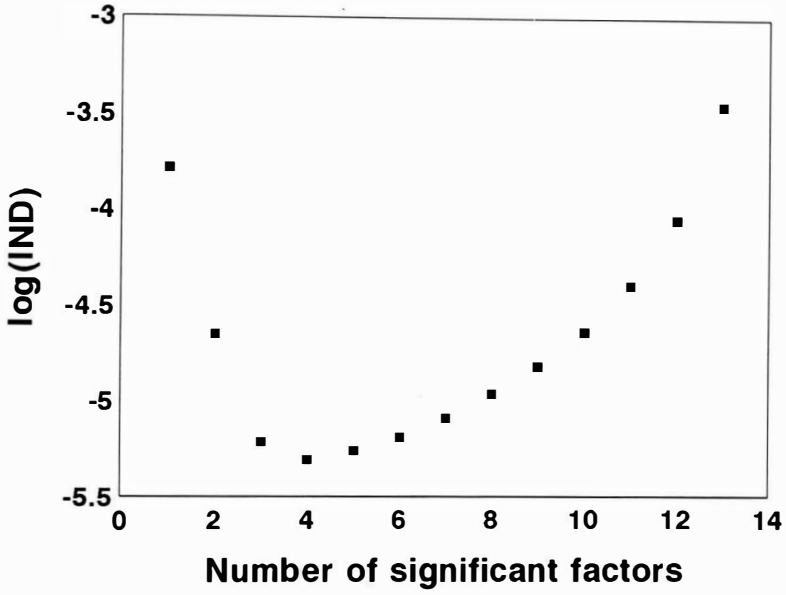

Figure 4-8. Plot of the factor indicator function (IND) vs. the factor level.

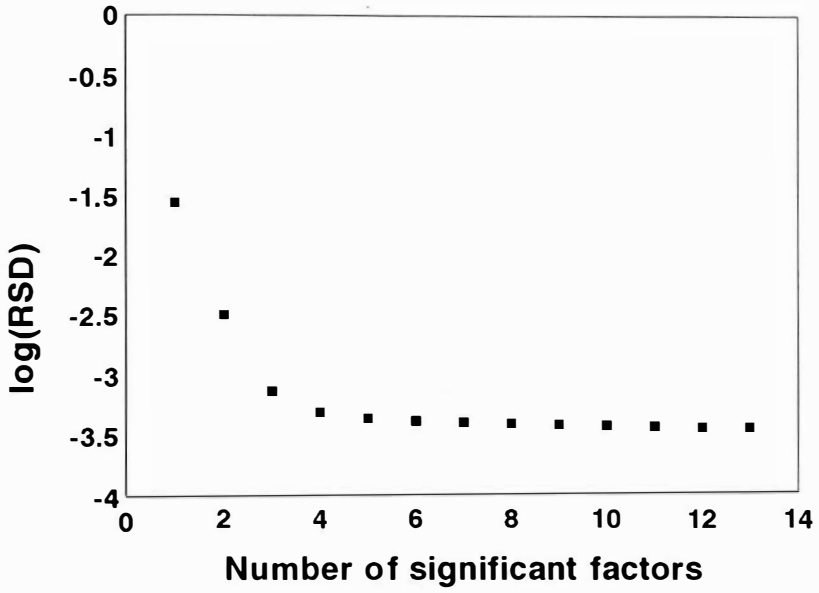

Figure 4-9. Plot of the residual standard deviation vs. the factor level.

abstract factor, can be obtained from the eigenvalues,

$$variance = \frac{\lambda_j}{\sum_{j=1}^{c} \lambda_j} \qquad (4\text{-}7)$$

The variances for the 1st, 2nd, 3rd, and 4th most significant factors account for 81.72, 15.56, 1.70, and 0.29% of the total variance, respectively. The cumulative variance for the first 3 largest factors accounts for 98.98% of the total variance. To concentrate on the major factors, the 4th most significant factor, though statistically significant, is not considered in the following target transformation.

4-3-4 Target Transformation

To our knowledge, there are no basic factors, i.e., physicochemical parameters, suitable for this problem. Target transformation based on typical factors, i.e., data columns in the original data matrix, was performed.

As a first try, the spectra of solutions 1 and 14 were chosen as typical factors because the spectra of the other solutions can be considered as linear combinations of these two spectra, as a first approximation. The third typical factor is a spectrum of one of the other solutions. The transformation vector for each factor is obtained by

$$t_j = \mathbf{S}(1{:}3,1{:}3)^{-2} \cdot (\mathbf{U}(:,1{:}3) \cdot \mathbf{S}(1{:}3,1{:}3))' \cdot \mathbf{D}(:,j) \qquad (4\text{-}8)$$

The transformation matrix is formed by

$$\mathbf{T} = [t_1\ t_j\ t_{14}] \tag{4-9}$$

The key combination set is formed by

$$\mathbf{D}_{key} = [\mathbf{D}(:,1)\ \mathbf{D}(:,j)\ \mathbf{D}(:,14)] \tag{4-10}$$

The reproduced data matrix is obtained by

$$\mathbf{D}_r = \mathbf{D}_{key} \cdot \mathbf{T}^{-1} \cdot \mathbf{V}(:,1:3)' \tag{4-11}$$

The residual error matrix

$$\mathbf{E} = \mathbf{D}_r - \mathbf{D} \tag{4-12}$$

The third typical factor is chosen when the square of the norm of matrix **E**, i.e., $\Sigma\Sigma e_{ij}^2$, is minimal. From the plot of $\Sigma\Sigma e_{ij}^2$ vs. j, as shown in Figure 4-10, the spectrum of solution 11 is considered the best choice for the third factor.

An alternative approach, where the spectra of solutions 11 and 14 were chosen as the first two factors, was attempted. From Figure 4-11 the spectrum of solution 5 is chosen as the third factor.

A third approach, the spectra of solutions 5 and 11 were chosen as the first two factors. From Figure 4-12 the spectrum of solution 14 is chosen as the third factor. Again the spectra of solutions 5 and 14 were chosen as the first two factors. From Figure 4-13 the spectrum of solution 11 is still chosen as the third factor.

The best key combination set is composed of the spectra of solutions 5, 11, and 14, which contain 20, 2, and 0% (v/v) of ethyl ether, respectively.

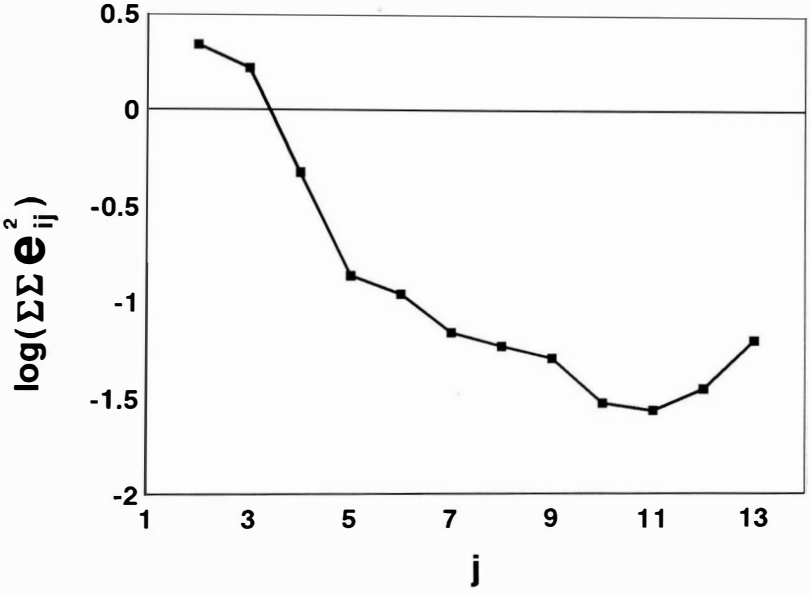

Figure 4-10. Square of the norm of the residual error matrix **E** vs. the choice of the third significant factor when the spectra in mixtures 1 and 14 have been chosen as the significant factors.

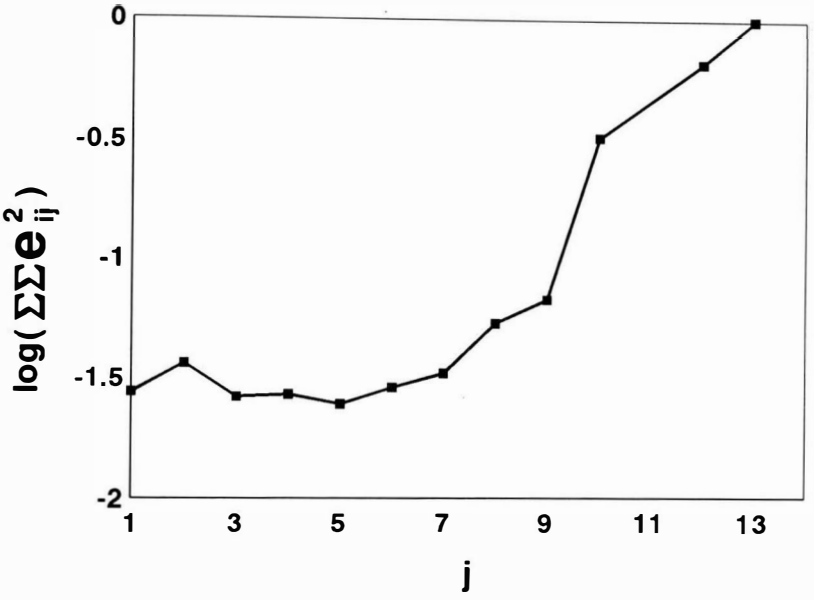

Figure 4-11. Square of the norm of the residual error matrix **E** vs. the choice of the third significant factor when the spectra in mixtures 11 and 14 have been chosen as the significant factors.

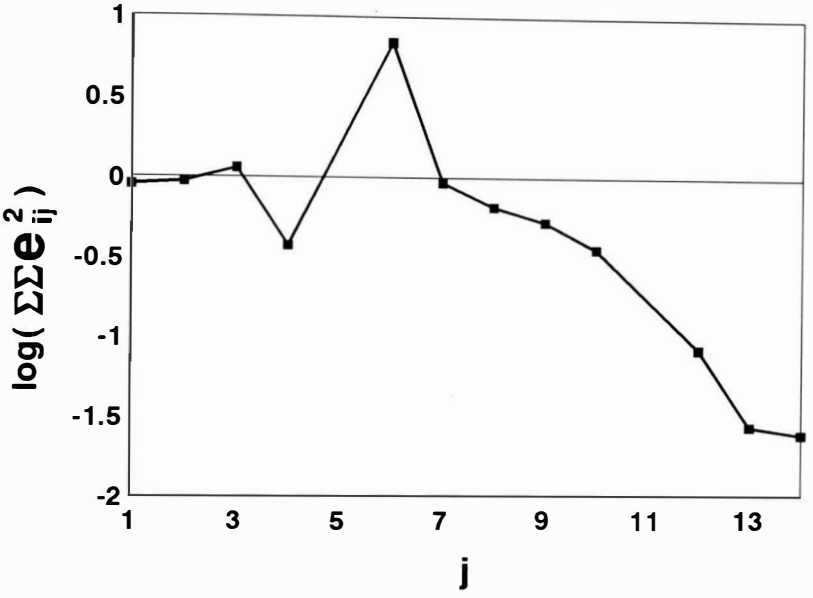

Figure 4-12. Square of the norm of the residual error matrix **E** vs. the choice of the third significant factor when the spectra in mixtures 5 and 11 have been chosen as the significant factors.

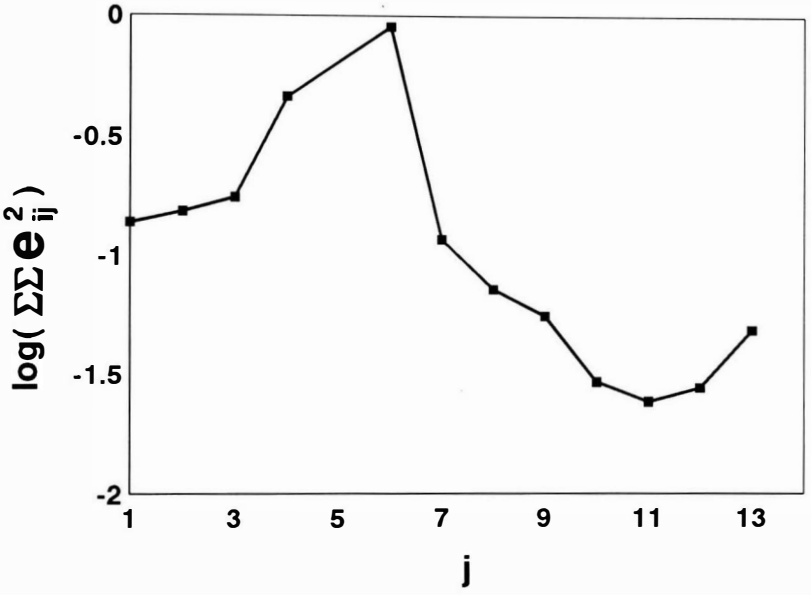

Figure 4-13. Square of the norm of the residual error matrix **E** vs. the choice of the third significant factor when the spectra in mixtures 5 and 14 have been chosen as the significant factors.

4-4 Discussion

From the target factor analysis results it can be concluded that a linear combination of the spectra of N,N-dimethyl-4-nitroaniline in *n*-hexane and ethyl ether is not a good model for the spectra in mixtures of *n*-hexane and ethyl ether. In mixtures of *n*-hexane and ethyl ether, the dye may exist in three different microenvironments. The three different microenvironments may be assigned to *n*-hexane, ethyl ether molecules not interacting with other ethyl ether molecules (segregated ethyl ether molecules), and ethyl ether molecules interacting with other ethyl ether molecules (ethyl ether clusters). Ethyl ether molecules prefer to interact among themselves, and the dye is preferentially solvated by ethyl ether molecules, as evidenced by the more rapid increase of π^* values with the content of ethyl ether when the content of ethyl ether is very low, as described in Chapter 3. Therefore, the second microenvironment may only exist in a mixture of *n*-hexane and ethyl ether with a very low content of ethyl ether. According to these arguments, the first two typical factors should be the spectrum of the dye in *n*-hexane and the spectrum of the dye in a mixture of *n*-hexane and ethyl ether with a very low content of ethyl ether. When the content of ethyl ether is above certain value, most of the ethyl ether molecules exist as ethyl ether clusters. Any one

of the spectra of the dye in the mixtures of *n*-hexane and ethyl ether with the content of ethyl ether above that value can be taken as the third typical factor, without changing the reproduced data significantly. The flatness of the curve in Figure 4 with the *j* value from 1 to 7 (100% to 8% (v/v) of ethyl ether) confirms this argument.

Evolving factor analysis,[126] i.e., factor analysis of a series of data matrices constructed by successively adding spectra to the previous matrix, may be very useful to observe the effects of the ethyl ether content on the nature of *n*-hexane-ethyl ether mixtures. Evolving target factor analysis both in the direction of increasing ethyl ether content and in the direction of decreasing ethyl content may be performed to further understand solvent effects and test the above arguments.

If the above arguments about the nature of *n*-hexane-ethyl ether mixtures are correct, target factor analysis of the spectra of other π^* dyes in the mixtures should also give same or similar results.

The error in this experiment may come from instrumental measurements, impurities in the dye, and impurities in the solvent. Some of the error sources, e.g., trace amounts of water, may result in non-random disturbance of the spectra of the dye, requiring additional significant factors.

4-5 Conclusion

Four significant factors were found in factor analysis of the spectra of N,N-dimethyl-4-nitroaniline in mixtures of *n*-hexane and ethyl ether. The largest three significant factors account for 99% of the total variance in the original data matrix. The possible reason for this phenomenon is that there may be three microenvironments in a mixture of *n*-hexane and ethyl ether, including *n*-hexane, ethyl ether molecules not interacting with other ethyl ether molecules (segregated ethyl ether molecules), and ethyl ether molecules interacting with other ethyl ether molecules (ethyl ether clusters).

Chapter 5

Wetting and Wetting Hysteresis of Alkyl Bonded Silicas in Organic-Water Mixtures

5-1 Introduction

When alkyl bonded silica is in contact with the eluent, a solid/liquid boundary is formed. On the molecular scale, however, it is more appropriate to refer to the boundary as an interphase region,[53,131] which has a finite width and is composed of the bonded alkyl chains, residual silanol groups, and sorbed eluent solvent molecules. The composition and width of the interphase region will depend on the eluent composition.

The composition and properties of the interphase region are determined by interactions between alkyl bonded silica and the eluent on the molecular level, including chain-chain interactions, chain-eluent interactions, and residual silanol-eluent interactions.[56,57] Wetting refers to the macroscopic manifestations of such molecular interactions. The wetting of bonded alkyl phases may strongly affect various chromatographic behaviors of the bonded phases, including column efficiency,[68] dead volume,[132] solute retention,[59,62,63] column equilibration time,[59,69] interactions between residual silanols and basic solutes,[69] adsorption of pairing agents in ion pair chromatography,[133] and solvent migration rate in reversed-phase thin layer chromatography.[75]

Though the wetting of bonded alkyl phases has been studied for a long time, a clear and complete picture of

wetting under chromatographic conditions has yet to appear. Most wetting experiments for alkyl bonded phases were conducted on alkyl derivatized silica plates and capillary inner surfaces, instead of octadecylsilylated silica particles. None of the methods that have been applied to the study of the wetting of planar surfaces can be used to study porous particles. In our preliminary experiments, it was found that alkyl bonded silica in eluents with different compositions showed different degrees of transparency.[134] Therefore, optical transmittance of light through alkyl bonded silica packed in a flow cell was used here to study the wetting of the stationary phase. Besides optical transmittance measurements, direct wetting tests, dipolarity-polarizability measurements based on the solvatochromic comparison method, and chromatographic measurements were also performed to study the wetting of the stationary phase. In direct wetting tests, stationary phase materials were brought into contact with the eluent to observed the amount of the immersed (or wetted) stationary phase materials and the amount of floating (or nonwetted) stationary phase materials. In dipolarity-polarizability measurements, a solvatochromic π^* dye was applied to the interphase region to observe the dipolarity-polarizability in this region. Chromatographic measurements were carried out to correlate the wetting and the retentive behavior of the stationary phase.

In this research, the wetting of various types of alkyl bonded silica was studied by methods cited above. The effects of the organic solvent, bonding density, particle size, pore size, and chain length on wetting were investigated. The effects of wetting on column equilibration time and solute retention were studied. The nature of the wetting behavior of alkyl bonded silicas was discussed.

5-2 Experimental

5-2-1 Materials and Chemicals

Different types of silica and alkyl bonded silica used in this research, their characteristics, and their suppliers are listed in Table 5-1. N,N-Diethyl-4-nitroaniline was obtained Frinton Laboratories (Vineland, NJ, USA). MeOH and ACN of HPLC grade were from EM Science (Gibbstown, NJ). THF of HPLC grade was from Fisher Scientific Company (Fair Lawn, NJ).

5-2-2 Optical Transmittance Measurements

All optical transmittance measurements were made on a Shimadzu UV-265 spectrophotometer equipped with an integrating sphere attachment. A flow cell with a path length of 1 mm was packed with about 0.05 g of the stationary phase of interest,

Table 5-1. Different types of silica and alkyl bonded silica, and their characteristics

Packing materials	Alkyl bonded	Size (μm) and shape	Pore size (Å)	Surface area (m^2/g)	% C (w/w)	End-capping	Other characteristics	Producer
HDG $C_{18}H_{37}$	C18	125-150		250-400	24.09			Tianjin No. 2 Chemical Manufacturer (Tianjin, China)
LiChroprep RP-18	C18	25-40						E. Merck (Darmstadt, Germany)
LiChrosorb SI 100	bare silica	30						
Spherisorb ODS1	C18	5 spherical	80	220	7	partial	monomeric; bonding density 1.47 μmol/m^2	Phase Separations (Deeside, UK)
Spherisorb ODS2	C18	5 spherical	80	220	12	yes	monomeric; bonding density 2.72 μmol/m^2	
SUPELCOSIL LC-18	C18	5 spherical	100	170		yes	pore volume 0.6 mL/g	SUPELCO (Bellefonte, PA)
YMC ODS-A 120A	C18	50 spherical	120	300	17	yes	pore volume 1.0 mL/g	YMC (Wilmington, NC)
		25 spherical						
		10 spherical						
YMC ODS-A 200A	C18	25 spherical	200	200	12	yes	pore volume 0.95 mL/g	
YMC ODS-A 300A	C18	25 spherical	300	150	6	yes	pore volume 0.7 mL/g	
YMC Octyl 120A	C8	15 spherical	120	300	10	yes	monomeric; pore volume 1.0 mL/g	
YMC Butyl 120A	C4	25 spherical	120	300	7	yes	monomeric; pore volume 1.0 mL/g	
YMC TMS 120A	C1	15 spherical	120	300	4		pore volume 1.0 mL/g	

as shown in Figure 3-5. After the stationary phase was equilibrated with an eluent, the transmittance of the stationary phase/eluent system at 550 nm was measured. The transmitted light is highly diffuse, so an integrating sphere attachment was used for these measurements.

5-2-3 Direct Wetting Tests

In direct wetting tests without prewetting, stationary phase particles were brought into contact with an organic-water mixture of interest directly. A series of 3 ml-glass tubes with a ground glass cap were filled with about 2 ml of organic-water mixtures with different compositions. To each of the tubes was added 0.050 g of alkyl bonded silica. The tubes were capped and shaken vigorously, then left undisturbed for 24 hours to let the particles either settle to the bottom of the tubes or rise above the liquid. The amount of the particles on the bottom of the tubes and the amount of floating particles were observed.

In direct wetting tests with prewetting, stationary phase particles were prewetted by organic modifier before contacting an organic-water mixture of interest. The procedure includes the following steps:

1. A 3 ml-glass tube with a ground glass cap was filled with about 2 ml of organic modifier. 0.050 g of

alkyl bonded silica was added to the tube. The tube was capped and shaken vigorously for 10 seconds.

2. The tube was left undisturbed for 10 minutes to let the particles settle to the bottom.
3. The supernatant was removed carefully with a pasteur pipet, without letting the particles contact air.
4. About 2 ml organic-water mixture of interest was carefully added along the wall into the tube without disturbing the stationary phase particles.
5. The suspension was stirred, without letting the particles contact air, to mix the residual liquid with the added mixture.
6. Steps 2-5 were repeated four times to ensure the complete replacement of organic modifier by the organic-water mixture of interest.
7. The amount of particles on the bottom of the tube and the amount of floating particles were observed.
8. The tube was capped and shaken vigorously, then left undisturbed for 24 hours to let the particles either settle to the bottom of the tube or rise above the liquid.
9. The amounts of immersed and floating particles were observed again.

5-2-4 Spectroscopic Measurements

To measure the dipolarity-polarizability of the stationary phase, the electronic absorption spectra of a π^* dye, N,N-diethyl-4-nitroaniline, sorbed in the stationary phase were measured after the stationary phase was equilibrated with the dye solution in an eluent, as described in Chapter 3. The spectroscopic measurements to obtain the π^* values for LiChroprep RP-18 in Figure 5-30 were made on a CARY 1E UV-Visible spectrophotometer equipped with a diffuse reflectance accessory, setting the bandpass to 4 nm. All the other spectroscopic measurements were made on a Shimadzu UV-265 spectrophotometer equipped with an integrating sphere attachment, setting the bandpass to 5 nm. The experimental setup for these spectroscopic measurements is identical to that for the optical transmittance measurements.

5-2-5 Chromatographic Measurements

Chromatographic measurements were performed on a Hewlett-Packard 1050 series liquid chromatograph. A 10 x 4.6 mm LiChroprep RP-18 (25-40 μm) column was packed by Peter W. Carr's group at the University of Minnesota, Minneapolis. A 75 x 4.6 mm Spherisorb ODS2 (3 μm) column was purchased from MetaChem Technologies (Redondo Beach, CA).

5-3 Results and Discussion

5-3-1 Optical Transmittance Measurements

An alkyl bonded silica/eluent system is composed of the silica support, the interphase region, and the bulk eluent, as shown in Figure 5-1. The interphase region includes residual silanol groups, the bonded alkyl chains, solvent molecules intercalated within the chains, and a solvent layer which may have a composition different from the bulk eluent because of the preferential sorption of some components in the eluent. With a change of the eluent, the composition of the interphase region changes, leading to a change in the refractive index. Therefore, the transmittance of light through the whole system changes also. The transmittance value may be used to monitor the change in the condition, e.g., solvation or wetting, of the interphase region. The thickness of the interphase region is only on the order of nanometer. Therefore, each interphase region may only have a very small effect on the transmittance value. The effects of the interphase region are magnified many times, however, by the fact that light passes through many interphase regions due to the small particle size, the porous nature of the particles, and the small pore size. The importance of the interphase region can also be recognized by its volume, which can be roughly estimated from the specific

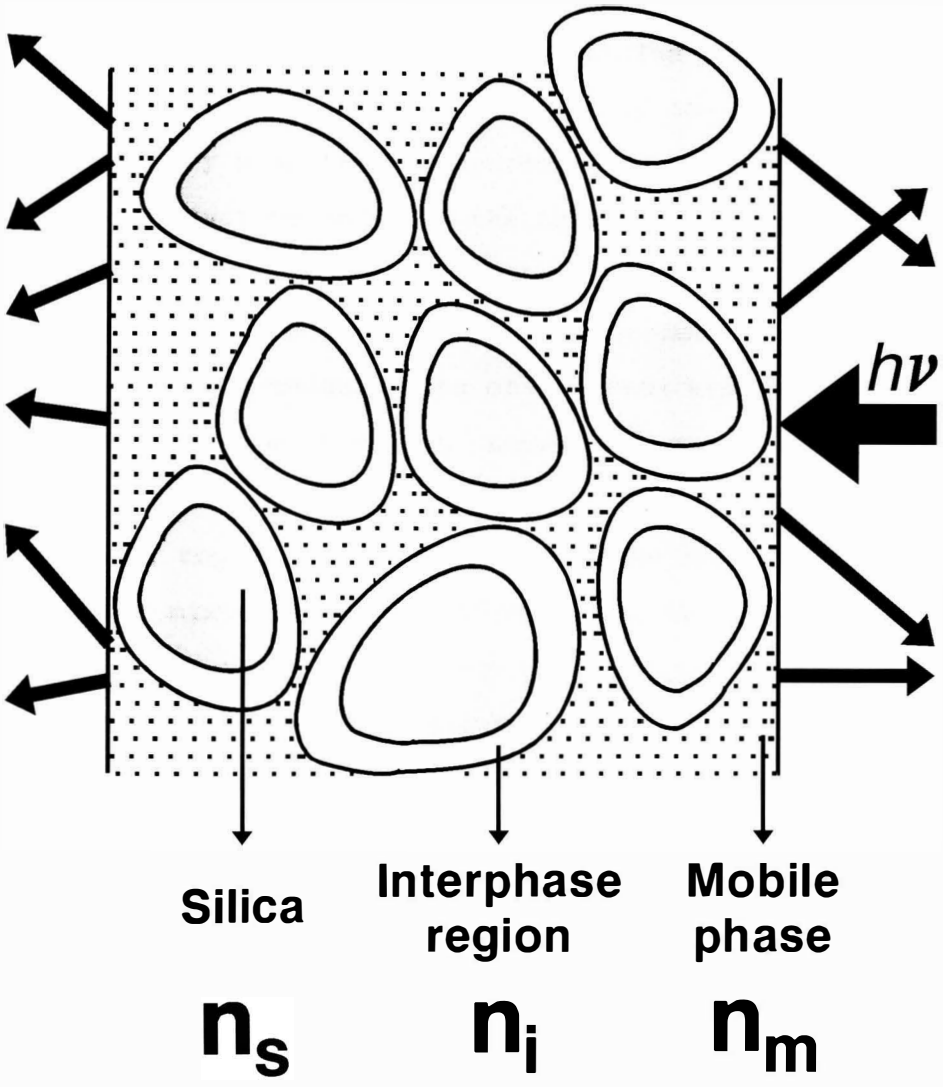

Figure 5-1. Optical transmittance through an alkyl bonded silica/mobile phase system. The sizes of the particles, especially the interphase regions, are exaggerated.

surface area (in the order of 100 m^2/g) and the carbon content of alkyl bonded silica (around 10%). The interphase volume accounts for at least several percent of the total volume of the stationary phase/eluent system.

The refractive index of the bulk eluent also depends on its composition. The transmittance change caused by the change in the refractive index of the eluent can be observed by transmittance measurements of the bare silica (LiChrosorb SI 100)/eluent system, as shown in Figure 5-2. The transmittance of bare silica in MeOH-water is plotted again in Figure 5-3, together with the curve of the refractive index of MeOH-water mixtures, obtained using the data from reference 30. From Figure 5-3 it is clear that the two curves resemble each other and there is no significant difference in the peak position of the two curves. Therefore, the changes in transmittance for the bare silica/eluent system can be attributed to changes in the refractive index of the eluent.

Various physical characteristics, e.g., particle size and pore size, may affect the absolute optical transmittance. The absolute optical transmittance also depends on the wavelength used in the measurements. The relative changes in the optical transmittance over the eluent composition, not the absolute transmittance value, however, are most informative about the composition and structure of the interphase region.

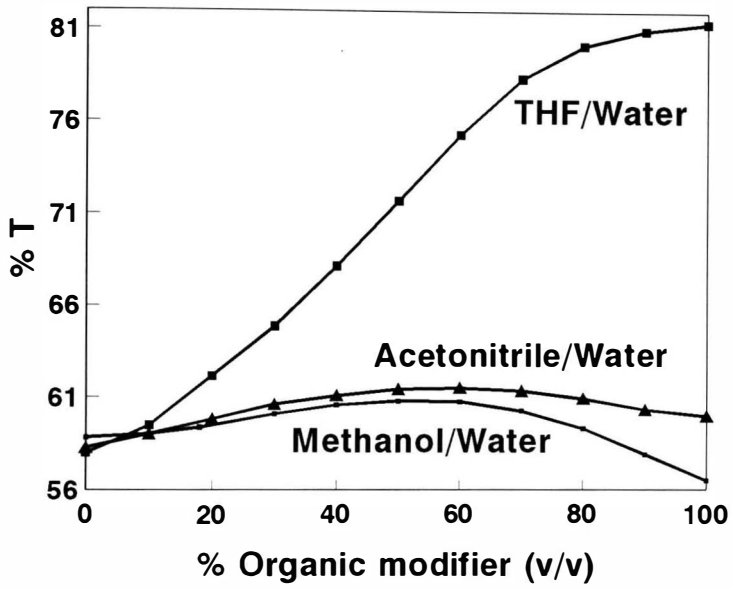

Figure 5-2. Transmittance of the bare silica/mobile phase (MeOH-water, ACN-water, and THF-water) system at 550 nm vs. mobile phase composition.

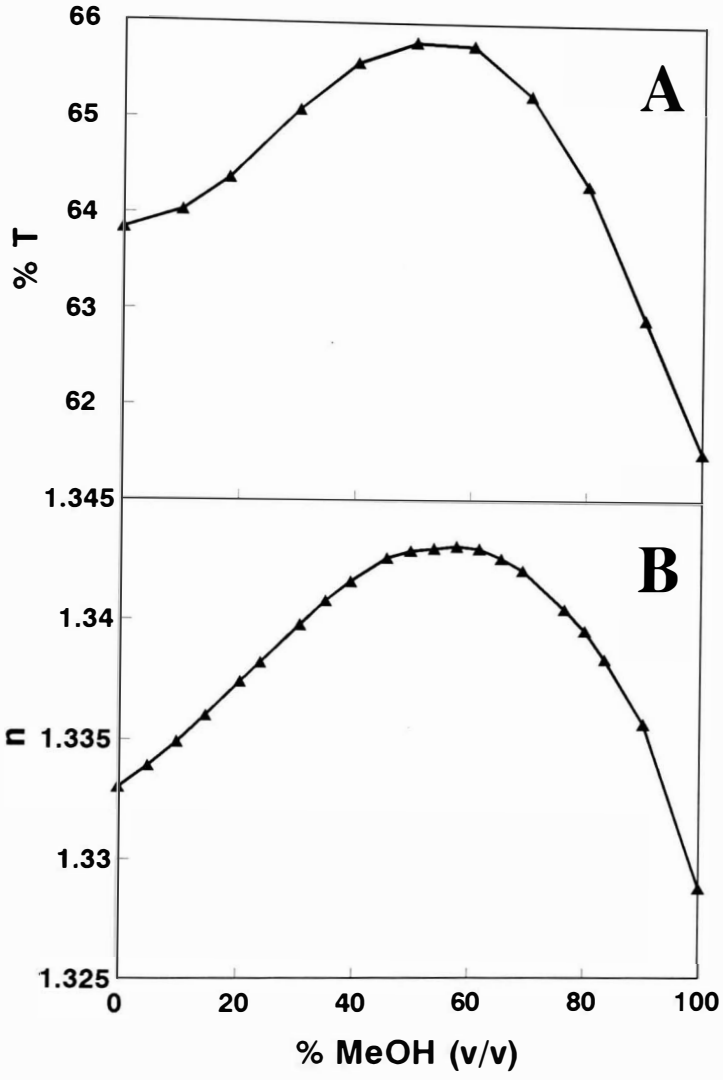

Figure 5-3. Transmittance of the bare silica/MeOH-water mobile phase system at 550 nm vs. mobile phase composition (A) and the refractive index of MeOH-water mixtures at 589.3 nm (sodium light) vs. solvent composition (B).

5-3-2 Transmittance of the Alkyl Bonded Silica/Eluent System vs. Eluent Composition

A plot of the transmittance of HDG $C_{18}H_{37}$ in MeOH-water eluent vs. the eluent composition is shown in Figure 5-4. The stationary phase was first equilibrated with MeOH. Then it was equilibrated with eluents containing decreasing amount of MeOH, specified as *downward equilibration*. The percent transmittance was measured once the value for transmittance had stabilized after changing to a new eluent. The data from downward equilibration are shown by the solid curve in Figure 5-4. After equilibration with water, the stationary phase was equilibrated with eluents containing increasing amount of MeOH, and this process is called *upward equilibration*. The dashed curve in Figure 5-4 represents the data from the upward equilibration experiment.

As the MeOH content, φ, decreases, the curve from downward equilibration shows five distinct regions, as shown in Figure 5-4. In region 1, as φ changes from 100% to 55%, the transmittance value for HDG $C_{18}H_{37}$ increases gradually. This is followed by a slight decrease over region 2, as φ changes from 55% to 20%. The changes in transmittance for HDG $C_{18}H_{37}$ in these two regions resemble those observed for bare silica in MeOH-water eluent, as shown in Figure 5-2. It can be concluded that there is no dramatic change in the

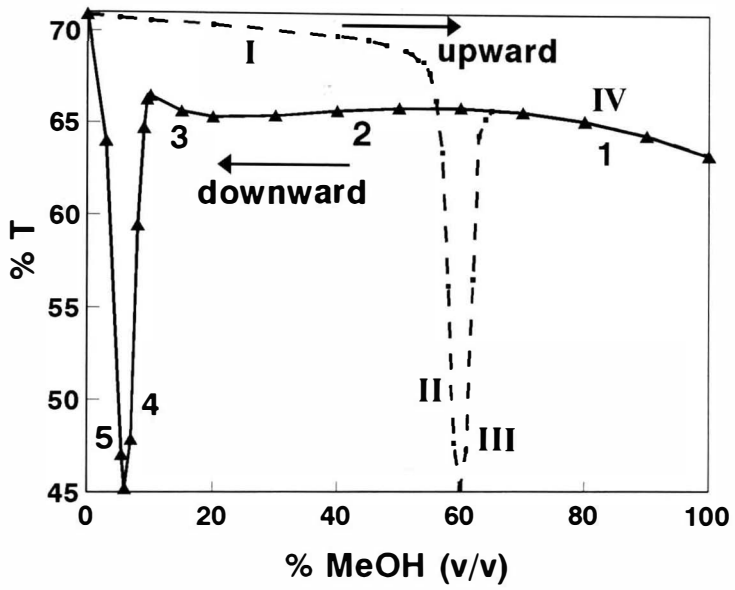

Figure 5-4. Transmittance of HDG $C_{18}H_{37}$ in MeOH-water eluent vs. eluent composition. The solid and dashed curves were obtained from downward and upward equilibration experiments, respectively.

interphase region over these eluent compositions. In region 3, as φ decreases from 20% to 10%, the transmittance of HDG $C_{18}H_{37}$ increases, which is not consistent the bare silica curve. The magnitude of this increase is small. Then the transmittance value decreases by a large amount in region 4, as φ decreases from 10% to 6%, followed by a pronounced increase in region 5, as φ decreases further from 6% to 0%. These dramatic changes in the transmittance value cannot be caused by changes in the refractive index of the eluent. They must be caused by significant changes in the interphase region.

With increasing φ, the curve from the upward equilibration experiment can be divided into four regions, labelled I through IV, as shown in Figure 5-4. In region I, as φ increases from 0% to 50%, the transmittance value for the HDG $C_{18}H_{37}$ phase decreases gradually. There is no dramatic change in the refractive index of the interphase region. Then there is an abrupt drop in the transmittance value over region II, as φ increases from 50% to 60%, followed by a sharp rise in transmittance in region III, when φ increases from 60% to 65%. In region IV, as φ increases from 65% to 100%, the curve overlaps with the one observed during the downward equilibration experiment.

When φ is lower than 65%, a hysteresis in the transmittance of the HDG $C_{18}H_{37}$ phase was observed. Different

transmittance values for the stationary phase were observed with the same eluent, depending on the eluent exposure history of the stationary phase.

Similar results were obtained for HDG $C_{18}H_{37}$ in ACN- and THF-water mixtures, as shown in Figures 5-5 and 5-6. Transmittance vs. composition plots were also obtained for other alkyl bonded phases, as shown in Appendix II. All these curves can be separated into different regions as in Figure 5-4, though some curves only exhibit some of the regions specified in Figure 5-4. All the regions are correlated to or associated with different physical processes, based on the results from direct wetting tests and some other experiments, as described in the following sections.

5-3-3 Theoretical Considerations in Direct Wetting Tests

The wetting of a stationary phase particle in an eluent is a total immersion of the solid particle in a liquid, i.e., a solid/vapor interface is replaced by a solid/liquid interface. The understanding of such a process is instructive to elucidate the process of interest in liquid chromatography, switching from one mobile phase to another mobile phase. A contact angle of less than 90° is required for the whole wetting process to be spontaneous. For an ideal solid cube particle as shown in Figure 2-2, the whole wetting process is

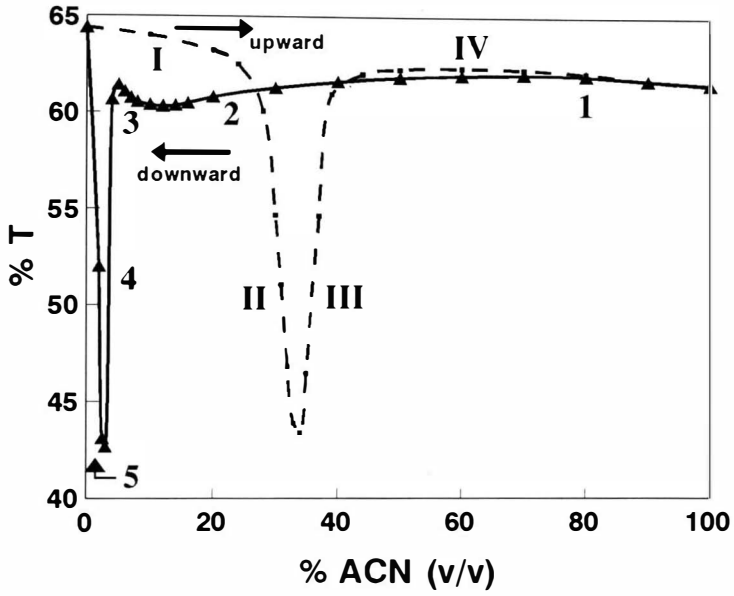

Figure 5-5. Transmittance of HDG $C_{18}H_{37}$ in ACN-water eluent vs. eluent composition. The solid and dashed curves were obtained from downward and upward equilibration experiments, respectively.

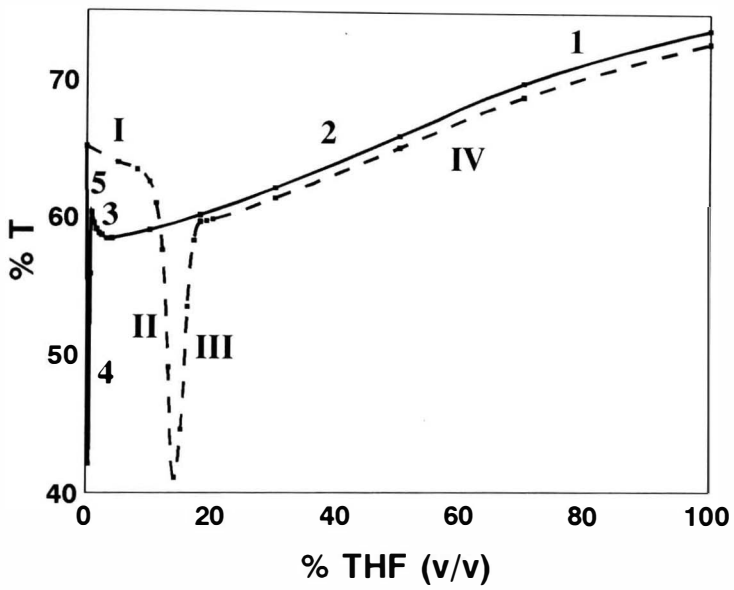

Figure 5-6. Transmittance of HDG $C_{18}H_{37}$ in THF-water eluent vs. eluent composition. The solid and dashed curves were obtained from downward and upward equilibration experiments, respectively.

composed of, in order, adhesional wetting, immersional wetting, and spreading wetting. The whole wetting process for a real stationary phase particle, however, is a combination of adhesional wetting, immersional wetting, spreading wetting, and capillary penetration, because of the porous nature and irregular shape of the particle. Each of the wetting steps must be spontaneous to make the whole wetting process spontaneous, requiring a contact angle of 0°. Without satisfying such a condition, the particle tends to float on the surface of the eluent. Work must be done to immerse the particle in the eluent. Such work can be provided by shaking or stirring the suspension. If the work required is of a very small magnitude, thermal convection and regular room vibration may cause the particle to become immersed.

In the above discussion, gravitational force has not been considered. For an ideal solid ball of radius r and density d_S, with exactly half of the ball above a liquid of density d_L and surface tension γ^{LV}, as shown in Figure 5-7, the total upward force is

$$F_u = - \gamma^{LV} \cdot \cos\theta \cdot 2\pi r \qquad (5\text{-}1)$$

The downward force equals to the weight of the ball minus the weight of the displaced liquid,

$$F_d = (4/3)\pi \cdot r^3 \cdot (d_S - 0.5 \cdot d_L) \cdot g \qquad (5\text{-}2)$$

The ratio of the upward force from surface tension to the gravitational force is

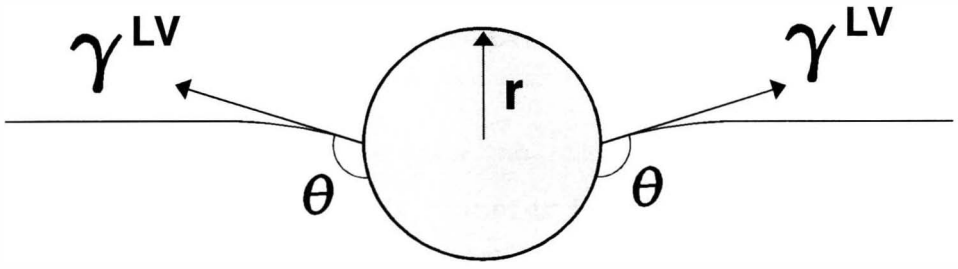

Figure 5-7. Floatation of a solid ball on a liquid.

$$F_u/F_d = - 3\gamma^{LV}\cdot\cos\theta/[2r^2\cdot(d_S - 0.5\cdot d_L)\cdot g] \quad (5\text{-}3)$$

Substituting values typical in RPLC, γ^{LV} 0.07275 N/m (water at 20°C), θ 93°,[79] r 5 μm, d_S 2200 kg/m^3 (fused quartz), d_L 998.2 kg/m^3 (water at 20°C), and g 9.8 m/s^2 into equation 5-3, a ratio of 1.4 x 10^4 is obtained. Even with a contact angle very close to 90°, e.g., 90.01°, the ratio is still 47. These calculations indicate that for particles with the magnitude of their size typical in HPLC, the contribution of gravitational force on the immersion of the particles into the eluent is in most cases negligible.

The contact angle has no direct bearing in liquid chromatography. The mass transfer between the eluent and the stationary phase is affected by the interfacial tension γ^{SL}. According to Young's equation, however, γ^{SL} can be obtained by knowing the contact angle. From wetting tests of the stationary phase particles, it is possible to obtain the eluent composition at which the contact angle becomes larger than 90°. At this point, γ^{SL} starts to be larger than the surface tension of the solid, γ^{SV}.

5-3-4 Direct Wetting Tests without Prewetting

Figure 5-8 shows the results from direct wetting tests without prewetting for YMC ODS-A 120A (25 μm) in ACN-water mixtures. Experimental observations are noted as followed:

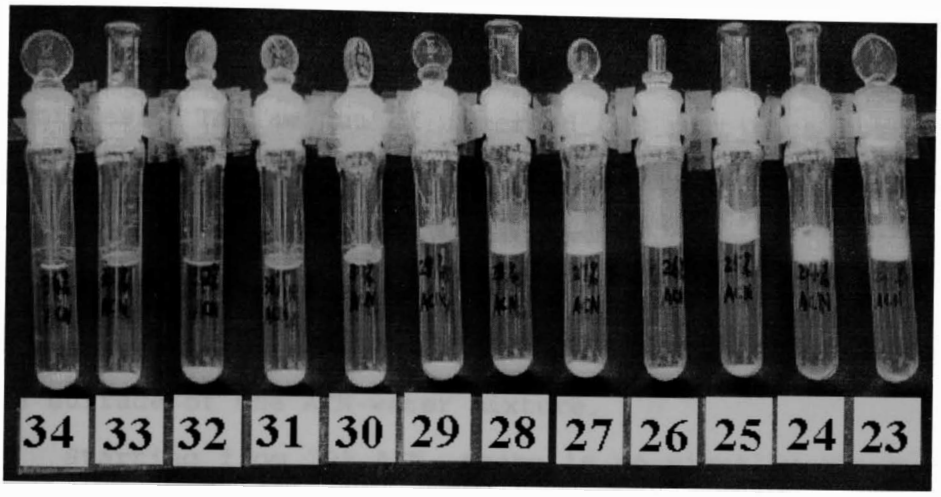

Figure 5-8. Octadecylsilylated silica (YMC ODS-A 120A, 25 μm) immersed in and floated on ACN-water mixtures. 0.050 g of ODS was added to each tube. The number below each tube indicates % ACN (v/v).

In 23% and 24% ACN (v/v) aqueous mixtures, only a minute amount of the ODS phase is on the bottom of the tubes. All the remaining ODS particles float on the surface of the ACN-water mixtures.

The amount of immersed ODS particles starts to increase at 25% ACN at the expense of the amount of floating ODS particles. The amount of immersed ODS particles increases continuously at 26%, 27%, 28%, and 29% ACN at the expense of the amount of floating ODS particles. The amount of floating ODS particles is still considerable at 28% ACN. At 29% ACN, however, only a minute amount of ODS particles still floats on the surface of the ACN-water mixture.

Starting from 29% ACN, there is no visually observable changes in the amount of immersed ODS particles. With 29% and 30% ACN, there is still a minute amount of ODS particles floating.

With 31% or more ACN, only a small patch of film formed by ODS particles is still on the surface of the ACN-water mixtures. A small patch of film persists even in pure ACN.

From the above wetting tests it can be concluded that 31% ACN is required to make dry YMC ODS-A 120A (25 μm) particles wetted. The amount of immersed ODS particles changes significantly in the range from 25% to 30% ACN.

Experimental observations from direct wetting tests without prewetting on YMC Butyl 120A (25 μm) in ACN-water

mixtures are described below:

At 30% ACN, only a very minute amount of butyl silica is immersed.

At 31% ACN, the amount of immersed butyl silica is several times of that at 30% ACN. However, the amount of floating butyl silica is still about 10 times of that immersed.

At 32% ACN, there is a huge increase in the amount of immersed butyl silica, accounting for about 80% of the total amount of butyl silica.

With 33% or more ACN, the amount of immersed butyl silica is not distinguishable. At 33% ACN, the amount of floating butyl silica is still considerable. At 34% ACN, there is only a minute amount of butyl silica floating. The decrease in the amount of floating butyl silica is very obvious from 31% to 35% ACN.

At 35% or 36% ACN, the amount of floating butyl silica is insignificant, though a small patch of butyl silica film persists. The experimental observations for the two tubes are not distinguishable.

Direct wetting tests performed for YMC Butyl 120A (25 μm) in ACN-water mixtures indicate that 35% ACN is required to wet the dry butylsilylated silica. The amount of immersed butyl silica particles changes significantly in the range from 31% to 34% ACN.

Using a single composition to describe the wetting of alkyl bonded silica, however, conceals the fact that particles of the same stationary phase have different wettabilities, indicated by gradual changes in the amount of immersed particles. A very small percentage of particles is not wetted even in ACN. Therefore, an ideal wetting test should be a curve of the amount of immersed particles vs. the solvent composition.

Wetting tests on YMC ODS-A 120A (25 μm) by titrating the ODS suspension in water using ACN as titrant have also been carried out. The disappearance of the film formed by ODS particles, as described in the literature,[57,60] never happened, consistent with the observation that a small patch of film persists even in ACN. The same problem exists for titration wetting tests on YMC Butyl 120A (25 μm). One solution is to neglect the small patch of low wettability particles in determining the end-point. Still, one must decide how small the size of the film is small enough to justify the arrival of the end-point. Therefore, the presence of a very small percentage of low wettability stationary phase makes the determination of the end-point in titration wetting tests a little subjective. Besides problems in end-point determination, wetting hysteresis, described later in the chapter, also makes titration wetting tests less reliable than direct wetting tests using premixed organic-water mixtures.

Particles of the same stationary phase have significantly different wettabilities. A more homogeneous stationary phase, however, is preferred for high separation efficiency. It is possible to use the direct wetting experiment to separate particles with different wettabilities, making stationary phases more homogeneous in wettability.

5-3-5 Correlation between the Results from Optical Transmittance Measurements and Those from Direct Wetting Tests——Physical Origin of Regions II and III

To compare the results from direct wetting tests and those from optical transmittance measurements, the transmittance vs. composition plots for YMC ODS-A 120A (25 μm) and YMC Butyl 120A (25 μm) in ACN-water mixtures are shown in Figures 5-9 and 5-10, respectively.

From Figure 5-9 it is clear that the composition range for dramatic changes in optical transmittance in regions II and III, 25% to 30% ACN, is the same as the range in which the amount of immersed ODS particles changes significantly.

Figure 5-10 shows that the composition range for the dramatic increase in optical transmittance in region III, 32% to 34% ACN, closely resembles the composition range in which the amount of immersed butyl silica particles changes significantly, 31% to 34% ACN.

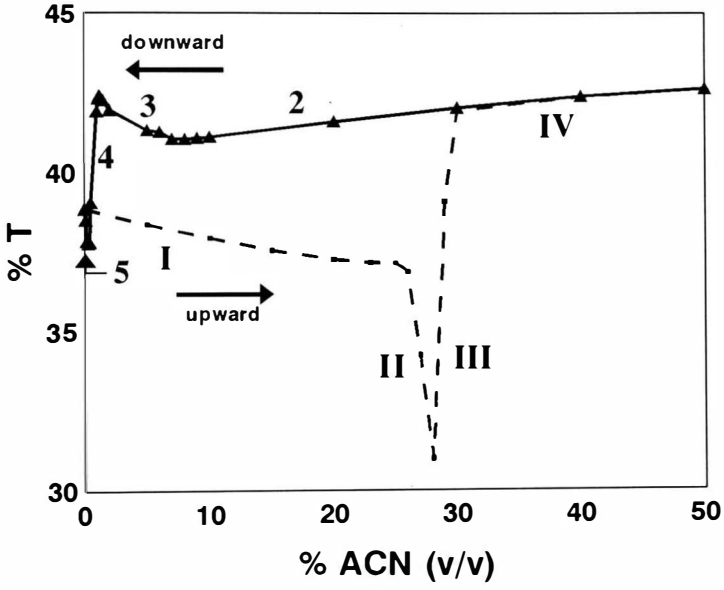

Figure 5-9. Transmittance of YMC ODS-A 120A (25 μm) in ACN-water eluent vs. eluent composition. The solid and dashed curves were obtained from downward and upward equilibration experiments, respectively.

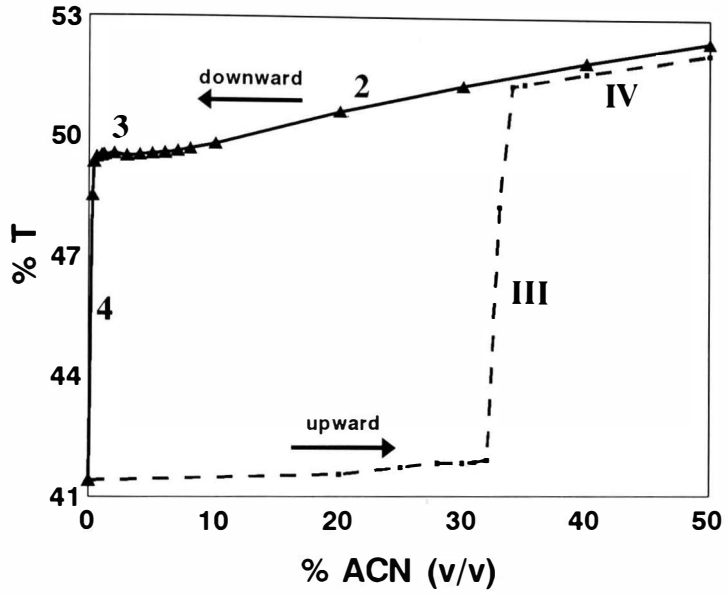

Figure 5-10. Transmittance of YMC Butyl 120A (25 μm) in ACN-water eluent vs. eluent composition. The solid and dashed curves were obtained from downward and upward equilibration experiments, respectively.

From the comparison between the results from optical transmittance measurements and those from direct wetting tests, it can be concluded that the dramatic changes in optical transmittance in regions II and III are correlated with immersional wetting of alkyl bonded silica particles.

5-3-6 Relation between the Dramatic Transmittance Changes in the Downward and Upward Equilibration Experiments——Physical Origin of Regions 4 and 5

LiChroprep RP-18 was chosen to study the relation between the dramatic transmittance changes in the downward and upward equilibration experiments. The transmittance vs. composition plot for LiChroprep RP-18 in MeOH-water mixtures is shown in Figure 5-11. The downward equilibration experiment depicted in Figure 5-11 ended with water. If the downward equilibration experiment ends before a certain region, *i*, appears, from the disappearance of a certain region, *j*, in the following upward equilibration experiment, it can be concluded that region *j* is the reversal of region *i*. By changing the direction of equilibration at different eluent compositions, different regions in the downward and upward equilibration experiments can be related to each other, if there exists a relationship.

With the downward equilibration ending at 1% MeOH, in

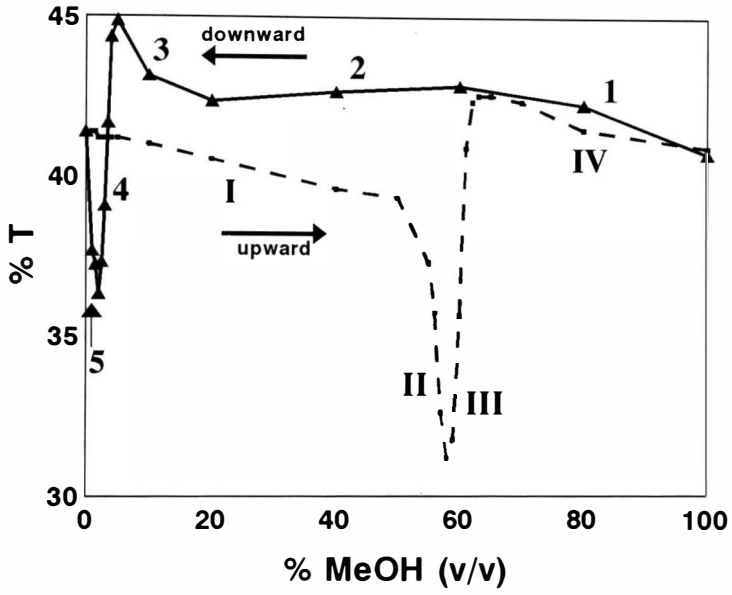

Figure 5-11. Transmittance of LiChroprep RP-18 in MeOH-water eluent vs. eluent composition. The solid and dashed curves were obtained from downward and upward equilibration experiments, respectively.

region 5, as shown in Figure 5-12, all the 4 regions in the upward equilibration experiment still exist. The magnitude of transmittance decrease in region II, however, is significantly smaller than that in Figure 5-11.

With the downward equilibration ending at 3% or 5% MeOH, before the appearance of region 5, as shown in Figures 5-13 and 5-14, region II disappears in the following upward equilibration experiment. This indicates that region II in upward equilibration is the reversal of region 5 in downward equilibration.

With the downward equilibration ending at 6% MeOH, before the appearance of region 4, as shown in Figure 5-15, region III disappears in the following upward equilibration experiment. This indicates that region III in upward equilibration is the reversal of region 4 in downward equilibration.

Considering the observation that alkyl bonded silica particles become wetted in regions II and III, it can be concluded that alkyl bonded phases are becoming nonwetted in regions 4 and 5. The eluent composition at the boundary between region 3 and region 4, is therefore defined as *the nonwetting limit*. Correspondingly, the composition at the boundary between region III and region IV, is defined as *the rewetting limit*.

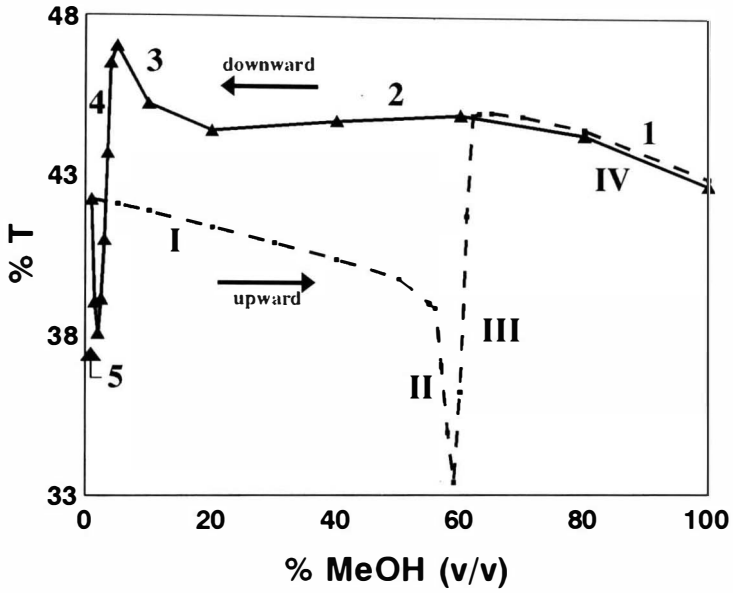

Figure 5-12. Transmittance of LiChroprep RP-18 in MeOH-water eluent vs. eluent composition. The solid and dashed curves were obtained from downward and upward equilibration experiments, respectively. The direction of equilibration was changed at 1% MeOH.

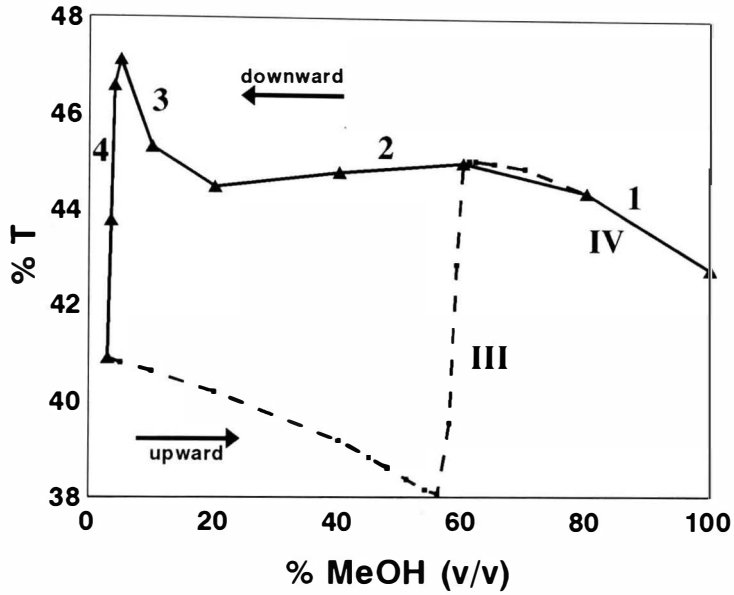

Figure 5-13. Transmittance of LiChroprep RP-18 in MeOH-water eluent vs. eluent composition. The solid and dashed curves were obtained from downward and upward equilibration experiments, respectively. The direction of equilibration was changed at 3% MeOH.

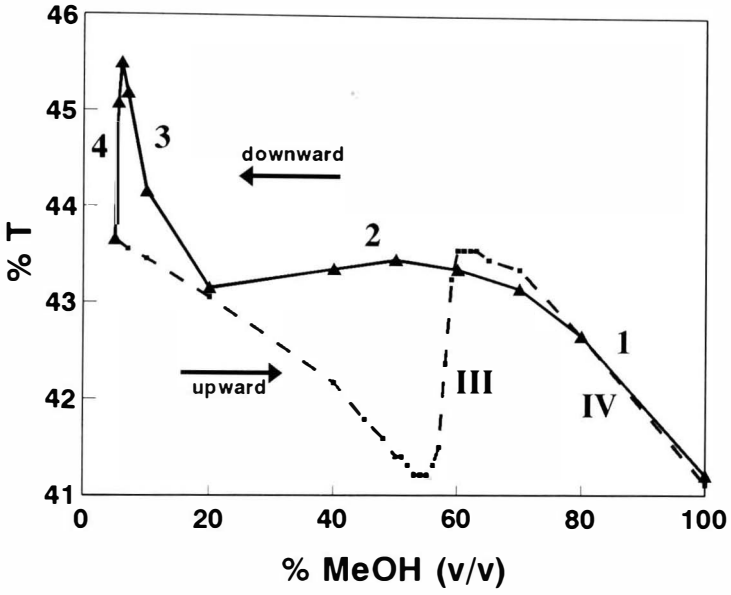

Figure 5-14. Transmittance of LiChroprep RP-18 in MeOH-water eluent vs. eluent composition. The solid and dashed curves were obtained from downward and upward equilibration experiments, respectively. The direction of equilibration was changed at 5% MeOH.

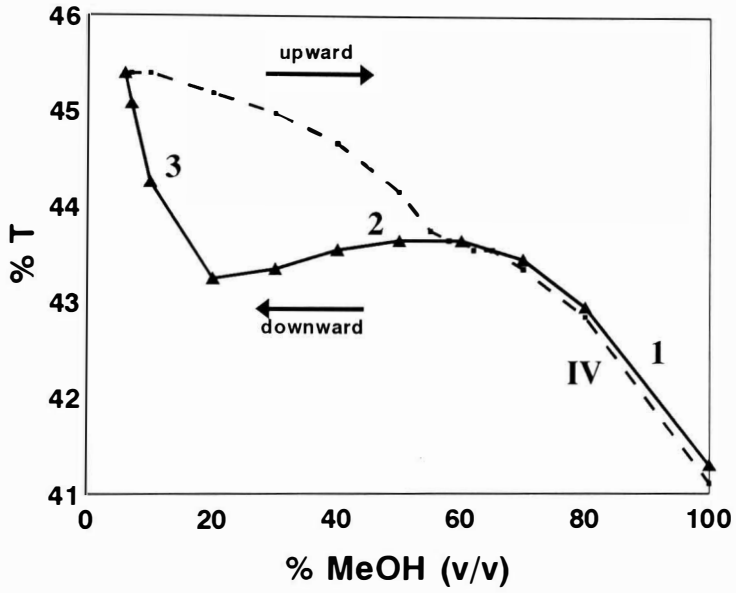

Figure 5-15. Transmittance of LiChroprep RP-18 in MeOH-water eluent vs. eluent composition. The solid and dashed curves were obtained from downward and upward equilibration experiments, respectively. The direction of equilibration was changed at 6% MeOH.

5-3-7 Wetting of Dry Alkylsilylated Silica by Upward Equilibration——Physical Origin of Regions II and III

In earlier transmittance vs. composition plots, a dry stationary phase was first equilibrated with an organic modifier, followed by downward and upward equilibration experiments. As an alternative approach, a dry alkyl bonded phase was first equilibrated with water. Then the stationary phase was equilibrated with eluents containing increasing amount of organic modifier. The transmittance vs. composition plot for LiChroprep RP-18 in MeOH-water mixtures obtained in such a way is shown in Figure 5-16. The curve closely resembles the upward equilibration curve shown in Figure 5-11 and can be separated into four regions in the same way. The MeOH content at which region IV starts is defined as *the initial wetting limit*. The initial wetting limit for LiChroprep RP-18, 65% MeOH (v/v), is a little higher than the rewetting limit, 63% MeOH (v/v). The results for LiChroprep RP-18 and other ODS phases are summarized in Table 5-2. Though SUPELCOSIL LC-18 and Spherisorb ODS1 are wetted in water after initial wetting with MeOH, the initial wetting of these phases starting with the dry state can only be achieved with an eluent containing a certain amount of MeOH.

The transmittance of the LiChroprep RP-18 phase in air, i.e., before the introduction of water, is only 8.9%, which is

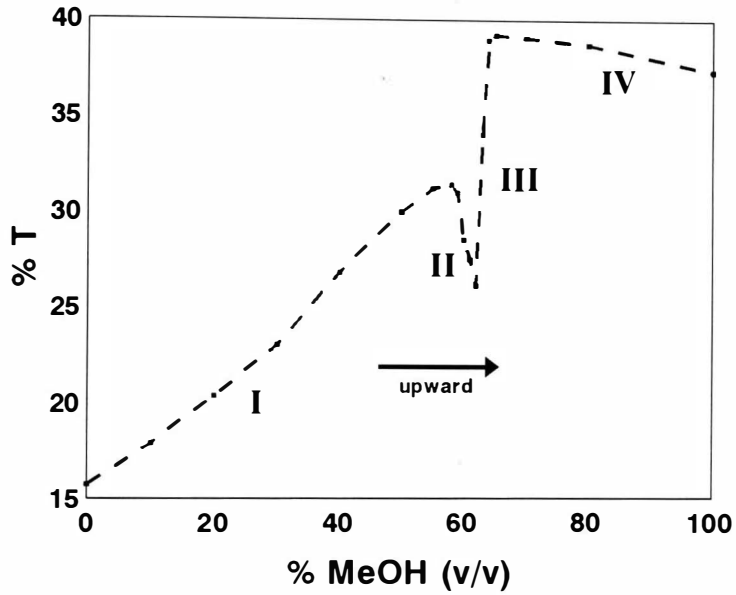

Figure 5-16. Transmittance of LiChroprep RP-18 in MeOH-water eluent vs. eluent composition. The plot was obtained by upward equilibration experiment starting with dry stationary phase.

Table 5-2. Composition range in % MeOH (v/v) for various regions in the wetting of dry octadecylsilylated silica, by upward equilibration

Stationary phase	I	II	III	IV
LiChroprep RP-18	0-58	58-62	62-65	65-100
SUPELCOSIL LC-18	0-53	53-57	57-59	59-100
Spherisorb ODS1	0-10	10-15	15-20	20-100

much lower than the value in the presence of MeOH-water mixtures. The low transmittance value in air is caused by the large difference in the refractive index between the stationary phase and air, as indicated later in this chapter.

The transmittance of the LiChroprep RP-18 phase in water is very low, due to the inability to replace all the air in the pores between and in the LiChroprep RP-18 particles. Air replacement with solvent by capillary action is unfavorable when the eluent cannot wet the stationary phase particles. In Figure 5-16, the increase in transmittance in region I may result from a gradual replacement of air by the eluent. As the MeOH content increases, more and more air is replaced by the eluent.

For a dry alkyl bonded silica, the bonded alkyl chains can only interact among themselves to form a hydrocarbon film on the surface of the silica support. The increase in transmittance in region I has been attributed to the gradual replacement of air by the eluent. The disruption of the hydrocarbon film is likely to happen in regions II and III. Regions 4 and 5 are the reversal of regions III and II, respectively. Therefore, it can be proposed that bonded alkyl chains collapse to form a hydrocarbon film in regions 4 and 5.[79,135]

5-3-8 Physical Origin of Region 3

From the effects of various parameters of alkyl bonded silica on the transmittance change in region 3, the physical origin of region 3 can be investigated. One parameter which significantly affects the magnitude of the transmittance change in region 3 is chain length. YMC ODS-A 120A (25 μm), YMC Octyl 120A, and YMC Butyl 120A were used to study the chain length effects. The transmittance vs. composition plots for YMC ODS-A 120A (25 μm) and YMC Butyl 120A in ACN-water mixtures are shown in Figures 5-9 and 5-10. The plot for YMC Octyl 120A in ACN-water eluent is shown in Figure 5-17. The transmittance change in region 3 for the octadecyl, octyl, and butyl phase is 1.38, 0.23, and 0.06, respectively.

The most likely physical process involved in region 3 is the desolvation of bonded alkyl chains. In eluents with high organic modifier concentrations, the bonded alkyl chains are solvated by organic modifier.[89] In regions 4 and 5, when the stationary phase is not wetted, the bonded alkyl chains collapse onto the silica support to form a hydrocarbon film.[79,135] Therefore, a desolvation process should be involved in region 3, just before the collapse of bonded alkyl chains. More organic modifier is likely to be enriched in the bonded alkyl layer with a longer chain length. Therefore, the desolvation process should have a more significant effect on

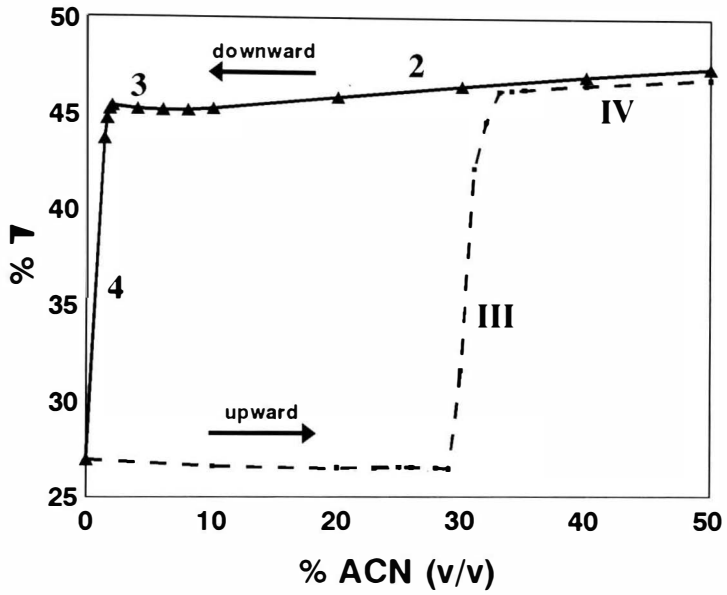

Figure 5-17. Transmittance of YMC Octyl 120A (15 μm) in ACN-water eluent vs. eluent composition. The solid and dashed curves were obtained from downward and upward equilibration experiments, respectively.

the transmittance change for alkyl bonded silica with a longer chain length, as observed for the three YMC phases.

5-3-9 Wetting Hysteresis

It is clear now that the transmittance hysteresis in the transmittance vs. composition plots is caused by hysteresis in the wetting or solvation of alkyl bonded silica. Sections 5-3-2 and 5-3-6 presented some observations for wetting hysteresis. Figures 5-11 to 5-15 in Section 5-3-6 indicate that wetting hysteresis becomes less significant as the downward equilibration ends with increasing MeOH content, from 0% to 6%. Figures 5-18, 5-19, and 5-20 show the transmittance vs. composition plots with the downward equilibration ending with 10%, 15%, and 25% MeOH, respectively. From Figure 5-20 it can be concluded that there is no hysteresis if the direction of equilibration is changed in regions 1 and 2. If the direction of equilibration is changed in regions 3 to 5, as shown in Figures 5-11 to 5-15, 5-18, and 5-19, hysteresis exists when the MeOH content in the eluent is lower than the rewetting limit, 63% (v/v).

Wetting hysteresis appears when alkyl bonded silica is nonwetted or not well solvated. It coexists with slow kinetics, as described later in this chapter.

The existence of wetting hysteresis indicates that the

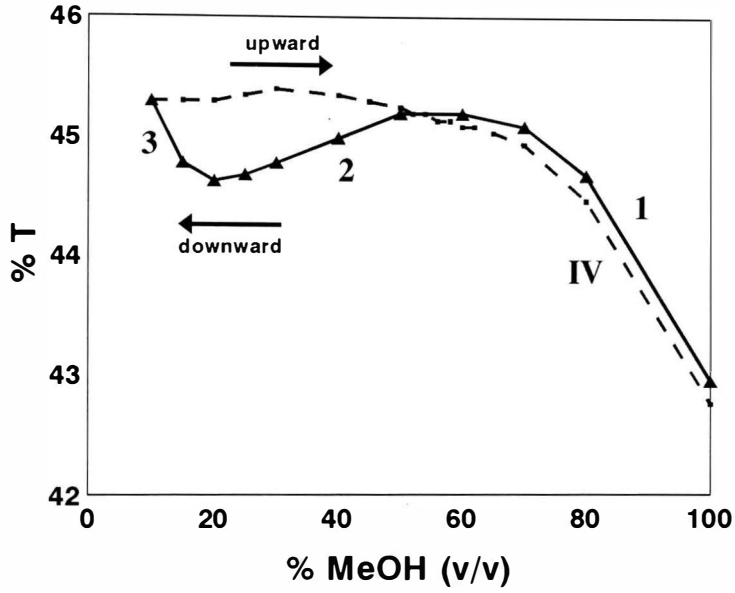

Figure 5-18. Transmittance of LiChroprep RP-18 in MeOH-water eluent vs. eluent composition. The solid and dashed curves were obtained from downward and upward equilibration experiments, respectively. The direction of equilibration was changed at 10% MeOH.

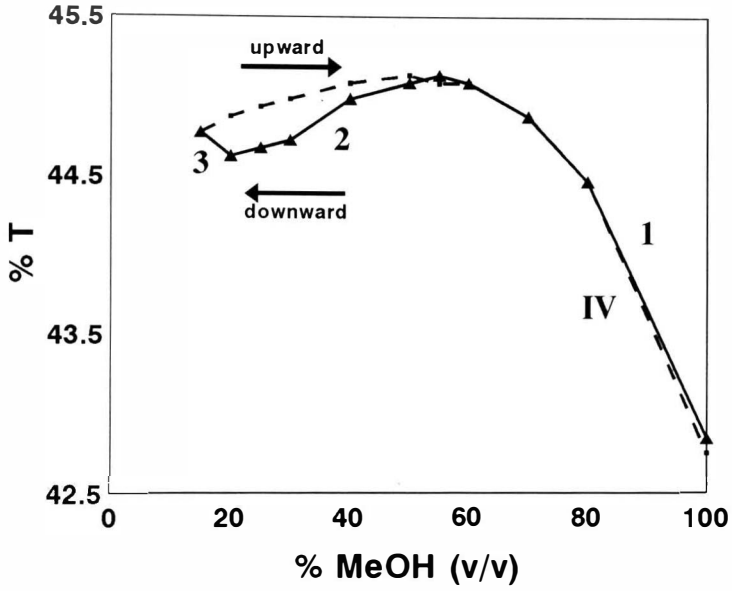

Figure 5-19. Transmittance of LiChroprep RP-18 in MeOH-water eluent vs. eluent composition. The solid and dashed curves were obtained from downward and upward equilibration experiments, respectively. The direction of equilibration was changed at 15% MeOH.

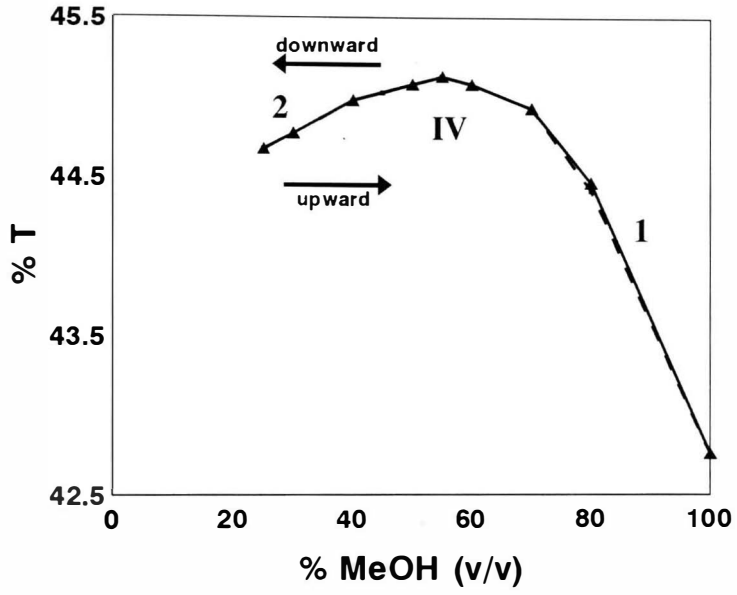

Figure 5-20. Transmittance of LiChroprep RP-18 in MeOH-water eluent vs. eluent composition. The solid and dashed curves were obtained from downward and upward equilibration experiments, respectively. The direction of equilibration was changed at 25% MeOH.

stationary phase/mobile phase system may not reach a thermodynamic equilibrium when the organic modifier content in the mobile phase is less than the rewetting limit. The states of wetting reached in the downward and upward equilibration experiments should be considered as metastable.

5-3-10 Direct Wetting Tests with Prewetting

The direct wetting tests without prewetting have been correlated to upward equilibration experiments. The direct wetting tests with prewetting should be related to downward equilibration experiments. Wetting hysteresis should also be related to the differences between the results from direct wetting tests with and without prewetting.

ACN-water mixtures containing 23%, 10%, 1%, 0.6%, and 0% (v/v) ACN have been tested for the wetting of YMC Butyl 120A prewetted by ACN. After the replacement of ACN by any of the mixtures cited above, all the particles stay on the bottom of the tube before shaking. The nonwetting limit for the butyl phase is 0.6% ACN. Therefore, a contact angle (if applicable) larger than 90°, i.e., an interfacial tension γ^{SL} larger than the surface tension of the solid γ^{SV}, is expected for the butyl phase in water. The particles, however, remain on the bottom of the tube because the density of the particles is higher than water.

The rise of the particles above the liquid can only be facilitated by an upward force, which can be obtained by bringing the particles into contact with the gas phase. The contact of the particles with the gas phase can be conducted by bringing air bubbles to the bottom of the tube. The air bubbles are likely to attach to the particles when the interfacial tension γ^{SL} is larger than the surface tension of the solid γ^{SV}, then lift the particles above the liquid. Shaking can bring air bubbles into contact with the particles or bring the particles into the gas phase directly, lift the particles above the liquid.

After shaking, all the particles in water float on the surface of liquid. In 10% ACN, only a minute amount of particles stays on the bottom of the tube. In 23% ACN, however, only a minute amount of particles floats on the mixture, comparable with the direct wetting test without prewetting where this occurs for 34% ACN.

Direct wetting tests on YMC ODS-A 120A (25 μm) (prewetted by ACN) in water gave the same results as those on YMC Butyl 120A.

Direct wetting tests with prewetting are similar with the titration wetting test starting with a suspension of stationary phase particles in organic modifier, using water as the titrant.[73] From the wetting hysteresis phenomenon observed in our wetting tests it can be concluded that this titration

wetting test[73] should produce different results from the titration wetting test starting with a suspension of stationary phase particles in water.[57,60] Both of the two titration wetting tests described in the literature are complicated by temporary high local concentration of titrant, which introduces wetting hysteresis during the titration process.

In the literature, there are often difficulties in producing alkyl bonded phase suspensions in water-rich eluents. Such a suspension, however, can be easily produced using the procedure for the direct wetting test with prewetting, described in the experimental section.

Overall, direct wetting tests are much less informative in studying the wetting of alkyl bonded silica than optical transmittance measurements.

5-3-11 Wetting Affected by the Characteristics of Alkyl Bonded Silica and by the Nature of Organic Modifier

The composition ranges for different regions in the transmittance vs. composition plots for various alkyl bonded phases are tabulated in Table 5-3. The results for three YMC ODS-A 120A phases with different particle sizes show no correlation between the wetting and the particle size. From Table 5-3 it can be seen that the YMC ODS-A phase with a

Table 5-3. Composition range in % organic modifier (v/v) for various regions in the transmittance vs. composition plots for alkyl bonded phases

Stationary phases				Downward				Upward			
				1&2	3	4	5	I	II	III	IV
HDG $C_{18}H_{37}$			MeOH	100-20	20-10	10-6	6-0	0-50	50-60	60-65	65-100
			ACN	100-12	12-5	5-3	3-0	0-20	20-34	34-41	41-100
			THF	100-3.6	3.6-0.8	0.8-0.4	0.4-0	0-10	10-14	14-18	18-100
LiChroprep RP-18†			MeOH	100-20	20-5	5-2	2-0	0-50	50-58	58-63	63-100
			ACN	100-11	11-1.9	1.9-0.3	0.3-0	0-28	28-33	33-38	38-100
			THF	100-3.2	3.2-0.15	0.15-0.04	0.04-0	0-11	11-14	14-16	16-100
SUPELCOSIL LC-18			MeOH	100-10	10-0	N/A	N/A	N/A	N/A	N/A	60-100
			ACN	100-6	6-0	N/A	N/A	N/A	N/A	N/A	30-100
			THF	100-3.2	3.2-0	N/A	N/A	N/A	N/A	N/A	14-100
Spherisorb ODS2			MeOH	100-15	15-0	N/A	N/A	N/A	N/A	N/A	60-100
Spherisorb ODS1			MeOH	100-0	N/A	N/A	N/A	N/A	N/A	N/A	0-100
YMC ODS-A	120A	10 μm	ACN	100-5	5-0	N/A	N/A	N/A	N/A	N/A	20-100
		25 μm	ACN	100-7	7-1.2	1.2-0.3	0.3-0	0-25	25-28	28-30	30-100
		50 μm	ACN	100-10	10-0	N/A	N/A	N/A	N/A	N/A	20-100
	200A	25 μm	ACN	100-4	4-0	N/A	N/A	N/A	N/A	N/A	30-100
	300A	25 μm	ACN	100-3	3-0	N/A	N/A	N/A	N/A	N/A	30-100
YMC Octyl 120A			ACN	100-7	7-1.9	1.9-0	N/A	N/A	N/A	29-33	33-100
YMC Butyl 120A			ACN	100-6	6-0.6	0.6-0	N/A	N/A	N/A	32-34	34-100
YMC TMS 120A			ACN	100-0	N/A	N/A	N/A	N/A	N/A	N/A	0-100

† Without any pretreatment, the transmittance vs. composition plots for LiChroprep RP-18 in MeOH-water and ACN-water mixtures resemble the plot for bare silica, exhibiting only regions 1 and 2 and no hysteresis. The data in the table were obtained by rinsing LiChroprep RP-18 with THF, chloroform, or 1,2-dichloroethane before equilibration with MeOH or ACN. LiChroprep RP-18 was always pretreated with THF in this research, if not otherwise specified. Such pretreatment effects were not observed for the other stationary phases listed in the table.

larger pore size is easier to wet. More experimental work should be performed, however, to obtain a conclusive relationship between the wetting and pore size of alkyl bonded silica.

Comparing the results for Spherisorb ODS1 and ODS2 in Table 5-3, it is clear that the higher the surface coverage of an ODS phase, the more difficult to wet, consistent with other reports in the literature.[57,73,76] Chain length is expected to affect the wetting of alkyl bonded silica.[57,76] The methyl phase is obviously easier to wet than silica bonded with longer alkyl groups, probably due to the shielding of the hydrophilic silica surface. A correlation between the wetting and chain length of alkyl bonded phase cannot be obtained solely based on the data presented in Table 5-3, however.

The less polar the organic modifier, the lower the organic modifier content required to wet an ODS phase, which agrees with observations in the literature[73] and validates our wetting test using optical transmittance measurements.

5-3-12 Monitoring of the Equilibration Process by Optical Transmittance

In the literature, the stationary phase equilibration process has only been monitored indirectly by measuring the retention of model compounds. When a stationary phase reaches

equilibrium, all its physical and chemical characteristics, including solute retention and optical transmittance, should become constant. Therefore, the equilibration of the stationary phase can also be evaluated by measuring its optical transmittance. When the eluent was changed from MeOH to a MeOH-water mixture, the equilibration process was monitored by recording the transmittance value of the HDG $C_{18}H_{37}$ phase as a function of time. The equilibration processes from MeOH to MeOH-water mixtures in regions 2, 3, and 4, with 30%, 15%, and 7% of MeOH, respectively, are plotted in Figure 5-21. For all the measurements described in this section, the flow rate is 0.25 mL/min.

The equilibration curves in Figure 5-21 follow the same trend observed in Figure 5-4 for downward equilibration. The different regions defined for the downward equilibration curve in Figure 5-4 can also be found in the corresponding equilibration curves in Figure 5-21. This implies that the same sequence of events resulting in changes in the wetting of the stationary phase is followed by the two processes.

To show the details of the curves, the plots in Figure 5-21 present the equilibration processes for the first 60 min. The complete equilibration process may take a much longer time. The time required to bring the HDG $C_{18}H_{37}$ phase to a constant transmittance value, or equilibrium, from MeOH to a MeOH-water mixture, is plotted vs. the eluent composition in

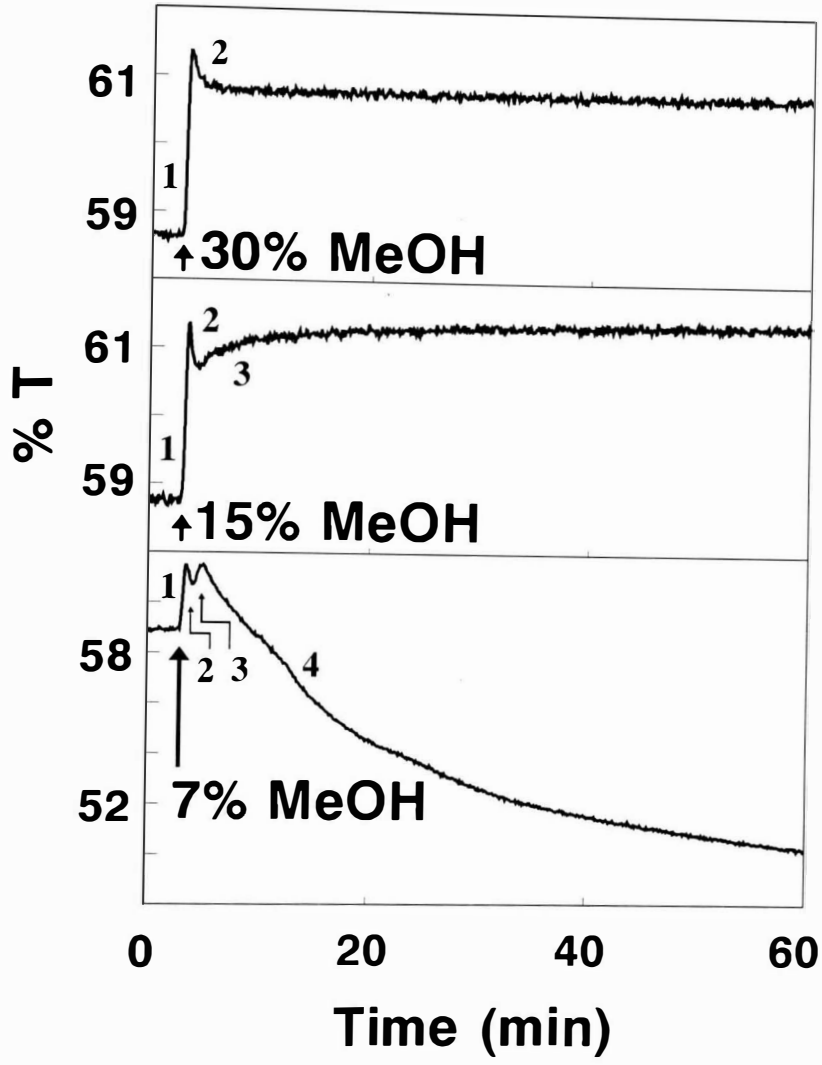

Figure 5-21. Transmittance of HDG $C_{18}H_{37}$ vs. time. The mobile phase was changed from MeOH to a MeOH-water eluent with 30%, 15%, and 7% MeOH. Arabic numbers are used to label different regions of the equilibration curves.

Figure 5-22. From the inset in Figure 5-22, it can be seen that it took about 1 min to equilibrate the HDG $C_{18}H_{37}$ phase when the eluent was changed from MeOH to a MeOH-water mixture in region 1. From MeOH to MeOH-water mixtures in region 2, the equilibration time increases with decreasing MeOH content, but the time required for equilibration is still less than 5 min. In regions 3, 4, and 5, with φ less than 20%, the equilibration time increases rapidly with decreasing MeOH content. From the dramatic increase in the equilibration time from region 2 to region 3, it can be concluded that the solvation or wetting of the HDG $C_{18}H_{37}$ phase is significantly different in these two regions.

Wetting hysteresis appears when the direction of equilibration changes in regions 3, 4, or 5, indicates that slow kinetics may be a requirement for the appearance of wetting hysteresis.

5-3-13 Adsorption of Water onto Residual Silanol Groups Observed by Optical Transmittance Measurements

Interactions of water with residual silanol groups are indispensable in the wetting of alkyl bonded silica. In the transmittance vs. composition plot for YMC Butyl 120A in ACN-water mixtures, as shown in Figure 5-23, a small decrease in transmittance can be observed when the eluent is changed from

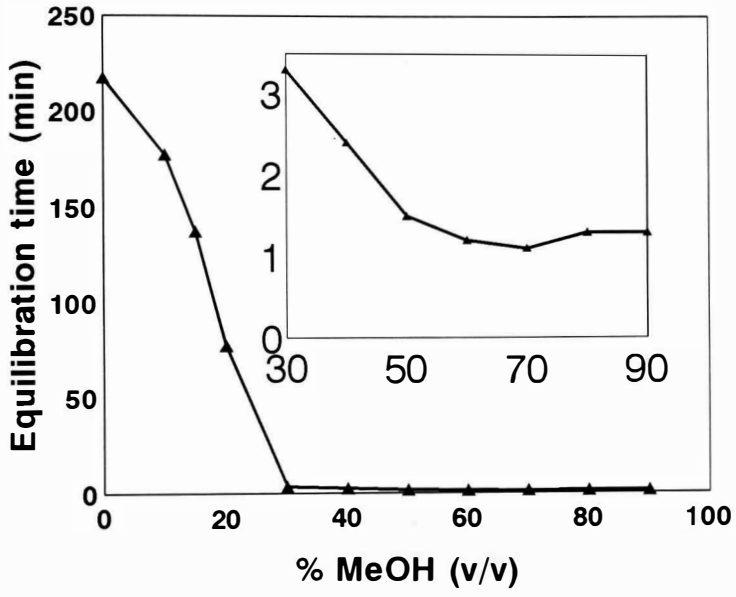

Figure 5-22. Equilibration time for HDG $C_{18}H_{37}$, from MeOH to a MeOH-water eluent, vs. eluent composition. The flat part of the curve is plotted in the inset with a different ordinate scale.

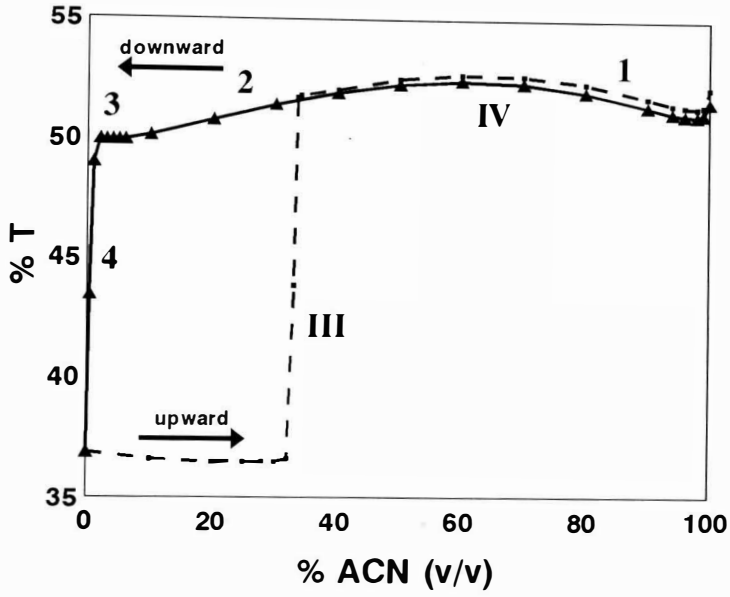

Figure 5-23. Transmittance of YMC Butyl 120A (25 μm) in ACN-water eluent vs. eluent composition. The solid and dashed curves were obtained from downward and upward equilibration experiments, respectively.

organic modifier to an organic-water mixture containing a small amount of water, which cannot be explained by the change in the refractive index of the eluent. The most likely reason for the small decrease in transmittance is the adsorption of water onto the residual silanol groups. The same phenomenon was also observed for all the other stationary phases tested, including YMC ODS-A 120A (25 μm), 200A, and 300A.

The equilibration process for the butyl phase when the eluent was changed from ACN to 98% ACN, then back to ACN, is shown in Figure 5-24. The equilibration from ACN to 98% ACN took 2 minutes. The reversal process, the equilibration from 98% ACN to ACN, however, took 12.6 minutes. This is consistent with the water adsorption hypothesis. The strong interactions between water and residual silanol groups make the removal of water from the silica surface much more difficult than the adsorption of water onto residual silanol groups.

The amount of adsorbed water may only be several molecular layers. The optical transmittance measurements, however, can easily detect such adsorption. This indicates that the transmittance of the stationary phase/eluent system is very sensitive to the change of the composition and structure of the interphase region.

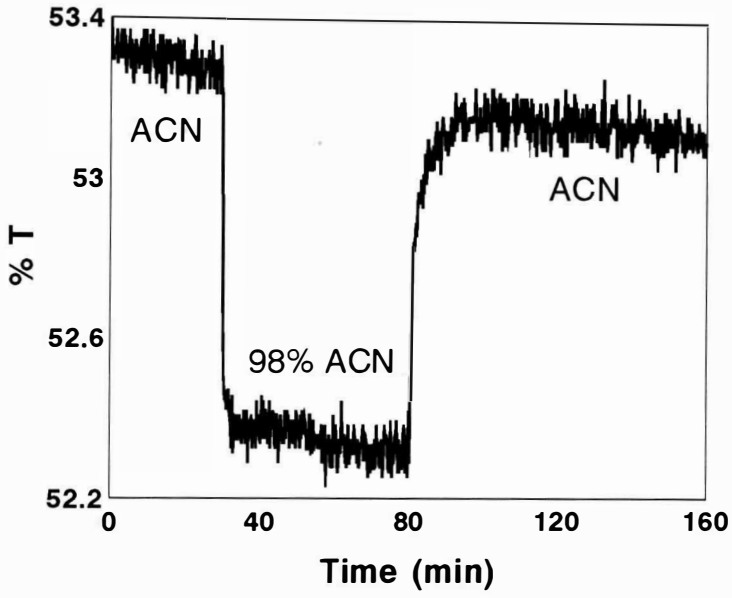

Figure 5-24. Transmittance of YMC Butyl 120A (25 μm) vs. time. The mobile phase was changed from ACN to 98% ACN-water, then back to ACN.

5-3-14 Effect of Flow and Temperature on the Equilibration Process as the Eluent is Switched from MeOH to Water

As shown in Figure 5-22, it takes a very long time to equilibrate the HDG $C_{18}H_{37}$ phase with water as the eluent. During the equilibration process, MeOH is replaced by water, and, in addition, we propose that the C_{18} chains on the silica surface are reorganizing to form a more energetically favorable configuration. We questioned whether these two processes occur over the same time frame. If not, how much longer does it take the C_{18} chains to reorganize after MeOH is replaced with water? To answer these questions, the following experiments were carried out.

For the measurement of the equilibration time from MeOH to water in Figure 5-22, the eluent was kept at a flow rate of 0.25 mL/min during the whole equilibration process. If the flow of water is stopped before the stationary phase reaches equilibrium, the optical transmittance of the HDG $C_{18}H_{37}$ particles keeps changing, as shown in Figure 5-25. Monitoring of the transmittance is continued until a constant value is finally reached. The dependence of *the final constant transmittance* on the volume of water passed through the cell before the flow is stopped is shown in Figure 5-26. The final constant transmittance does not change as long as the volume of water passed through the cell is larger than 4.35 mL. The

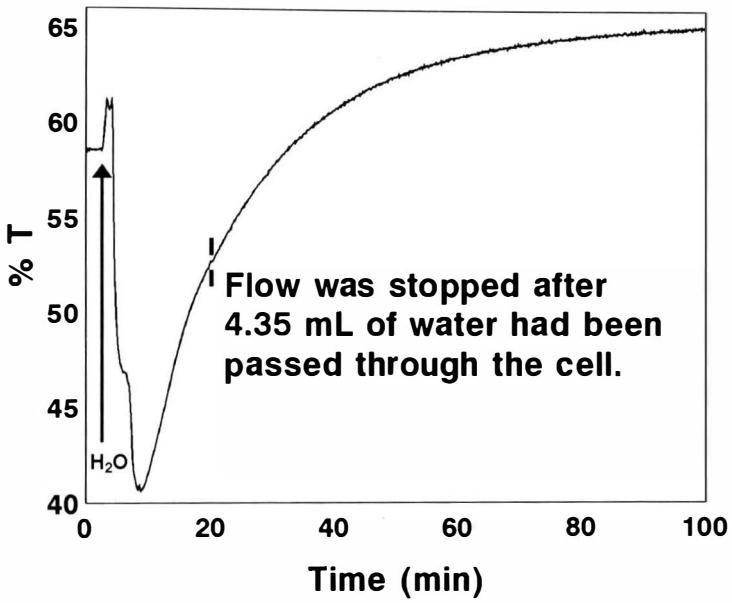

Figure 5-25. Transmittance of HDG $C_{18}H_{37}$ vs. time. The mobile phase was changed from MeOH to water, at a flow rate of 0.25 mL/min. After 4.35 mL of water was passed through the flow cell, the flow was stopped.

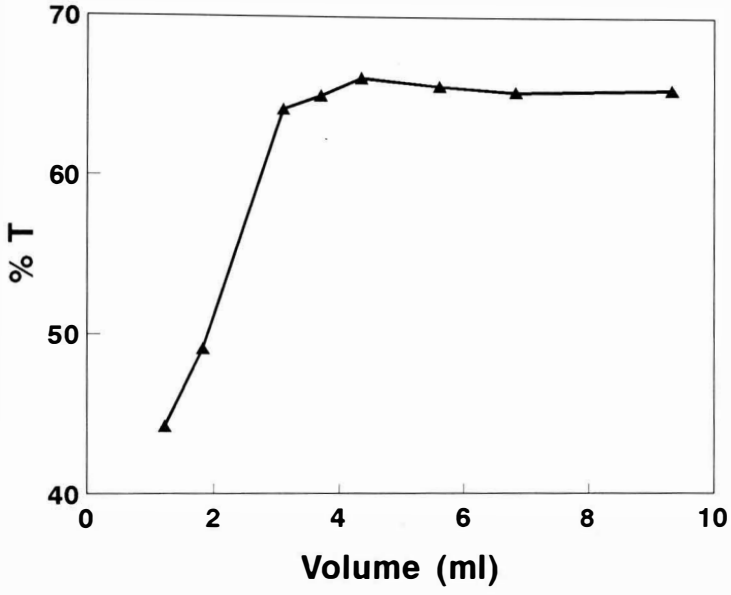

Figure 5-26. Final constant transmittance of HDG $C_{18}H_{37}$ vs. the volume of water passed through the flow cell before the flow was stopped.

final constant transmittance at this point, 66.2%, is within the experimental error of the constant transmittance when the flow is not stopped, which is (66.0 ± 0.2) %. It can be concluded that MeOH is completely replaced by water after 4.35 mL of water is passed through the cell. Eluent replacement is a relatively fast process. We propose that the slow change in the transmittance after eluent replacement is caused by C_{18} chain reorganization.

The equilibration process, from MeOH to water, was monitored both at 23°C and 48°C. The equilibration curves for the first 100 min are shown in Figure 5-27. For both equilibration processes in Figure 5-27, the eluent was kept at a flow rate of 0.25 mL/min. The difference between the final constant transmittance values at the two temperatures is small. We interpret this to mean that the difference in the final configuration of the chains of the HDG $C_{18}H_{37}$ phase at the two temperatures is not significant. As shown in Figure 5-27, it takes much less time to reach equilibrium at 48°C than at 23°C. One possible explanation is that chain reorganization is a slow process and requires a significant activation energy. An increase in temperature can significantly accelerate this chain reorganization process.

Hydrocarbon films formed by association among bonded alkyl chains in contact with water can be transformed to a different state after heating.[56,70-72] Gilpin et al.[56,70,71]

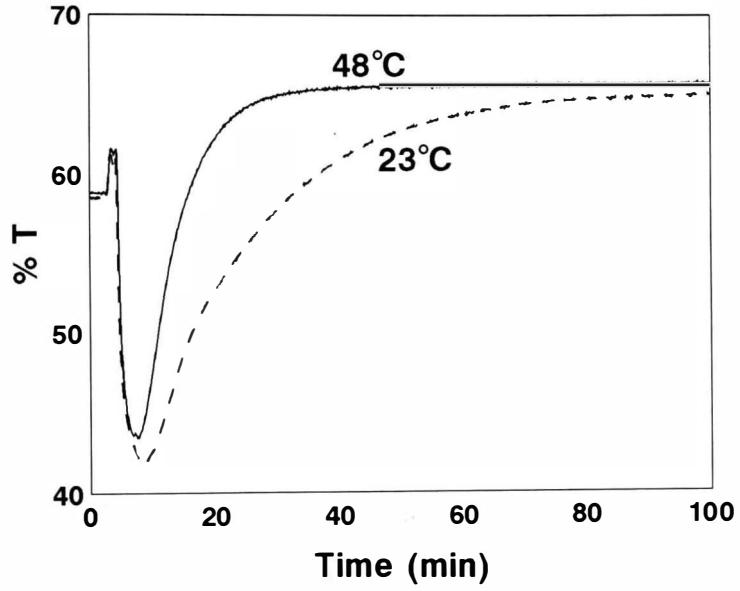

Figure 5-27. Effect of temperature on the equilibration process for HDG $C_{18}H_{37}$ when the eluent was switched from MeOH to water. The eluent flow rate was 0.25 mL/min.

believe that bonded alkyl chains rearrange to an extended state upon heating and remain in such a configuration after cooling. A different surface model was proposed by Hammers and Verschoor[72] with convincing experimental evidence. They believe that a rough hydrocarbon film is first formed because the degree of ordering among bonded alkyl chains is low. After heating, the bonded alkyl chains rearrange to an extended pattern. During cooling, a smoother hydrocarbon film is obtained because of the more ordered associations among the bonded alkyl chains. Retention times before heating were larger than the ones obtained after heating.[70,72] Retention times on a column with a higher cooling rate after heating were larger than the ones on a column with a lower cooling rate.[72] Two elution peaks were obtained for one solute if the column was rapidly cooled while a solute was on the column.[72] All of this evidence strongly favors the latter model. In our experiment, no evidence for differences in chain organization at room temperature, 23°C, and elevated temperature, 48°C, was observed. A temperature higher than 48°C may be required to rearrange C_{18} chains to an extended state or the extended state does not have a big change in refractive index.

5-3-15 Factors Affecting the Transmittance of the Stationary Phase/Eluent System

Though the changes in transmittance in the transmittance vs. composition plots have been associated with the solvation or wetting of alkyl bonded silica, it is still not clear why the solvation and wetting of alkyl bonded silica can introduce such changes in the transmittance of the stationary phase/eluent system. To solve this problem, it is necessary to understand how the transmittance of the stationary phase/eluent system is affected by various parameters of the system.

The first parameter to be investigated is the refractive index of the eluent. The transmittance values of a bare silica, LiChrosorb SI 100, and an ODS phase, SUPELCOSIL LC-18, in water and various pure organic solvents were measured and plotted against the difference in the refractive index between the stationary phase and the solvent, as shown in Figure 5-28. The refractive index of the stationary phase is taken as that of fused silica, 1.458. The refractive index values of fused silica and the solvents are from reference 136. It is obvious from the bare silica curve in Figure 5-28 that the smaller the difference in the refractive index between the stationary phase and the eluent, the higher the transmittance of the stationary/eluent system, which is consistent with optical

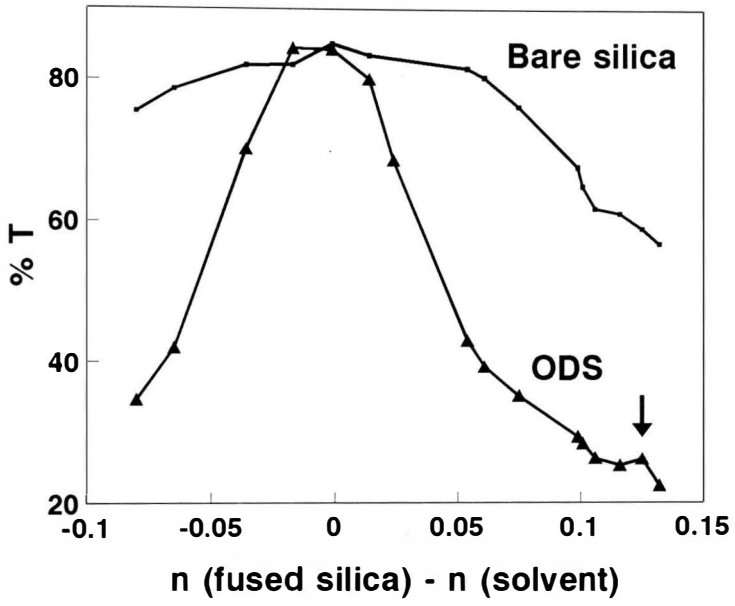

Figure 5-28. Transmittance of LiChrosorb SI 100 and SUPELCOSIL LC-18, in water and various pure organic solvents vs. the difference in the refractive index between silica and the solvent. The point indicated by an arrow is for SUPELCOSIL LC-18 in water.

theory for a two phase system. For the ODS curve, the above rule holds except for the point indicated by an arrow, which is for ODS in water. The interphase region may not form a distinct third phase when the C_{18} chains are significantly solvated. In water, however, the C_{18} layer on the surface of silica may form a distinct third phase, leading to the breakdown of the rule holding only for a two phase system. In addition, the decrease in transmittance with an increase in the refractive index difference is much more pronounced with the ODS phase as compared to the silica phase, which is probably due to the smaller particle size of the ODS phase.

The transmittance values of various stationary phases in MeOH and ACN are listed in Table 5-4 to show the effects of particle size, pore size, alkylsilylation, and chain length on the transmittance of the stationary phase/eluent system. Comparing the transmittance values for YMC ODS-A 120A (25 μm), 200A, and 300A in ACN, it can be concluded that the pore size does not have a significant effect on the transmittance of the stationary phase/eluent system. It is obvious that the larger the particle size, the higher the transmittance of the stationary phase/eluent system. Alkylsilylation, which adds one more phase in the stationary phase/eluent system, decreases the transmittance of the stationary phase/eluent system. From Table 5-4 it is also obvious that the longer the chain length, i.e., the larger the size of the interphase

Table 5-4. Transmittance of various stationary phases in ACN and MeOH

Stationary phases	Particle size (μm)	Pore size (Å)	% T	
			in ACN	in MeOH
LiChrosorb SI 100	30		59.99	56.51
HDG $C_{18}H_{37}$	125-150		61.52	58.37
LiChroprep RP-18	25-40		40.49	38.37
SUPELCOSIL LC-18	5	100	26.17	22.07
Spherisorb ODS2	5	80	22.60	19.19
Spherisorb ODS1	5	80		20.00
YMC ODS-A 120A	10	120	39.08	
YMC ODS-A 120A	25	120	42.34	
YMC ODS-A 120A	50	120	53.98	
YMC ODS-A 200A	25	200	47.81	
YMC ODS-A 300A	25	300	41.88	
YMC Octyl 120A	15	120	46.99	
YMC Butyl 120A	25	120	53.17	
YMC TMS 120A	15	120	55.72	

region between the silica support and the bulk eluent, the lower the transmittance value of the stationary phase/eluent system.

The decrease in the transmittance upon the adsorption of water onto the silica surface may be explained by the addition of another phase, though very thin, in the stationary phase/eluent system. It was also found that sorption of hexadecane to alkyl bonded silica in MeOH, which enlarged the interphase region, reduced the transmittance of the stationary phase/eluent system.

5-3-16 Interpreting the Transmittance Changes in Various Regions

The increase in transmittance in region 1 is caused by the increase in the refractive index of the eluent, as shown in Figure 5-3, which reduces the difference in refractive index between the stationary phase and the eluent. The transmittance decreases in region 2 because the refractive index of the eluent decreases.

The increase in optical transmittance in region 3 may be attributed to the desolvation of the bonded alkyl chains, which reduces the size of the interphase region.

When the bonded alkyl chains collapse on the silica surface to form a hydrocarbon film, a distinct boundary

between the stationary phase and the eluent is formed. This discontinuity in substance introduces a discontinuity in refractive index, resulting in the dramatic decrease in transmittance in region 4. Other processes may also be solely or partially responsible for the dramatic decrease in transmittance in region 4. When alkyl bonded silica is not wetted, air dissolved in the mobile phase and mobile phase vapor may accumulate in the pores in alkyl bonded silica particles to form gas phase pockets, leading to a decrease in transmittance.

In region 5, the rough hydrocarbon film formed in region 4 may reorganize itself to produce a smoother and denser layer. Though the distinct boundary still exists, the size of the interphase region is reduced, resulting in the increase in transmittance. Hydrocarbon films formed on different particles may associate with one another to reduce the exposure of the hydrophobic films to the mobile phase. Such a process can reduce the number of interfaces, resulting in a increase in transmittance.

5-3-17 Solvatochromic Studies

Solvatochromic studies were conducted to correlate the surface polarity of the stationary phase with the wetting of the stationary phases. The π^* value for the LiChroprep RP-

18/eluent system, measured using N,N-diethyl-4-nitroaniline, vs. the MeOH content in the eluent, φ, is plotted in Figure 5-29. The π^* value for the eluent is also plotted in Figure 5-29 as a reference.

When φ is high, however, the retention of the π^* dye is low. With decreasing φ, the π^* value on the curves for the stationary phase first increases, which simply reflects the increase in the dipolarity of the eluent because more dye molecules are present in the eluent than in the stationary phase. Then the curves for the stationary phase descend and deviate from the curve for the eluent because of the increase in retention. In the downward equilibration experiment, when φ decreases from 50% to 0%, the π^* value for the stationary phase increases, indicating the π^* dye molecules retained by the stationary phase are at least partially exposed to the eluent. If the dye molecules are entirely within the bonded C_{18} layer, the desolvation and collapse of the bonded C_{18} chains would have resulted in a decreasing surface dipolarity. After equilibration with water, the decrease in the surface dipolarity with φ from 0 to 40% mainly reflects the decrease in the dipolarity of the eluent because no significant changes in the wetting or solvation of the bonded C_{18} layer were observed from the transmittance measurements, as shown in Figure 5-11. When φ is below the rewetting limit, different π^* values for the stationary phase were obtained with the same

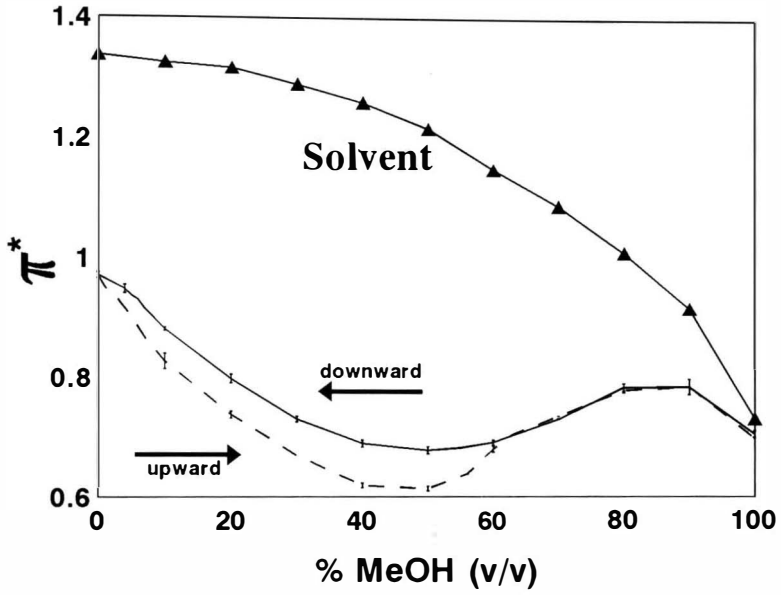

Figure 5-29. Dipolarity for MeOH-water eluent (specified as "Solvent") and LiChroprep RP-18 vs. eluent composition. The solid and dashed curves were obtained from downward and upward equilibration experiments, respectively.

eluent, when equilibrated from opposite directions. In the same eluent, the nonwetted stationary phase exhibits a lower surface dipolarity than the wetted stationary phase. The rewetting of LiChroprep RP-18 eliminates the hysteresis in surface dipolarity. There is no dramatic changes, or 'break', in surface dipolarity, as observed for the transmittance. This is understandable because dipolarity and transmittance are affected by different physical parameters.

If the direction of equilibration is changed in region 4, at 3% MeOH, before the appearance of region 5, the hysteresis in surface dipolarity is almost indistinguishable from experimental uncertainties, as shown in Figure 5-30. This indicates that the bonded C_{18} layer must have reorganized itself in region 5, as proposed earlier in this chapter. For N,N-diethyl-4-nitroaniline retained by the stationary phase, to reduce the exposure of the hydrophobic part of the molecule to water-rich eluent, the molecule may prefer to lie flat onto the hydrocarbon film formed by collapsed C_{18} chains. When the bonded C_{18} layer changes from a rough film to a smooth one, the contact area between the dye molecule and the hydrocarbon film increases, resulting in a lower surface dipolarity if contacting the same eluent.

No differences in the π^* value for SUPELCOSIL LC-18 with the same eluent equilibrated from opposite directions are observed.

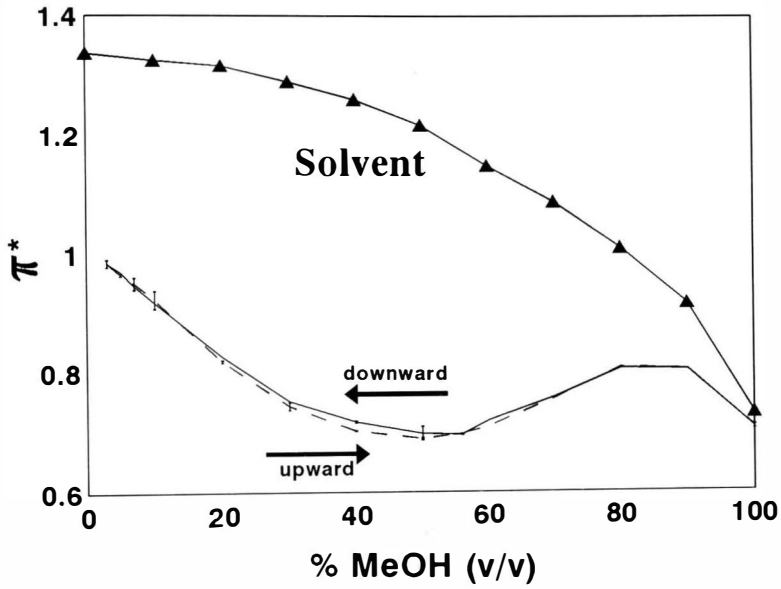

Figure 5-30. Dipolarity for MeOH-water eluent (specified as "Solvent") and LiChroprep RP-18 vs. eluent composition. The solid and dashed curves were obtained from downward and upward equilibration experiments, respectively.

Though hysteresis in transmittance is significant when the direction of equilibration is changed in regions 3, 4, or 5, hysteresis in surface dipolarity is only significant when the direction of equilibration is changed in region 5. This indicates that optical transmittance is more sensitive to the changes in the wetting or solvation of alkyl bonded silica.

The π^* values for HDG $C_{18}H_{37}$, SUPELCOSIL LC-18, and LiChroprep RP-18 from the downward equilibration experiment are plotted vs. the eluent composition in Figure 5-31. When the MeOH content, φ, is below 50%, the contribution from the π^* dye present in the eluent to the measured π^* value can be neglected. No significant differences in π^* value among the three ODS phases were observed when φ is above 10%, i.e., when all the three stationary phases are still wetted. The dipolarity for HDG $C_{18}H_{37}$ is significantly higher than that of the other two ODS phases when φ falls below 10%, the non-wetting limit for HDG $C_{18}H_{37}$. The π^* values for LiChroprep RP-18 are significantly lower than those for SUPELCOSIL LC-18 when φ is below 5%, the non-wetting limit for LiChroprep RP-18. It should be noted that the dipolarities of the two non-wetted ODS phases in water deviate in opposite directions, i.e., one non-wetted phase has a higher dipolarity, and the other has a lower dipolarity than the wetted phase, indicating diversities in the properties of different ODS phases.

An attempt was made to correlate the surface hydrogen

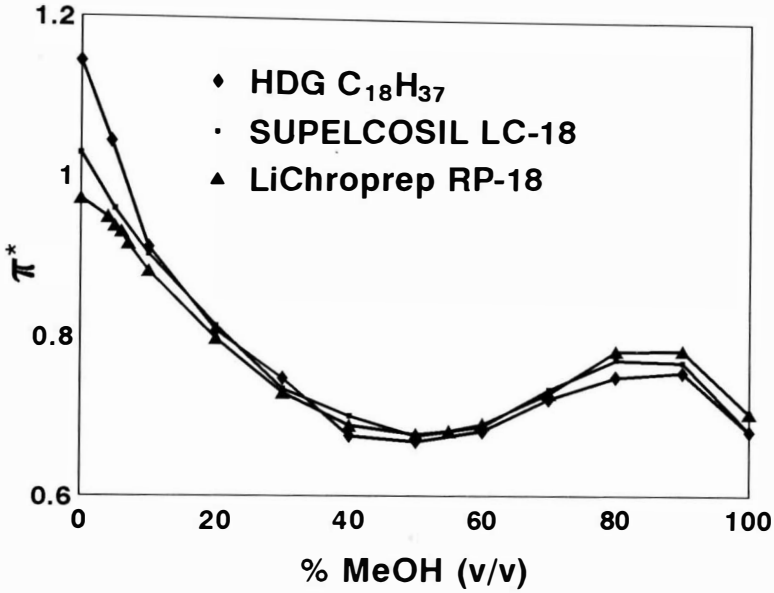

Figure 5-31. Dipolarity for HDG $C_{18}H_{37}$, SUPELCOSIL LC-18, and LiChroprep RP-18 in MeOH-water eluent vs. eluent composition. The curves were obtained from downward equilibration experiments.

bonding acidities, represented by α values,[102] of the ODS phases with their wetting behavior. Using two α dyes, ET-33[108] and DCMPVP,[109] LiChroprep RP-18 and SUPELCOSIL LC-18 were studied. Most of the α dye molecules, however, are protonated in the ODS phase/organic-water mixture system, making the α value measurement impossible. The accessibility of residual silanol groups, confirmed by the protonation of the α dyes, may be very important in the wetting of the ODS phases.

5-3-18 Chromatographic Studies

The retention of caffeine on a 10 x 4.6 mm LiChroprep RP-18 column in MeOH-water eluents was measured. The eluent flow rate was set to 0.5 mL/min. The column was equilibrated with MeOH and eluents with decreasing MeOH content. The plot of the retention time of caffeine vs. the MeOH content, φ, is shown in Figure 5-32. It took a long time to equilibrate the column and the reproducibility of the retention data is low. For each eluent, the retention time of caffeine was plotted against the equilibration time. After the retention time of caffeine became stabilized, more measurements were made. The average of the stabilized retention times was taken as the retention time of caffeine in that eluent.

In Figure 5-32, the retention time of caffeine on LiChroprep RP-18 initially increases with decreasing φ. When

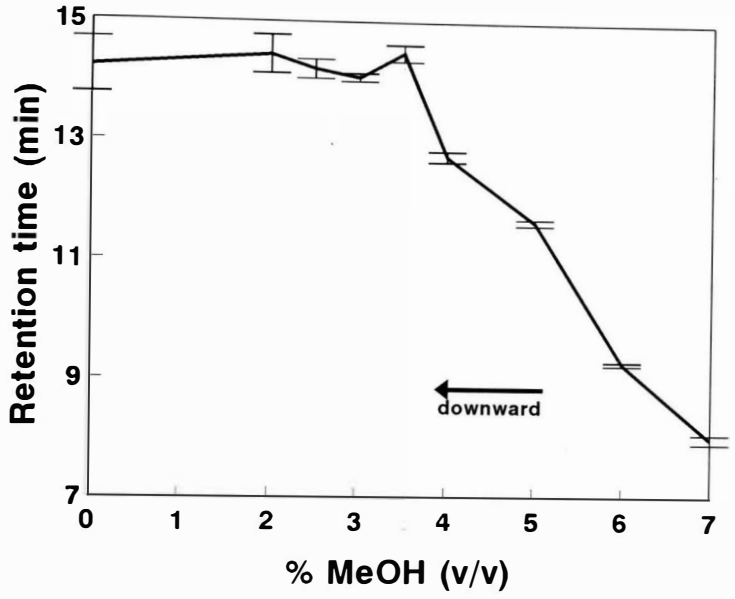

Figure 5-32. Retention of caffeine on LiChroprep RP-18 vs. the MeOH content in the eluent. The arrow indicates the direction of equilibration.

φ is lower than 3.5% (v/v), the retention time of caffeine does not change significantly or even decreases with decreasing φ.

After equilibration with water, the column was equilibrated by an eluent containing 3% (v/v) MeOH. The retention time of caffeine on LiChroprep RP-18, preequilibrated with water, in the eluent with 3% (v/v) of MeOH was measured. Then the column was equilibrated by an eluent with 10% (v/v) of MeOH. Again the retention time of caffeine in the eluent with 3% (v/v) of MeOH was measured. The retention time of caffeine on LiChroprep RP-18, preequilibrated with each of the eluents with 30%, 50%, 55%, 60%, 80%, and 100% (v/v) of MeOH, in the eluent with 3% (v/v) of MeOH was measured. The retention time of caffeine in the eluent with 3% (v/v) of MeOH vs. the MeOH content in the preequilibration eluent is plotted in Figure 5-33. When the MeOH content in the preequilibration eluent is in the range of 50 to 60% (v/v), there is a jump in the retention time of caffeine.

The results of the chromatographic studies on LiChroprep RP-18 are similar to those on HDG $C_{18}H_{37}$.[134] When the ODS phase is not wetted, chromatographic retention on it is significantly reduced. The nonwetted phase can only become more wetted using eluents with MeOH contents close to the rewetting limit. The column pressure during the retention

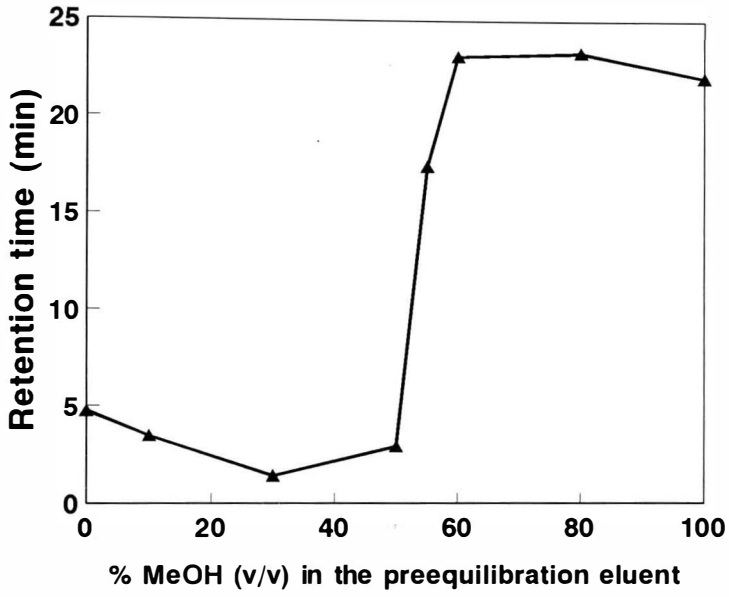

Figure 5-33. Retention of caffeine on LiChroprep RP-18 in 3% (v/v) MeOH-water eluent vs. the MeOH content in the preequilibration eluent (see text for explanation).

measurements on LiChroprep RP-18 is in the range of 30 to 45 atm, indicating that wetting effects are also significant at pressures much higher than ambient pressure.

The transmittance of Spherisorb ODS2, which only shows regions 1, 2, and 3, also depends on the eluent exposure history if the MeOH content in the eluent is less than 60% (v/v). Chromatographic measurements were performed to study the effect of eluent exposure history on retention to see if there is an effect similar to that for the LiChroprep RP-18 phase. The retention of caffeine in a 20% (v/v) MeOH eluent was measured. If the preequilibration eluent is MeOH, the retention time of caffeine on a 75 x 4.6 mm Spherisorb ODS2 (3 μm) column is 6.70 $\pm$ 0.04 min. If the preequilibration eluent is water, the retention time is 6.66 $\pm$ 0.04 min. The difference is statistically not significant. The wetting hysteresis observed when the direction of equilibration is changed in region 3 is not significant enough to affect retention. Optical transmittance is much more sensitive to the wetting of ODS phases than chromatographic measurements.

5-4 Conclusion

Optical transmittance of the alkyl bonded silica/eluent system is very sensitive to changes in the composition and structure of the interphase region. The changes in optical

transmittance over the eluent composition can be separated into different regions, which may be associated with various physical processes in the interphase region, including adsorption of water onto residual silanols, desolvation of bonded alkyl chains, collapse of alkyl chains onto silica to form a rough hydrocarbon film, and chain reorganization to form a smooth hydrocarbon film. Other processes, e.g., gas phase pocket formation in the pores and particle aggregation, may also be responsible for some of the transmittance changes.

Some changes in optical transmittance can be well correlated to the results from direct wetting tests. From this correlation, the rewetting limit and initial wetting limit have been defined. Direct wetting tests, however, cannot reveal the nonwetting limit.

Wetting hysteresis can be observed clearly in optical transmittance measurements, which indicates the alkyl bonded silica/eluent system may exist in metastable states, instead of thermodynamic equilibrium. Slow kinetics may be a prerequisite for the appearance of wetting hysteresis.

Different alkyl bonded phases have different wetting behaviors, depending on bonding density, alkyl chain length, etc. Alkyl bonded phases can be wetted more easily using a less polar organic modifier.

A much longer equilibration time is required if the stationary phase is nonwetted or not well solvated. Both the

surface dipolarity and solute retention are affected by the wetting of the stationary phase.

Several implications for chromatographic applications of alkyl bonded silica can be derived from this research. RPLC should be conducted above the nonwetting limit, if possible. A gradient elution should start at an eluent composition above the nonwetting limit. Otherwise a long equilibration time, a low efficiency, and a low reproducibility are expected. If it is necessary to perform chromatographic analysis below the nonwetting limit, make sure the column is equilibrated. Below the nonwetting limit, before switching to a eluent containing more organic modifier, it is recommended to rinse the column with pure organic modifier to rewet the stationary phase. Otherwise lower retention values are expected.

Optical transmittance has been well established in this research to study the wetting and solvation of stationary phase materials for RPLC. It is much more informative than other methods, including direct wetting tests and titration wetting tests. It is also much more sensitive to changes in the interphase region than surface dipolarity and solute retention. The mechanisms proposed for the changes in transmittance in various regions, however, may not be unique interpretations and are subject to further testing.

Chapter 6

Conclusions

The work here demonstrates that interactions among the stationary phase, the eluent, and the solute in liquid chromatography are complicated. The properties of the stationary phase, in both normal phase and reversed-phase liquid chromatography, may strongly depend on the eluent composition. The interactions of the solute with binary solvent mixtures deviate significantly from a linear function of the solvent composition.

The solvatochromic studies of the surface polarity of silica have shown that the surface of silica in *n*-hexane has a high dipolarity-polarizability, a high hydrogen-bonding acidity and a low hydrogen-bonding basicity. In *n*-hexane-chloroform mixtures, the dipolarity-polarizability and hydrogen-bonding acidity of the silica surface are independent of the solvent composition. The hydrogen-bonding basicity of the silica surface, however, decreases as the concentration of chloroform is increased, which may be attributed to hydrogen-bonding interactions between chloroform and the surface silanol groups. In *n*-hexane-ethyl ether mixtures, the dipolarity-polarizability of the surface of silica decreases as the concentration of ethyl ether is increased. The strength of interactions between ET-33, an α dye, and the silica surface, as indicated by the electronic transition energy of ET-33, also decreases with increasing ethyl ether content. Ethyl ether, which has a considerable hydrogen-

bonding basicity, may strongly interact with acidic surface silanol groups. This makes some strong adsorption sites unavailable to π^* and α dyes, resulting in a decrease in the surface dipolarity-polarizability of silica and a decrease in the strength of interactions between ET-33 and the silica surface. The same argument can be applied to the strong dependence of the surface dipolarity-polarizability of silica on drying of solvents. Water may have much stronger interactions with surface silanol groups. Therefore, even a trace amount of water may strongly affect the surface properties of silica. Because of the high hydrogen-bonding acidity of the silica surface, a solvent with a high hydrogen-bonding basicity is a strong eluent in normal phase liquid chromatography with silica as the stationary phase.

π^* measurements may be interfered with by hydrogen-bonding interactions in strongly acidic environments. Such interference may be different for different π^* dyes, resulting in the dependence of π^* values on the nature of π^* dyes. Unlike solvent molecules, due to orientational or steric reasons, surface silanol groups may interact with the basic functional group in different α dyes at different strengths. This leads to the dependence of α measurements on the nature of the α probes. Though the absolute π^* and α values of the silica surface are different using different π^* and α probes, the same solvent composition dependence of the π^* and α values

of the silica surface was observed using different probes.

The method developed for the solvatochromic measurements of the silica surface may also be applied to characterize other solid particles, e.g., alumina. Alumina is considered a little basic. If the disparity in the π^* measurements using different π^* dyes is caused by interference from hydrogen-bonding interactions, there should be no such disparity in the π^* measurements on alumina. The dependence of the solvatochromic parameters on the solvent composition should also be different from that for the silica surface.

Factor analysis studies indicate that the electronic absorption spectra of N,N-dimethyl-4-nitroaniline in 14 *n*-hexane-ethyl ether mixtures containing 0% to 100% (v/v) of ethyl ether cannot be reconstructed accurately from a linear combination of two spectra. At least three spectra are required to reproduce the 14 spectra within the experimental uncertainties. The best combination are the spectra in mixtures containing 0%, 2%, and 20% (v/v) of ethyl ether, respectively. It was proposed that the dye may exist in three different environments, *n*-hexane, ethyl ether molecules without interactions with other ethyl ether molecules (segregated ethyl ether molecules), and ethyl ether molecules interacting with other ethyl ether molecules (ethyl ether clusters).

Optical transmittance measurements were established in

this work to study the wetting or solvation of alkyl bonded silica in organic-water mixtures. Changes in optical transmittance of the alkyl bonded silica/eluent system over the eluent composition can be separated into different regions, which have been correlated with or assigned to various physical processes in the interphase region, including adsorption of water onto residual silanol groups, desolvation of bonded alkyl chains, collapse of bonded alkyl chains onto the silica support to form a rough hydrocarbon film, and chain reorganization to form a smooth hydrocarbon film. Other processes, e.g., gas phase pocket formation in the pores and particle aggregation may also be responsible for some of the transmittance changes. Wetting hysteresis is obvious from the difference in the transmittance vs. composition plots with opposite equilibration directions.

Surface silanol groups, which are mainly responsible for the high surface dipolarity-polarizability and high surface hydrogen-bonding acidity of silica, are indispensable in the wetting of alkyl bonded silica in organic-water mixtures. Residual surface silanol groups on alkyl bonded silica are obviously available for water adsorption, as observed by a decrease in optical transmittance of the alkyl bonded silica/eluent system when a small amount of water was introduced to organic modifier.

In the downward equilibration experiment, no significant

changes in the structure and composition of the interphase region were observed by optical transmittance measurements until the organic modifier content decreases to region 3. The increase in optical transmittance with decreasing organic modifier content in region 3 is attributed to the desolvation of bonded alkyl chains, which reduces the size of the interphase region. As the organic modifier content becomes lower than the nonwetting limit, bonded alkyl chains may collapse onto the silica surface to form a rough hydrocarbon film, which introduces a discontinuity in the refractive index between the stationary phase and the eluent, resulting in a dramatic decrease in optical transmittance. As the organic modifier content continues to decrease, to reduce the exposure of bonded alkyl chains to a water-rich eluent, bonded alkyl chains may reorganize themselves to form a smooth hydrocarbon film. Such a process may take place in region 5. As the size of the interphase region decreases, the optical transmittance increases. Other processes, e.g., gas phase pocket formation in the pores and aggregation among particles, may also be responsible for the changes in transmittance in regions 4 and 5. Gas phase formation decreases the optical transmittance, while particle aggregation may increase the transmittance by reducing the number of interfaces.

In the following upward equilibration experiment, the hydrocarbon film formed by bonded alkyl chains remains

unchanged until the organic modifier content in the eluent is in region II. The physical process involved in region II has been proved to be the reversal of the one involved in region 5. Region III was proved to be the reversal of region 4. As the organic modifier content increases above the rewetting limit, alkyl bonded silica is rewetted and bonded alkyl chains are resolvated.

Different alkyl bonded silica materials have different wetting behaviors. After initial wetting by organic modifier, some alkyl bonded silica materials exhibit only regions 1 to 4 in the downward equilibration experiment. Some alkyl bonded silica materials remain wetted even in water, exhibit only regions 1 to 3. There are two alkyl bonded silica materials exhibiting only regions 1 and 2. Lower bonding density obviously facilitates wetting in organic-water mixtures. The effects of other characteristics of alkyl bonded silica on wetting have yet to be clarified. Less polar organic modifier can wet alkyl bonded silica at a lower concentration.

Alkyl bonded silica particles are inhomogeneous in wettability, as proved by direct wetting tests. The organic modifier content required to wet dry alkyl bonded silica particles from direct wetting tests is well correlated to the rewetting limit obtained from optical transmittance measurements. Direct wetting tests showed that nonwetted particles remained immersed in the eluent until they were

brought into contact with air. For alkyl bonded silica materials without regions 4 and 5, a certain concentration of organic modifier is required for the initial wetting.

Wetting hysteresis appears when the direction of equilibration is changed in regions 3 to 5, but not regions 1 and 2. Slow kinetics may be a prerequisite for the existence of wetting hysteresis. The existence of wetting hysteresis indicates that the stationary phase/mobile phase system may not reach a thermodynamic equilibrium when the organic modifier content in the mobile phase is less than the rewetting limit.

A much longer column equilibration time is required if the eluent is in regions 3 to 5, i.e., when alkyl bonded silica is not wetted or well solvated. Column equilibration time is significantly reduced at an elevated temperature. In the same eluent, a significantly lower surface dipolarity is observed for the nonwetted phase if the direction of equilibration is changed in region 5, but not region 4. Solute retention is significantly lower than expected as the stationary phase is nonwetted. The wetting hysteresis observed by optical transmittance when the direction of equilibration is changed in region 3, however, does not cause any significant hysteresis in solute retention. The strong effects of wetting on column equilibration time and solute retention indicate the importance to understand the wetting of

alkyl bonded silica.

According to the results from this research, RPLC should be conducted above the nonwetting limit, if possible. A gradient elution should start at a mobile phase composition above the nonwetting limit. Otherwise a long column equilibration time, a low column efficiency, and a low reproducibility are expected. If chromatographic analysis must be performed below the nonwetting limit, make sure the column is equilibrated. Below the nonwetting limit, before switching to a mobile phase containing more organic modifier, it is recommended to rinse the column with pure organic modifier to rewet the stationary phase. Otherwise lower retention values are expected.

There are still many unresolved mysteries in the wetting of alkyl bonded silica, e.g., pretreatment effects observed for LiChroprep RP-18. The mechanism for wetting hysteresis is still very controversial. The mechanisms proposed here for the changes in transmittance in various regions may not be unique interpretations and are subject to further testing.

Optical transmittance is very sensitive to the changes in the structure and composition of the interphase region in solvated alkyl bonded silica. The methodology established here for studying the wetting of alkyl bonded silica may be used as a general method to study the interactions between porous particles and a liquid.

References

References

(1) Iler, R. K. *The Chemistry of Silica*; Wiley: New York, 1979.

(2) Unger, K. K. *Porous Silica*; Elsevier: Amsterdam, 1979.

(3) Cox, G. B. *J. Chromatogr.* **1993**, *656*, 353.

(4) Nawrocki, J.; Buszewski, B. *J. Chromatogr.* **1988**, *449*, 1.

(5) Nawrocki, J. *Chromatographia* **1991**, *31*, 177.

(6) Nawrocki, J. *Chromatographia* **1991**, *31*, 193.

(7) Köhler, J.; Chase, D. B.; Farlee, R. D.; Vega, A. J.; Kirkland, J. J. *J. Chromatogr.* **1986**, *352*, 275.

(8) Mauss, M.; Engelhardt, H. *J. Chromatogr.* **1986**, *371*, 235.

(9) Köhler, J.; Kirkland, J. J. *J. Chromatogr.* **1987**, *385*, 125.

(10) Zhdanov, S. P.; Kosheleva, L. S.; Titova, T. I. *Langmuir* **1987**, *3*, 960.

(11) Sindorf, D. W.; Maciel, G. E. *J. Am. Chem. Soc.* **1981**, *103*, 4263.

(12) Sindorf, D. W.; Maciel, G. E. *J. Am. Chem. Soc.* **1983**, *105*, 1487.

(13) Kinney, D. R.; Chuang, I.-S.; Maciel, G. E. *J. Am. Chem. Soc.* **1993**, *115*, 6786.

(14) Adams, J.; Giam, C. S. *J. Chromatogr.* **1984**, *285*, 81.

(15) Fubini, B.; Bolis, V.; Cavenago, A.; Garrone, E.; Ugliengo, P. *Langmuir* **1993**, *9*, 2712.

(16) Souteyrand, C.; Thibert, M.; Caude, M.; Rosset, R. *J. Chromatogr.* **1984**, *316*, 373.

(17) Kirkland, J. J.; Dilks, C. H., Jr.; DeStefano, J. J. *J. Chromatogr.* **1993**, *635*, 19.

(18) Hair, M. L. In *Silanes, Surfaces, and Interfaces*; Leyden, D. E., Ed.; Gordon and Breach: New York, 1986; p 25.

(19) Takeuchi, T.; Miwa, T.; Nagae, N. *Chromatographia* **1993**, *35*, 375.

(20) Zhuravlev, L. T. *Langmuir* **1987**, *3*, 316.

(21) Pfleiderer, B.; Bayer, E. *J. Chromatogr.* **1989**, *468*, 67.

(22) Nawrocki, J.; Moir, D. L.; Szczepaniak, W. *J. Chromatogr.* **1989**, *467*, 31.

(23) Sadek, P. C.; Koester, C. J.; Bowers, L. D. *J. Chromatogr. Sci.* **1987**, *25*, 489.

(24) Ohtsu, Y.; Shiojima, Y.; Okumura, T.; Koyama, J.-I.; Nakamura, K.; Nakata, O.; Kimata, K.; Tanaka, N. *J. Chromatogr.* **1989**, *481*, 147.

(25) Kimata, K.; Tanaka, N.; Araki, T. *J. Chromatogr.* **1992**, *594*, 87.

(26) Heidrich, D.; Volkmann, D.; Żurawski, D. *Chem. Phys. Lett.* **1981**, *80*, 60.

(27) Boudreau, S. P.; Cooper, W. T. *Anal. Chem.* **1987**, *59*, 353.

(28) Boudreau, S. P.; Cooper, W. T. *Anal. Chem.* **1989**, *61*, 41.

(29) Katz, E. D.; Ogan, K.; Scott, R. P. W. *J. Chromatogr.* **1986**, *352*, 67.

(30) Katz, E. D.; Lochmüller, C. H.; Scott, R. P. W. *Anal. Chem.* **1989**, *61*, 349.

(31) Easteal, A. J. *Aust. J. Chem.* **1979**, *32*, 1379.

(32) Kovacs, H.; Laaksonen, A. *J. Am. Chem. Soc.* **1991**, *113*, 5596.

(33) Chatterjee, P.; Bagchi, S. *J. Chem. Soc., Faraday Trans.* **1991**, *87*, 587.

(34) Reta, M. R.; Cattana, R.; Anunziata, J. D.; Silber, J. J. *Spectrochim. Acta* **1993**, *49A*, 903.

(35) Acree, W. E., Jr.; Tucker, S. A.; Wilkins, D. C. *J. Phys. Chem.* **1993**, *97*, 11199.

(36) Balakrishnan, S.; Easteal, A. J. *Aust. J. Chem.* **1981**, *34*, 943.

(37) Marcus, Y.; Migron, Y. *J. Phys. Chem.* **1991**, *95*, 400.

(38) Dawber, J. G.; Ward, J.; Williams, R. A. *J. Chem. Soc., Faraday Trans. 1* **1988**, *84*, 713.

(39) Dawber, J. G.; Etemad, S.; Beckett, M. A. *J. Chem. Soc., Faraday Trans.* **1990**, *86*, 3725.

(40) Bosch, E.; Rosés, M. *J. Chem. Soc., Faraday Trans.* **1992**, *88*, 3541.

(41) Chatterjee, P.; Laha, A. K.; Bagchi, S. *J. Chem. Soc., Faraday Trans.* **1992**, *88*, 1675.

(42) Cheong, W. J.; Carr, P. W. *Anal. Chem.* **1988**, *60*, 820.

(43) Migron, Y.; Marcus, Y. *J. Chem. Soc., Faraday Trans.* **1991**, *87*, 1339.

(44) Balakrishnan, S.; Easteal, A. J. *Aust. J. Chem.* **1981**, *34*, 933.

(45) Marcus, Y. *J. Chem. Soc., Perkin Trans. 2* **1994**, 3541.

(46) Marcus, Y. *J. Chem. Soc., Faraday Trans. 1* **1989**, *85*, 381.

(47) Cattana, R.; Silber, J. J.; Anunziata, J. *Can. J. Chem.* **1992**, *70*, 2677.

(48) Ramírez, C. B.; Carrasco, N.; Rezende, M. C. *J. Chem. Soc., Faraday Trans.* **1995**, *91*, 3839.

(49) Boggetti, H.; Anunziata, J. D.; Cattana, R.; Silber, J. J. *Spectrochim. Acta* **1994**, *50A*, 719.

(50) Israelachvili, J. N. *Intermolecular and Surface Forces*, 2nd ed.; Academic Press: London, 1992; p 323.

(51) Berg, J. C. In *Wettability*; Berg, J. C., Ed; Marcel Dekker: New York, 1993; pp 75-148.

(52) Johnson, R. E., Jr.; Dettre, R. H. In *Wettability*; Berg, J. C., Ed; Marcel Dekker: New York, 1993; pp 1-73.

(53) Jaycock, M. J.; Parfitt, G. D. *Chemistry of Interfaces*; Ellis Horwood Ltd.: Chichester, 1981; Chapters 1 and 5.

(54) Davies, J. T.; Rideal, E. K. *Interfacial Phenomena*, 2nd ed.; Academic Press: New York, 1963; p 435.

(55) Adamson, A. W. *Physical Chemistry of Surfaces*, 4th ed.; Wiley-Interscience: New York, 1982; Chapter XIII.

(56) Yang, S. S.; Gilpin, R. K. *J. Chromatogr.* **1987**, *394*, 295.

(57) Welsch, T.; Frank, H.; Vigh, Gy. *J. Chromatogr.* **1990**, *506*, 97.

(58) Heslot, F.; Fraysse, N.; Cazabat, A. M.; Levinson, P.; Carles, P. In *Wetting Phenomena*; De Coninck, J., Dunlop, F., Eds.; Springer-Verlag: Berlin, 1990; pp 41-48.

(59) Scott, R. P. W.; Simpson, C. F. *J. Chromatogr.* **1980**, *197*, 11.

(60) Engelhardt, H.; Mathes, D. *J. Chromatogr.* **1977**, *142*, 311.

(61) Melander, W. R.; Horváth, Cs. *Chromatographia* **1984**, *18*, 353.

(62) Schoenmakers, P. J.; Billiet, H. A. H.; de Galan, L. *J. Chromatogr.* **1983**, *282*, 107.

(63) Gilpin, R. K.; Gangoda, M. E. *J. Chromatogr. Sci.* **1983**, *21*, 352.

(64) Cole, L. A.; Dorsey, J. G. *Anal. Chem.* **1990**, *62*, 16.

(65) Jandera, P.; Kubát, J. *J. Chromatogr.* **1990**, *500*, 281.

(66) Hsieh, M.-M.; Dorsey, J. G. *J. Chromatogr.* **1993**, *631*, 63.

(67) Martire, D. E.; Boehm, R. E. *J. Phys. Chem.* **1983**, *87*, 1045.

(68) Foley, J. P.; May, W. E. *Anal. Chem.* **1987**, *59*, 110.

(69) Engelhardt, H.; Dreyer, B.; Schmidt, H. *Chromatographia* **1982**, *16*, 11.

(70) Gilpin, R. K.; Squires, J. A. *J. Chromatogr. Sci.* **1981**, *19*, 195.

(71) Gilpin, R. K.; Gangoda, M. E.; Krishen, A. E. *J. Chromatogr. Sci.* **1982**, *20*, 345.

(72) Hammers, W. E.; Verschoor, P. B. A. *J. Chromatogr.* **1983**, *282*, 41.

(73) Scott, R. P. W.; Kucera, P. *J. Chromatogr.* **1977**, *142*, 213.

(74) Riedo, F.; Czencz, M.; Liardon, O.; sz. Kováts, E. *Helv. Chim. Acta* **1978**, *61*, 1912.

(75) Guiochon, G.; Körösi, G.; Siouffi, A. *J. Chromatogr. Sci.* **1980**, *18*, 324.

(76) Park, J.-M.; Kim, J. H. *J. Colloid Interface Sci.* **1994**, *168*, 103.

(77) Wasserman, S. R.; Tao, Y.-T.; Whitesides, G. M. *Langmuir* **1989**, *5*, 1074.

(78) Schwartz, D. K.; Steinberg, S.; Israelachvili, J.; Zasadzinski, J. A. N. *Phys. Rev. Lett.* **1992**, *69*, 3354.

(79) Montgomery, M. E., Jr.; Green, M. A.; Wirth, M. J. *Anal. Chem.* **1992**, *64*, 1170.

(80) Allara, D. L.; Parikh, A. N.; Judge, E. *J. Chem. Phys.* **1994**, *100*, 1761.

(81) Parikh, A. N.; Liedberg, B.; Atre, S. V.; Ho, M.; Allara, D. L. *J. Phys. Chem.* **1995**, *99*, 9996.

(82) Montgomery, M. E., Jr.; Wirth, M. J. *Anal. Chem.* **1994**, *66*, 680.

(83) Montgomery, M. E., Jr.; Wirth, M. J. *Langmuir* **1994**, *10*, 861.

(84) Montgomery, M. E., Jr.; Wirth, M. J. *Anal. Chem.* **1992**, *64*, 2566.

(85) Burbage, J. D.; Wirth, M. J. *J. Phys. Chem.* **1992**, *96*, 5943.

(86) Fóti, G.; Martinez, C.; sz. Kováts, E. *J. Chromatogr.* **1989**, *461*, 243.

(87) Fóti, G.; sz. Kováts, E. *Langmuir* **1989**, *5*, 232.

(88) Koch, C. S.; Köster, F.; Findenegg, G. H. *J. Chromatogr.* **1987**, *406*, 257.

(89) Zhu, P. L. *Chromatographia* **1985**, *20*, 425.

(90) Alvarez-Zepeda, A.; Martire, D. E. *J. Chromatogr.* **1991**, *550*, 285.

(91) Sindorf, D. W.; Maciel, G. E. *J. Am. Chem. Soc.* **1983**, *105*, 1848.

(92) Albert, K.; Evers, B.; Bayer, E. *J. Magn. Reson.* **1985**, *62*, 428.

(93) Thompson, W. R.; Pemberton, J. E. *Anal. Chem.* **1994**, *66*, 3362.

(94) Hansen, R. L.; Harris, J. M. *Anal. Chem.* **1995**, *67*, 492.

(95) Carr, J. W.; Harris, J. M. *Anal. Chem.* **1987**, *59*, 2546.

(96) Lu, H.; Rutan, S. C. *Anal. Chem.* **1996**, *68*, 1387.

(97) Morel, D.; Serpinet, J. *J. Chromatogr.* **1980**, *200*, 95.

(98) Cole, L. A.; Dorsey, J. G. *Anal. Chem.* **1992**, *64*, 1317.

(99) Jones, J. L.; Rutan, S. C. *Anal. Chem.* **1991**, *63*, 1318.

(100) Bogar, R. G.; Thomas, J. C.; Callis, J. B. *Anal. Chem.* **1984**, *56*, 1080.

(101) Rangnekar, V. M.; Foley, J. T.; Oldham, P. B. *Appl. Spectrosc.* **1992**, *46*, 827.

(102) Kamlet, M. J.; Abboud, J. L. M.; Taft, R. M. *Prog. Phys. Org. Chem.* **1981**, *13*, 485.

(103) Reichardt, C. *Solvents and Solvent Effects in Organic Chemistry*, 2nd ed.; VCH: Weinheim, 1988.

(104) Kamlet, M. J.; Taft, R. W. *J. Am. Chem. Soc.* **1976**, *98*, 377.

(105) Taft, R. W.; Kamlet, M. J. *J. Am. Chem. Soc.* **1976**, *98*, 2886.

(106) Kamlet, M. J.; Abboud, J. L.; Taft, R. W. *J. Am. Chem. Soc.* **1977**, *99*, 6027.

(107) Taft, R. W.; Kamlet, M. J. *J. Chem. Soc., Perkin Trans. 2* **1979**, 1723.

(108) Kessler, M. A.; Wolfbeis, O. S. *Chem. Phys. Lipids* **1989**, *50*, 51.

(109) Lu, H.; Rutan, S. C. *Anal. Chem.* **1996**, *68*, 1381.

(110) Yokoyama, T.; Taft, R. W.; Kamlet, M. J. *J. Am. Chem. Soc.* **1976**, *98*, 3233.

(111) Lindley, S. M.; Flowers, G. C.; Leffler, J. E. *J. Org. Chem.* **1985**, *50*, 607.

(112) Handreck, G. P.; Smith, T. D. *J. Chem. Soc., Faraday Trans. 1* **1988**, *84*, 1847.

(113) Dutta, P. K.; Turbeville, W. *J. Phys. Chem.* **1991**, *95*, 4087.

(114) Michels, J. J.; Dorsey, J. G. *Langmuir* **1990**, *6*, 414.

(115) Spange, S.; Reuter, A.; Vilsmeier, E. *Colloid Polym. Sci.* **1996**, *274*, 59.

(116) Helburn, R. S.; Rutan, S. C.; Pompano, J.; Mitchem, D.; Patterson, W. T. *Anal. Chem.* **1994**, *66*, 610.

(117) Rutan, S. C. *Chemom. Intell. Lab. Syst.* **1989**, *6*, 191.

(118) Krygowski, T. M.; Milczarek, E.; Wrona, P. K. *J. Chem. Soc., Perkin Trans., 2* **1980**, 1563.

(119) Szepesy, L.; Combellas, C.; Caude, M.; Rosset, R. *J. Chromatogr.* **1982**, *237*, 65.

(120) Casassas, E.; Fonrodona, G.; de Juan, A.; Tauler, R. *Chemom. Intell. Lab. Syst.* **1991**, *12*, 29.

(121) Snyder, L. R. *Principles of Adsorption Chromatography*; Marcel Dekker: New York, 1968; Chapters 3, 8, and 10.

(122) Kagel, R. O. *J. Phys. Chem.* **1970**, *74*, 4518.

(123) Tan, L. C.; Carr, P. W.; Fréchet, J. M. J.; Smigol, V. *Anal. Chem.* **1994**, *66*, 450.

(124) Park, J. H.; Carr, P. W. *J. Chromatogr.* **1989**, *465*, 123.

(125) Spange, S.; Simon, F.; Heublein, G.; Jacobasch, H.-J.; Börner, M. *Colloid Polym. Sci.* **1991**, *269*, 173.

(126) Malinowski, E. R. *Factor Analysis in Chemistry*, 2nd ed.; Wiley-Interscience: New York, 1991.

(127) Fawcett, W. R.; Krygowski, T. M. *Can. J. Chem.* **1976**, *54*, 3283.

(128) Edward, J. T.; Wong, S. C. *J. Am. Chem. Soc.* **1977**, *99*, 4229.

(129) Casassas, E.; Fonrodona, G.; de Juan, A.; Tauler, R. *Anal. Chim. Acta* **1993**, *283*, 548.

(130) Bulmer, J. T.; Shurvell., H. F. *J. Phys. Chem.* **1973**, *77*, 256.

(131) Dill, K. A. *J. Phys. Chem.* **1987**, *91*, 1980.

(132) Gutnikov, G.; Hung, L.-G. *Chromatographia* **1984**, *19*, 260.

(133) Dreux, M.; Lafosse, M.; Agbo-Hazoume, P. *Chromatographia* **1984**, *18*, 15.

(134) Li, Z. M.Sc. Thesis, Beijing Medical University, Beijing, 1987.

(135) Lochmüller, C. H.; Hunnicutt, M. L. *J. Phys. Chem.* **1986**, *90*, 4318.

(136) *CRC Handbook of Chemistry and Physics*, 62nd ed.; Weast, R. C., Ed.; CRC Press: Boca Raton, 1981.

Appendices

Appendix A MATLAB Program for Determining the Number of Significant Factors

```
% sfa.m significant factor analysis - a program designed to
help determine the number of significant factors in a matrix.
function []=sfa(data)
% data=data matrix
format short e
[r,c]=size(data);
[u,s,v]=svd(data,0);
for j=1:c
ev(j)=s(j,j)*s(j,j);
rev(j)=ev(j)/((r-j+1)*(c-j+1));
end
sev(c+1)=0;
sdf(c+1)=0;
for k=c:-1:2
sev(k)=sev(k+1)+ev(k);
sdf(k)=sdf(k+1)+(r-k+1)*(c-k+1);
end
for l=1:c-1
re(l)=sqrt(sev(l+1)/(r*(c-l)));
ind(l)=re(l)/(c-l)^2;
end
semilogy(ind,'ok')
xlabel('FACTOR LEVEL')
ylabel('IND')
pause
```

Appendix B Transmittance vs. Composition Plots

All the transmittance vs. composition plots cited in Table 5-3 are shown here except those which have appeared in Chapter 5, including the plots for HDG $C_{18}H_{37}$ (Figures 5-4, 5-5, and 5-6), LiChroprep RP-18 in MeOH-water (Figure 5-11), YMC Octyl 120A (15 μm) in ACN-water (Figure 5-17), YMC Butyl 120A (25 μm) in ACN-water (Figure 5-23). The plot for YMC ODS-A 120A (25 μm) in ACN-water from 0% to 50% ACN has been shown in Figure 5-9. The plot from 0% to 100% ACN is shown here. The solid and dashed curves were obtained from downward and upward equilibration experiments, respectively. All these curves can be separated into different regions as in Figure 5-4, though some curves only exhibit some of the regions specified in Figure 5-4. For some stationary phase/mobile phase systems, optical transmittance measurements were only conducted from 0% to 30% or 0% to 50% organic modifier because the desolvation process or the nonwetting of the stationary phase only happened at relatively low organic modifier contents. The plots are arranged in the order as in Table 5-3.

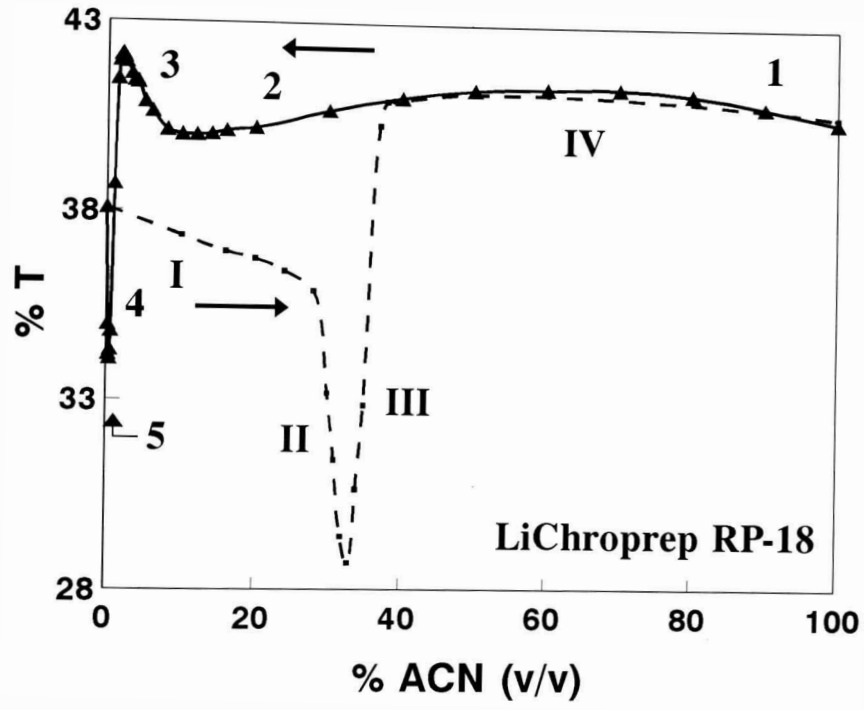

Figure B-1. Transmittance of LiChroprep RP-18 in ACN-water eluent vs. eluent composition. The solid and dashed curves were obtained from downward and upward equilibration experiments, respectively.

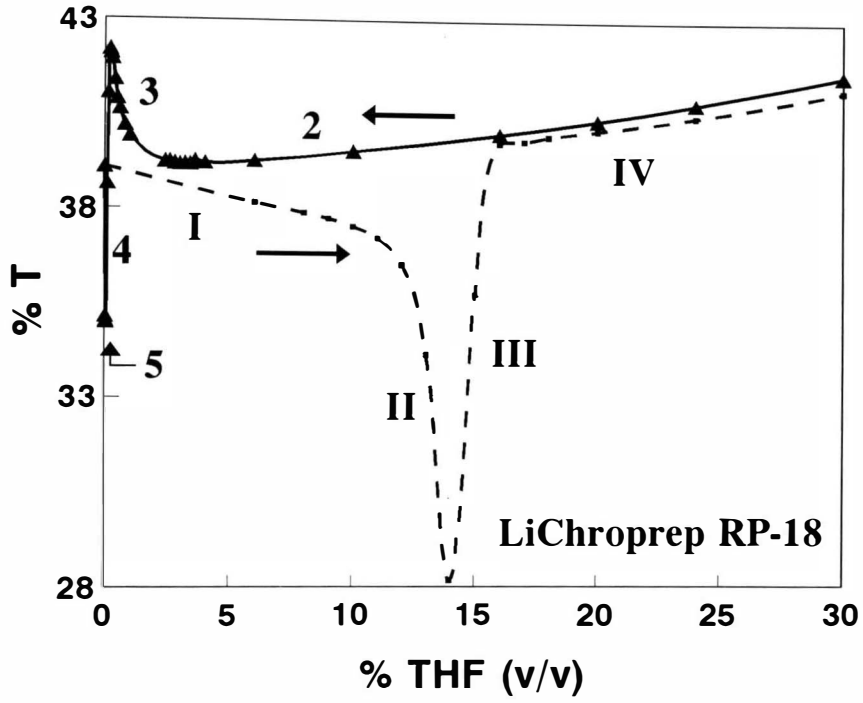

Figure B-2. Transmittance of LiChroprep RP-18 in THF-water eluent vs. eluent composition. The solid and dashed curves were obtained from downward and upward equilibration experiments, respectively.

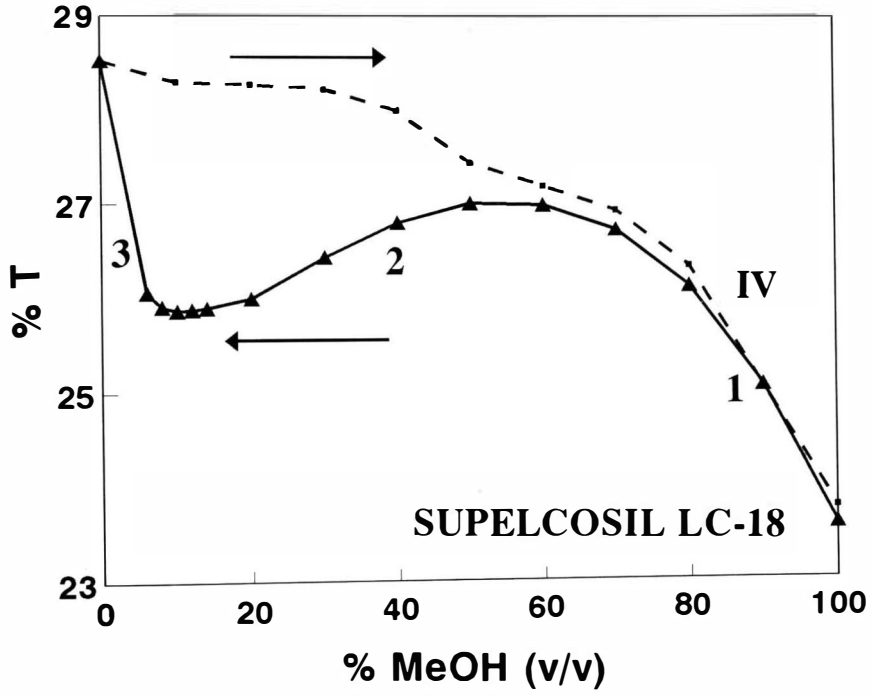

Figure B-3. Transmittance of SUPELCOSIL LC-18 in MeOH-water eluent vs. eluent composition. The solid and dashed curves were obtained from downward and upward equilibration experiments, respectively.

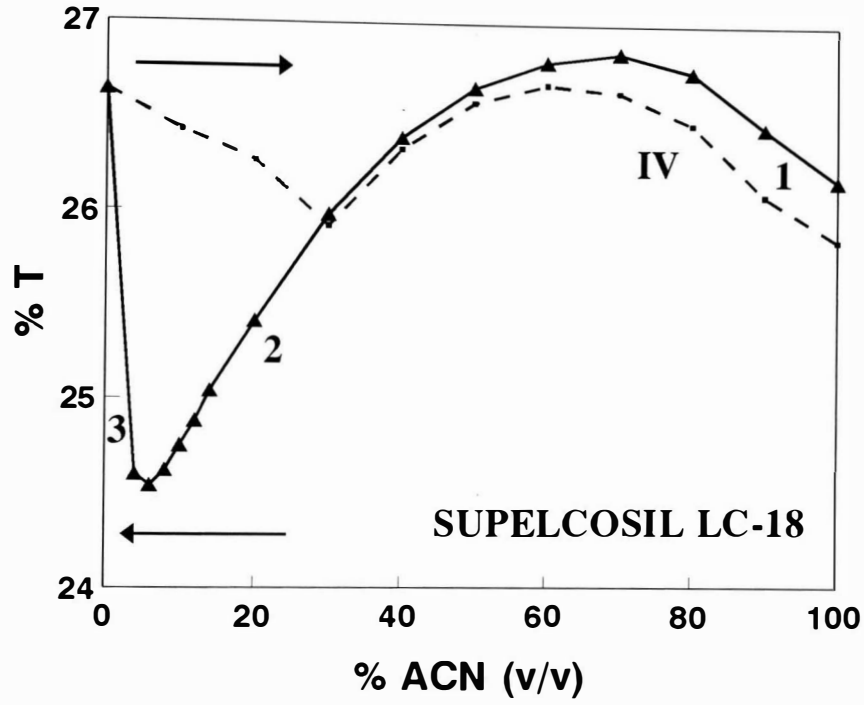

Figure B-4. Transmittance of SUPELCOSIL LC-18 in ACN-water eluent vs. eluent composition. The solid and dashed curves were obtained from downward and upward equilibration experiments, respectively.

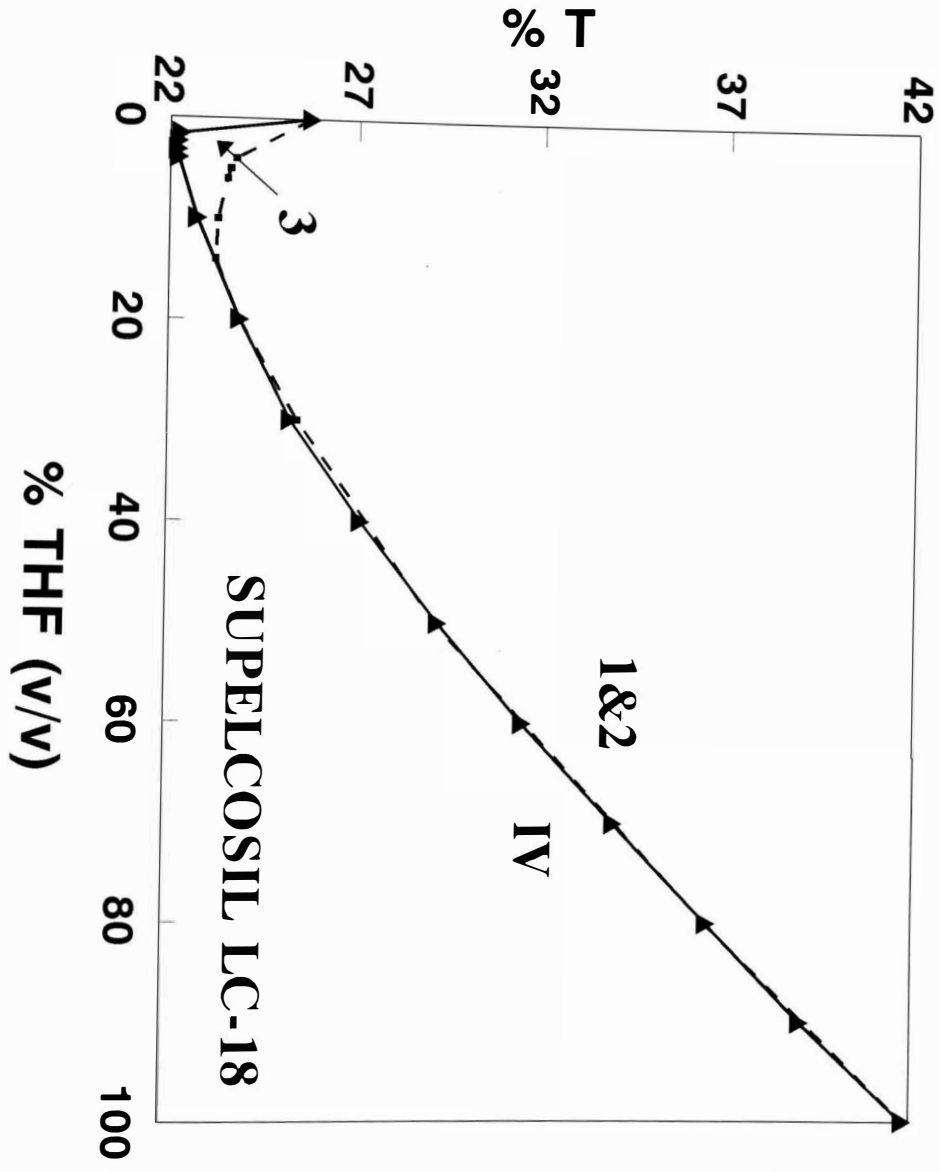

Figure B-5. Transmittance of SUPELCOSIL LC-18 in THF-water eluent vs. eluent composition. The solid and dashed curves were obtained from downward and upward equilibration experiments, respectively.

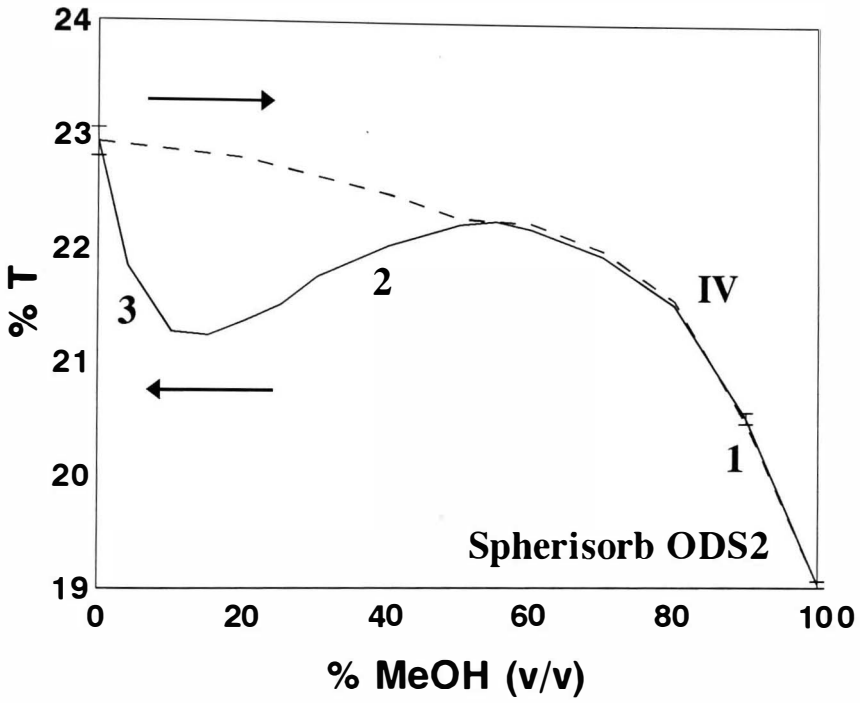

Figure B-6. Transmittance of Spherisorb ODS2 in MeOH-water eluent vs. eluent composition. The solid and dashed curves were obtained from downward and upward equilibration experiments, respectively.

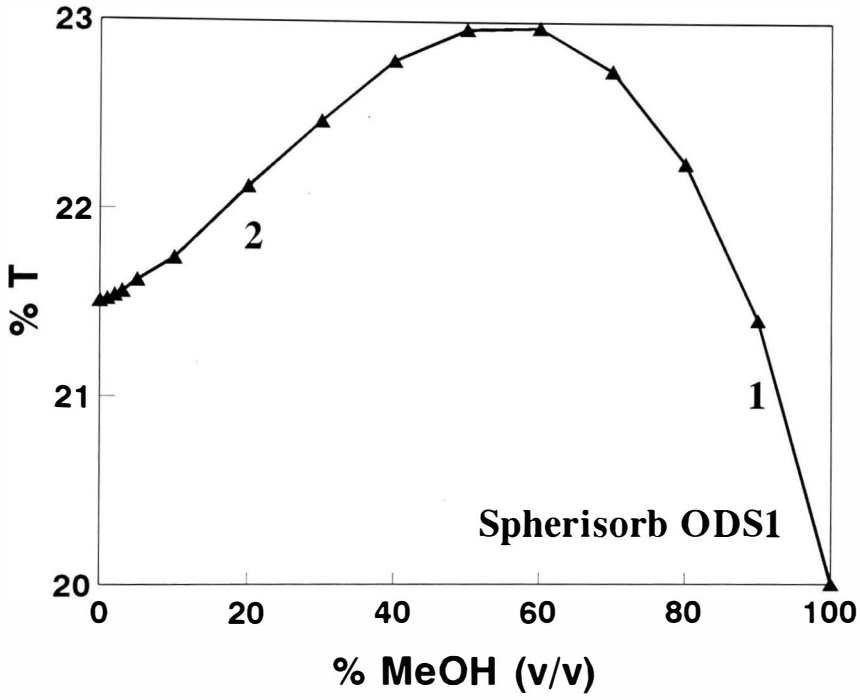

Figure B-7. Transmittance of Spherisorb ODS1 in MeOH-water eluent vs. eluent composition. The solid and dashed curves were obtained from downward and upward equilibration experiments, respectively.

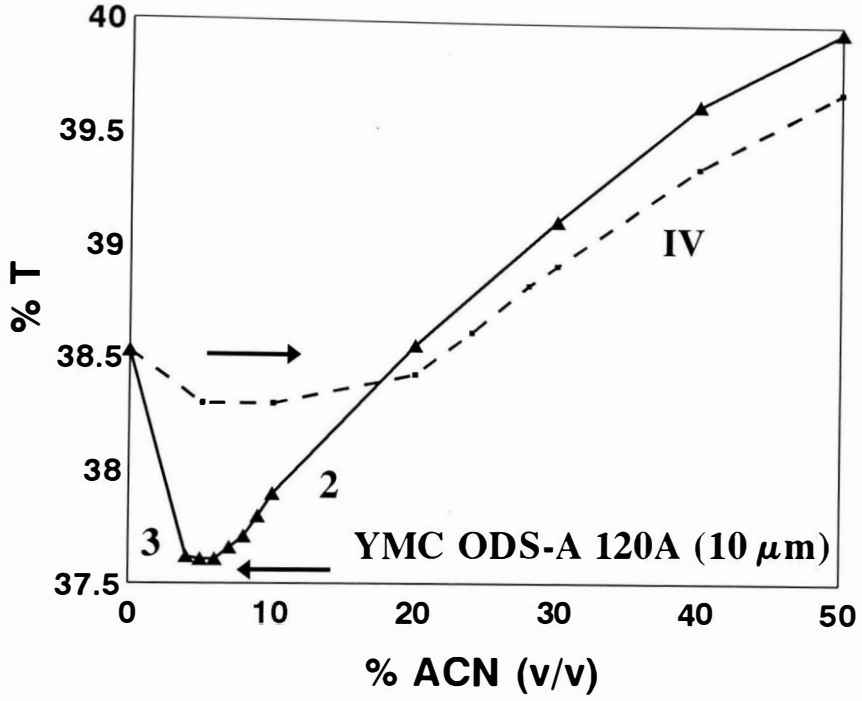

Figure B-8. Transmittance of YMC ODS-A 120A (10 μm) in ACN-water eluent vs. eluent composition. The solid and dashed curves were obtained from downward and upward equilibration experiments, respectively.

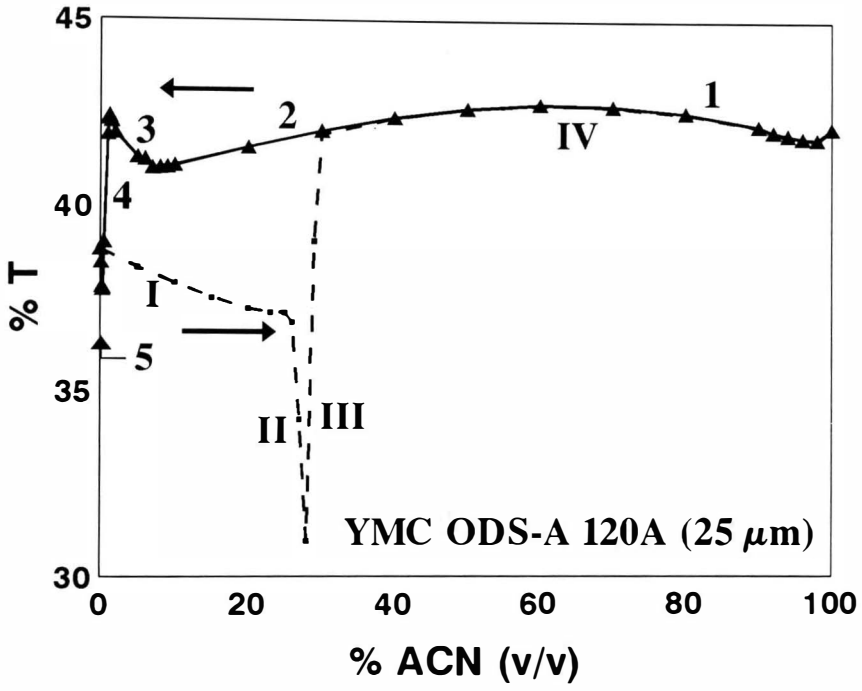

Figure B-9. Transmittance of YMC ODS-A 120A (25 μm) in ACN-water eluent vs. eluent composition. The solid and dashed curves were obtained from downward and upward equilibration experiments, respectively.

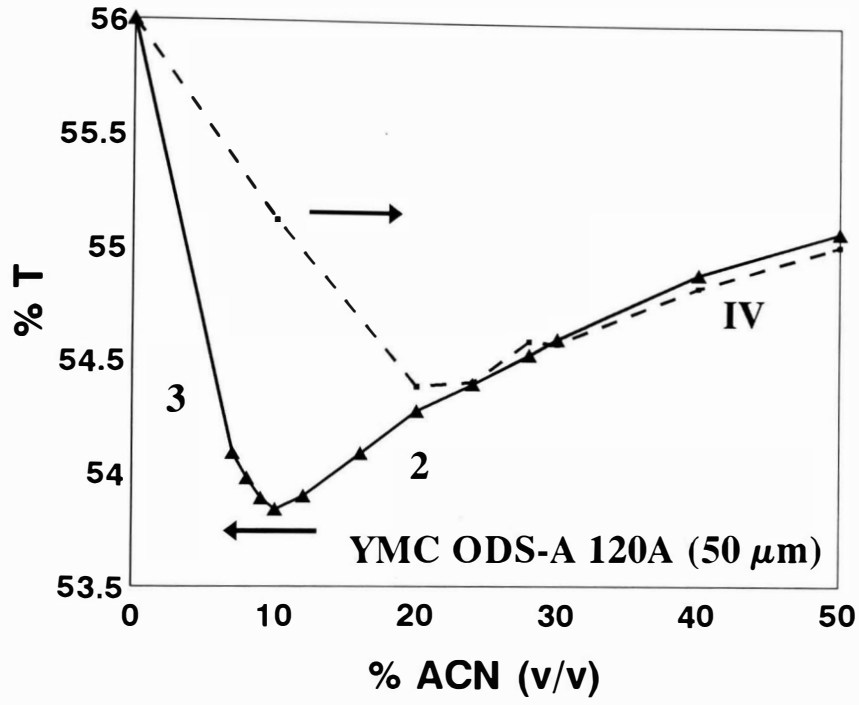

Figure B-10. Transmittance of YMC ODS-A 120A (50 μm) in ACN-water eluent vs. eluent composition. The solid and dashed curves were obtained from downward and upward equilibration experiments, respectively.

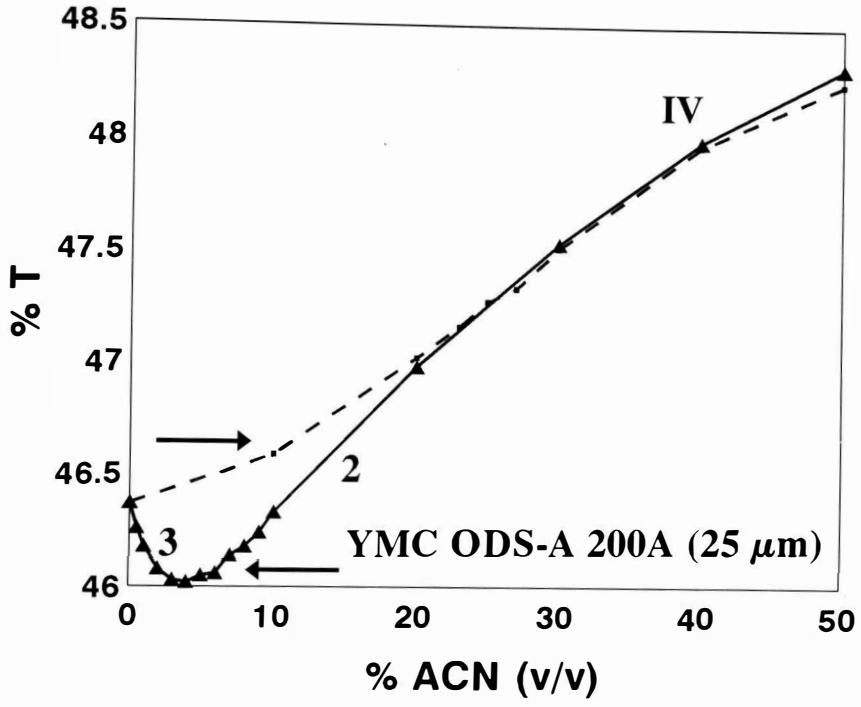

Figure B-11. Transmittance of YMC ODS-A 200A (25 μm) in ACN-water eluent vs. eluent composition. The solid and dashed curves were obtained from downward and upward equilibration experiments, respectively.

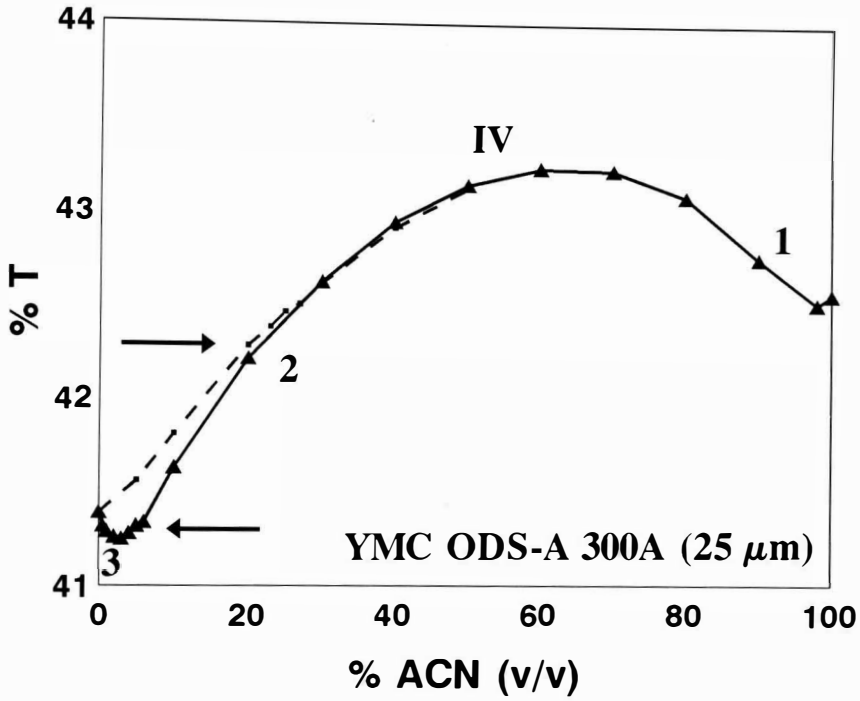

Figure B-12. Transmittance of YMC ODS-A 300A (25 μm) in ACN-water eluent vs. eluent composition. The solid and dashed curves were obtained from downward and upward equilibration experiments, respectively.

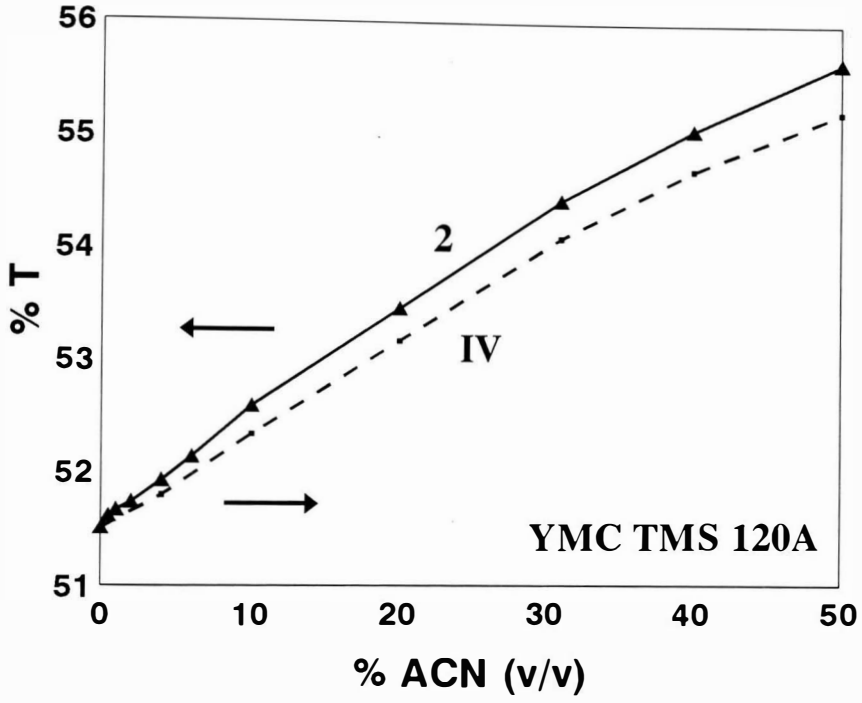

Figure B-13. Transmittance of YMC TMS 120A in ACN-water eluent vs. eluent composition. The solid and dashed curves were obtained from downward and upward equilibration experiments, respectively.

Vita